Universidade de Évora - Escola de Ciências e Tecnologia
Universidade Nova de Lisboa - Faculdade de Ciências e Tecnologias

Mestrado em Paleontologia

Dissertação

A new phytosaur from the Late Triassic of Jameson Land, Greenland.

Víctor López Rojas

Orientador | Octávio João Madeira Mateus

Évora 2021

Universidade de Évora - Escola de Ciências e Tecnologia

Universidade Nova de Lisboa - Faculdade de Ciências e Tecnologias

Mestrado em Paleontologia

Dissertação

A new phytosaur from the Late Triassic of Jameson Land, Greenland.

Víctor López Rojas

Orientador | Octávio João Madeira Mateus

Évora 2021
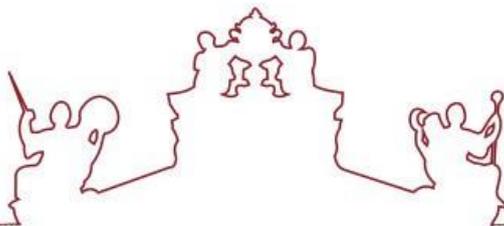
A dissertação foi objeto de apreciação e discussão pública pelo seguinte júri nomeado pelo Diretor da Escola de Ciências e Tecnologia:

Presidente | Carlos Alexandre Ribeiro (Universidade de Évora)

Vogais | Octávio João Madeira Mateus (Universidade Nova de Lisboa - Faculdade de Ciências e Tecnologias) (Orientador)
Richard Butler (UNIVERSITY OF BIRMINGHAM) (Arguente)

Évora 2021

ACKNOWLEDGMENTS

RESUMO

A descrição mais detalhada do primeiro material de fitossauro encontrado em Jameson Land, Fleming Fjord Group (Leste da Gronelândia). O material desagregado de restos de jovens, subadultos e adultos de vários espécimes, e a falta de grande parte dos ossos do crânio, permitiram fazer uma análise filogenética inicial.

As primeiras análises filogenéticas feitas aqui mostram que é do género *Mystriosuchus*, com potencial para ser uma nova espécie. *Mystriosuchus* é um género exclusivamente europeu, que sustenta a influência da fauna europeia da Leste da Gronelândia no Triásico. Este género também pode ser usado como um indicador de intervalo de tempo para as unidades em Malmros Klint Fm., já que *Mystriosuchus* viveu entre os Noriano Médio e Superior.

Esses restos de fitossauros, são importantes devido à posição central na Laurásia durante o Período Triássico, quando o Atlântico Norte começou a abrir, na altura em que a Gronelândia e a Europa ainda muito próximas.

Palavras-chave: *Mystrisosuchus*, filogenia, Malmros Klint, Norian, paleogeografia.

ABSTRACT

More detailed description of the first phytosaur material collected on Jameson Land, Fleming Fjord Group (East Greenland). The disaggregated material of young, sub-adult and adult remains of various specimens, and the lack of most of the skull bones, allowed doing only a preliminary phylogenetic analysis.

The first phylogenetic analyses made here show it is from the *Mystriosuchus* genus, with the potential to be a new species. *Mystriosuchus* is an exclusive European genus, which supports the European fauna influence of East Greenland in the Triassic. It also can be used as a time range indicator for those units in Malmros Klint Fm., as *Mystriosuchus* lived between the on Middle and Late Norian.

These phytosaur remains, are important due to the central Laurasia position during Triassic period, when the North Atlantic started to open, at the time Greenland and Europe were still connected.

Key-words: *Mystriosuchus*, phylogeny, Norian, Malmros Klint, paleogeography.

A new phytosaur from the Late Triassic of Jameson Land, Greenland.

GRAPHICAL ABSTRACT

TABLE OF CONTENTS

INTRODUCTION

A climatic instability at the end of the Permian and the Permian-Triassic Extinction Event (251 Million years ago) caused the extinction of 90% of marine and 70% of continental vertebrate families (Erwin, 1994; Tong et al., 2007). These events created a big gap in several ecological niches with the extinction of the dominant groups from the Permian. Then, the remaining opportunistic survivors were able to spread and conquer those empty ecological niches in the Early Triassic (Erwin, 1998).
Due to the environmental oscillations that the planet suffered at the beginning of the Triassic (Tong et al., 2007), the diversification was slowly recovering in most marine (Schubert & Bottjer, 1995; Tong et al., 2007) and land biotas (Sahney & Benton, 2008). In the case of land animals, Archosauriformes diversified faster than other groups after the Permian-Triassic Extinction, and started to become larger and gained importance in the Late Triassic ecosystems, represented by crocodylomorphs, pterosaurs and early dinosaurs (Sahney & Benton, 2008; Nesbitt et al., 2009; Turner & Nesbitt, 2013).

Phytosaurs

In Late Triassic, freshwater environments were mainly ruled by archosauriforms, in particular the phytosaurs, crocodile-like animals. Phytosaria was described by Jaeger (1828) as herbivorous reptiles, but then von Meyer & Plieninger (1844) accurately described them as semi-aquatic carnivorous animals, similar in life to actual crocodiles. Phytosaurs are characterized by two main traits that can be found in their skulls: (1) a strongly dorsoventrally compressed skull with mainly dorsally antorbital fenestrae and orbits; and (2) external nostrils displaced dorsally and posteriorly, reaching the anterior border part of the orbits (Ezcurra, 2016). The position of the nares and the modification in the skull caused by their migration can be used as a specific discriminator between phytosaurs (Datta et al., 2019b).
Their temporal range extends from the Late Middle Triassic (Ladinian, *Diandongosuchus fuyuanenis* Stocker et al., 2017) to the latest Triassic (Late Norian? - Rhaetian, *Redondasaurus gregorii* Hunt & Lucas, 1993). Older species (*Mesorhinosuchus fraasi*, Jaekel, 1910b, Early Triassic of Germany) and younger (Early Jurassic; Maisch & Kapitzke, 2010) have been found that could be enclosed as phytosaurs; however, as described in Stocker & Butler (2013), *M.fraasi* holotype was destroyed in WWII, and the Early Jurassic phytosaur remains need further studies.

Dentition in phytosaurs has been used as a feature to differentiate basal from more derived forms in the same family, based on character descriptions as "homodont" or "weakly-strong heterodonty" (Long & Murray, 1995), but the difference between that "weakly" to "strong heterodonty" feature was not clearly explained. Hungerbühler (2000) properly described the dentition in phytosaur and has been used to help determine species since then (Spielmann & Lucas, 2012; Datta et al., 2019a). As described by Hungerbühler (2000), phytosaur dentition can be homodont or heterodont. The different level of heterodonty can discriminate phytosaurs between "tripartite dentition" (tip of the snout, premaxilla and maxilla), or "bipartite dentition" (tip and post-tip of the snout). Mandible teeth share the structure of their upper-jaw relatives, but they are smaller and their morphology and transition between sets is less marked than the upper-jaw counterpart.

The relationships of the phytosaurs with crocodilians and, in further extant, with other archosaurs, have been part of a phylogenetic controversy since their discovery. They were

first enclosed as Thecodontia (Owen, 1859), a now obsolete clade supported until the late XX century, which related them with modern crocodiles (Colbert, 1947; Buffetaut & Ingavat, 1982). However, McGregor soon differentiated the phytosaurs from the crocodilian lineage and suggested similar morphology features in both groups were homoplastic (McGregor, 1906).

Modern phylogenies do not closely relate phytosaurs with crocodilians, ending the controversy (Sereno, 1991), but are now focused into the relationship between phytosaurs and other archosaurians: some describe them as the sister-taxa of Archosauria (Nesbitt, 2011; Fig.1A) while others introduce them within Archosauria, as the most basal clade of Pseudosuchia (Ezcurra, 2016; Fig.1B).
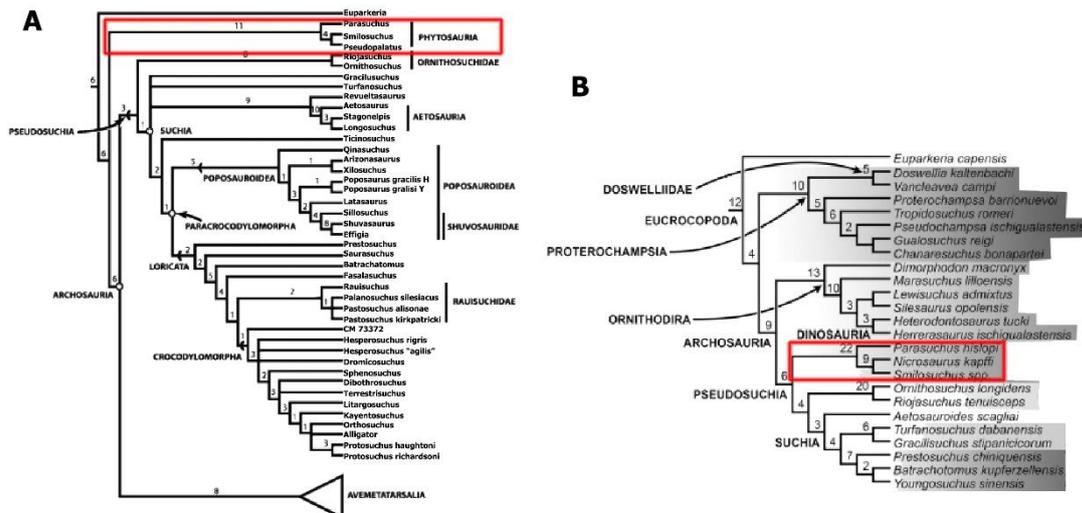
Figure 1. Archosauromorph phylogeny most parsimonious trees, modified from A. Nesbitt (2011), and B. Ezcurra (2016), with the Phytosauria clade marked in red.

The relationships among phytosaur remain under study. However, improvements related to detailed phylogenetic work to identify new and refine old characters, build larger datasets, and redescriptions of historically significant taxa, such as the ones from Stocker et al (2017) and Jones & Butler (2018), will result in better phytosaur phylogenies.

History of discoveries

Phytosaur record is common from Laurasia with occurrences in Europe (Austria, Butler et al., 2019; Germany, Kimmig & Arp, 2010; Italy, Gozzi & Renesto, 2003, Renesto, 2008; Lithuania, Brusatte et al., 2013; Luxembourg, Godefroit et al., 1998; Poland, Dzik, 2001; United Kingdom, Huene, 1908; Switzerland, von Huene, 1922; and recently Portugal, Mateus et al., 2014a); in North America (United States, Stocker, 2010); and in Asia (Thailand, Buffetaut & Ingavat, 1982; Turkey, Buffetaut et al., 1988; and China, Li et al., 2012).

Remains have been also recovered from Gondwana with occurrences in North Africa (Morocco, Lagnaoui et al., 2016) and South Africa (Zimbabwe, Barrett et al., 2020; Madagascar, Burmeister et al., 2006); South America (Brazil, Kischlat & Lucas, 2003); and India (Datta et al, 2019a-b).

In 2012 and 2016, the US-Danish expedition recovered the first material related with phytosaurs from the Triassic lake deposits of East Greenland (Mateus et al., 2014b; Marzola et al., 2017a). Even so there are possible phytosaur remains described by Jenkins et al.

2

(1994), the ones from the US-Danish expeditions are the first detailed phytosaur material. East Greenland lake deposits are well known since the 1970s, with many vertebrate fossils from the main groups of the Mesozoic recovered (Clemmensen et al. 1998, 2015, 2020; Nøttved et al., 2008; Mateus et al., 2014a-b; Marzola et al., 2017a-b). Marzola PhD thesis (2019) described most of the material from the expeditions of 2012 and 2016, including sarcoterygians, temnospondyls, aetosaurians, testudines and dinosaurs, and an early description and comparison of the phytosaur material.

Late Triassic Continental environments

The break of Pangea into the supercontinents Laurasia (northern) and Gondwana (southern), in addition to the Great Extinction event at the end of the Permian, provoked global environmental changes (Erwin, 1994; Tong et al., 2007).

The continental deposits from the Triassic are characterized by an arid or semi-arid global paleoclimate with short humid seasons, even more "climate-sensitive" in some parts of Laurasia (Clemmensen et al., 1998). However, as the Triassic progressed, the paleoclimate evolved into a more humid one (Manspeizer, 1988; Zerfass et al., 2003).

The same rifting that started separated Pangea, caused the break of North Laurasia and the opening of North Atlantic (Golonka, 2007), starting with the separation of Greenland from North Europe during the Late Triassic (Nøttved et al., 2008; Clemmensen et al., 2015) and continuing until its complete separation in the Middle Jurassic (Golonka, 2007).

The rifting caused a paleoclimate change for most of the regions to an arid or semi-arid climate with short seasonal precipitations (Zerfass et al., 2003), and a cyclicity between desert to steppe and back in these regions (Clemmensen et al., 1998).

During the Late Triassic, East Greenland was located in the central part of Laurasia, with a paleolatitude between 35-40º N (Clemmensen et al., 1998). However, it has been migrating towards northern regions since the Early Triassic (Clemmensen et al., 1998; Guarnieri et al., 2017), where seasonal changes had a stronger influence on its climate and environment than in equatorial regions (Clemmensen et al., 1998), combined with cycling periods of transgressions and regressions due to its proximity with the Northern seas (Clemmensen et al., 1998; Ziegler, 1988).

Jameson Land Basin, in the East Greenland coast, was part of a marine bay of the Boreal Sea in the earliest Triassic, but northern drift of the basin and regression processes at the end of Early Triassic transformed it into emerged lands (Clemmensen et al., 2015). The basin is divided into four groups (Clemmensen et al., 2020), from Lower Triassic to Lower Jurassic deposits (Pingo Dal, Gipsdalen, Fleming Fjord, and Kap Stewart), where the environments ranged from freshwater (alluvial fan to lake deposits) to shallow marine and brackish waters, with more moisture, less dry and warmer climate than other laurasian regions (Clemmensen et al., 1998; Nøttved *et al*., 2008; Clemmensen et al., 2020).

Fleming Fjord Group is predominantly made by cyclically lacustrine deposits of continental origin of Norian-Rhaetian (Sulej et al., 2014; Clemmensen et al., 2015). It is divided in three formations: the lowermost Edderfugledal Formation (lacustrine dolomitic mudstone), the middle Malmros Klint Formation (fresh water deposits of lowermost sandstone-siltstones rich and uppermost claystone rich), and the uppermost Ørsted Dal Formation (complex internal stratigraphy due to the proximity of Carlsberg Fjord and Tait Bjerg Members; Clemmensen et al., 1998; Sulej et al., 2014; Guarnieri et al., 2017).
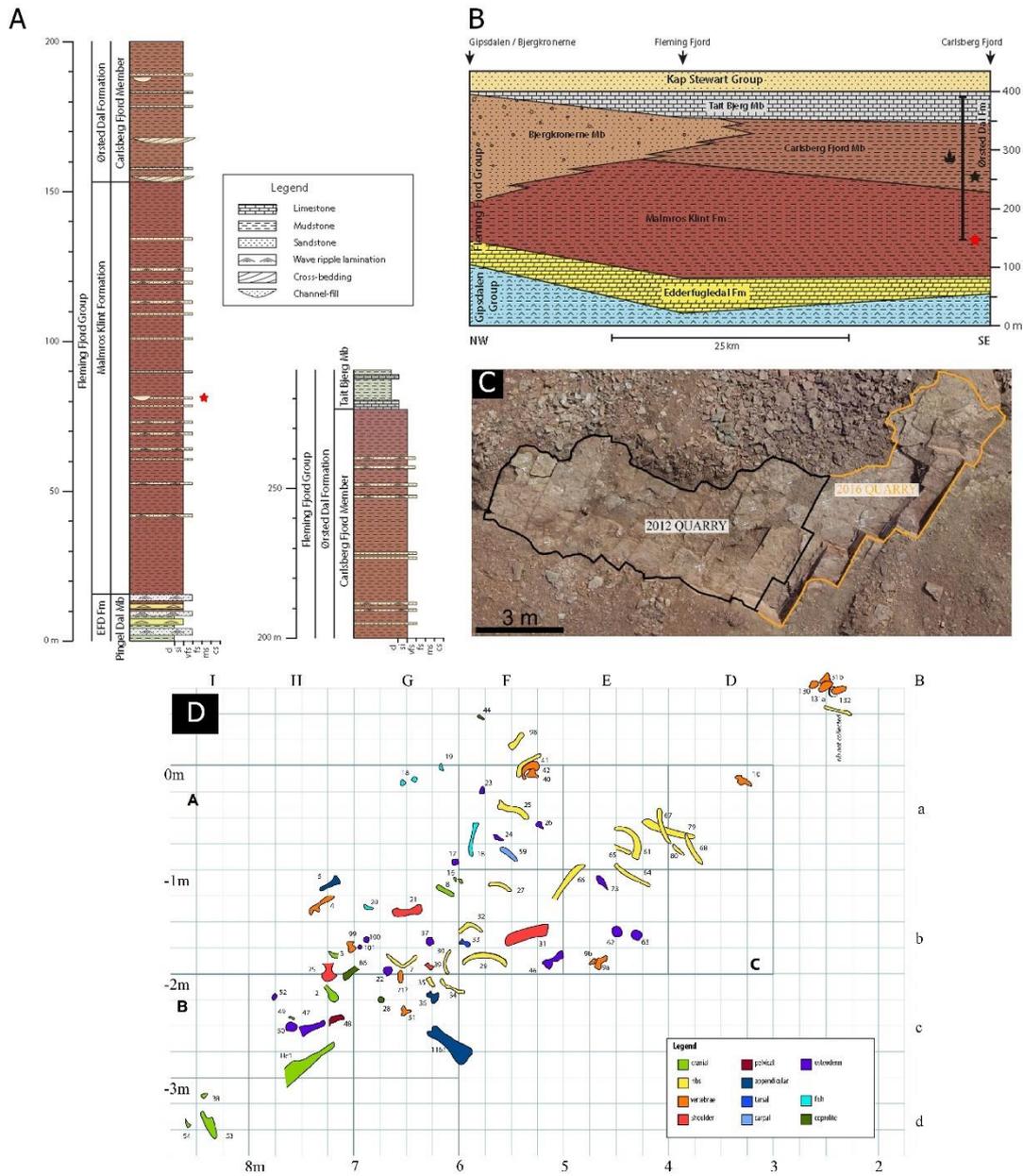
Figure 2. A. Malmros Klint Formation stratigraphy section; B. Cross-section of the lithostratigraphical units in Fleming Fjord Group; C. Map of "Mateus Quarry" at Lepidopteris elv, Malmros Klint; D. Phytosaur Site, digital field map. The red star marks where the phytosaur remains were found in A and B. Figures A-B modified from Clemmensen et al. (2020), and C from Marzola et al. (2017a)

Fleming Fjord Group is rich in vertebrate fossils, such as testudinates, amphibians, lung fish, stem-mammals, pterosaurs and dinosaurs, and other archosaurs (Clemmensen et al., 2015). This fauna shows an European biogeographic affinity (Clemmensen et al., 1998; Sulej et al., 2014; Clemmensen et al., 2015; Marzola et al., 2017b), with the first phytosaur remains found in Malmros Klint Formation in 2012 and 2016 (Clemmensen et al., 2015; Marzola et al., 2017a).

Malmros Klint is a formation of high cliffs of monotonous brownish to red-bed units of mudstones and fine-grained sandstones (Clemmensen et al., 2020). The Formation is comprised of a sedimentary cyclicity, and divided into a lower sandstone-siltstone rich unit,

an upper claystone-rich unit, and topped by a dolomitic paleosol (Clemmensen et al., 1998; Clemmensen et al., 2015).

The Malmros Klint Formation paleoenvironment at the end of the Triassic (Late Norian-Early Rhaetian; Clemmensen et al., 2015) was interpreted as a shallow fresh-water playa-lake with low energy movement as the ripples and horizontal lamination are the most common structure found (Clemmensen, 1979; Clemmensen et al., 1998, Clemmensen et al., 2015). The appearance of mud-cracks suggests the lake would have suffered aerial exposure and, intense desiccation even in humid climatic phases (Clemmensen, 1979; Clemmensen et al., 1998).

This interpretation matches with the Jameson Land Basin one, which was more influenced by seasonal changes and where the lake could have been entirely dry in arid seasons (Clemmensen et al., 1998).

The "Phytosaur Bone Bed" (Fig.2), from where the phytosaur remains were collected, is located in Mateus Quarry, at Lepidopteris Elv locality, in the middle of Malmros Klint Formation (Late Norian, ≃211-210 Ma; Mateus et al., 2014b; Clemmensen et al., 2015).

OBJECTIVES

The objectives of this Master Thesis were focused on describing the taxonomy of the Greenland phytosaur specimens and exploring its implications.

MATERIAL AND METHODS

This Master Thesis is focused into the material collected during the expeditions to Malmros Klint Formation from 2012 and 2016 (Table 1). The material collected is related to, at least, four individuals of different ontogenetic stages with no major intraspecific variation to referred them as different species of phytosaurs. All material is part of the Natural History Museum of Denmark (NHMD) collections. During the study, part of the material was hosted by the Museu da Lourinhã (Portugal) and the other part by the GeoCenter MønsKlint (Denmark). Most of the material in Portugal was prepared during Marzola PhD thesis (2019), but some material required more preparation to allow more detailed description.

Some material was prepared in Museu da Lourinhã by me (specimen NHMD-NOID, a partial radius), and the volunteers (specimens NHMD-6E13-92, possible lacrimal; and NHMD-6E14, sacral vertebrae). To remove the sediment, we used the air scribes HW10 and HW322, and 50% Paraloid B72 in acetone to glue the broken parts. For the specimens NHMD-6E13-92 and NHMD-NOID, when half the preparation was done, they were covered in polyethylene glycol (4000 molecular weight) to protect that part while preparing the other half. The polyethylene glycol coverage was easily removed with hot water and brushes once the preparation was done.

Photographs were taken using a Canon EOS 350 DIGITAL DS126071, and a DinoLite AM411T for the serration counting in the teeth.

For the phylogeny, TnT version 1.5 (Goloboff & Catalano, 2016) was used. Following the data matrix from Jones & Butler (2018), in which they work with operational taxonomic units (OTUs) to facilitate the comparisons between known species and specimens of undetermined taxa.

Here, I used those 43 OTUs plus the Greenland's phytosaur, and the 94 characters related to the cranial region, plus an additional character (character 95) about the degree of heterodonty, obtained from Hungerbühler (2002; character 5: 0 – homodont, 1 – bipartite upper dentition, 2 – tripartite upper dentition).

The "degree of heterodonty" was added into the matrix of Jones & Butler (2018) because of the good number of teeth found. Only eleven species (*Euparkeria capensis* Broom, 1913; *Ebrachosuchus neukami* Kuhn, 1936; *Nicrosaurus kapffi* Fraas, 1866; *N. meyeri* Hungerbühler & Hunt, 2000; *Machaeroprosopus pristinus* Mehl & Branson, 1928; *M. buceros* Cope, 1881; *M. mccauleyi* Ballew, 1989; *Redondasaurus gregorii* Hunt & Lucas, 1993; *R. bermani* Hunt & Lucas, 1993; *Mystriosuchus planirostris* von Meyer, 1863; and *M. westpali* Hungerbühler & Hunt, 2000) appeared in Hungerbühler (2002) which are shared with Jones & Butler (2018), so another six species (*Angistorhinus grandis* Mehl, 1913; *A. talainti* Dutuit, 1977; *Leptosuchus crosbiensis* Case, 1922; *Parasuchus hislopi* Lydekker, 1885; *Paleorhinus parvus* Mehl, 1928; *Rutiodon carolinensis* Emmons, 1856) with the "degree of heterodonty" were collected from Hungerbühler (2000) to better complete the matrix.

Table 1. List of bone and teeth of *Mystriosuchus* from Greenland. All field numbers are under NHMD (Natural History Museum of Denmark).

Field number	Bone
Gb8	Left premaxilla
126a	Right premaxilla+maxilla
Kc121	Right jugal
Hc87	Left jugal
Jc72	Left postorbital
Hc47b	Right quadrate
6E12-84	Left ectopterygoid?
6,00E+14	Right quadratojugal?
6C4-36	?
6F12	?
6E13-92	Left lacrimal?
6D2/3 - FCT-UNL	Mandible
Hc1	Mandible (dentary)
Hc1	Mandible (posterior)
Gb95c	Angular
Jd53	Angular
6G12	Premaxilla (snout)
6F12	Premaxilla (snout)
A011	Premaxilla (snout)
NO ID	Premaxilla (anterior)
6E12-59	Premaxilla (anterior)
6E12.	Premaxilla (anterior)
6C14	Premaxilla (anterior)
6E11.	Premaxilla (anterior)

A000	Premaxilla (anterior)?
A001	Premaxilla (anterior)?
A002	Premaxilla (anterior)?
A004	Premaxilla (anterior)
A009	Premaxilla (anterior)
A010	Premaxilla (anterior)
Gb93a	Premaxilla (anterior)
Hc2	Premaxilla (anterior)
Hc49	Premaxilla (anterior)
Hc78	Premaxilla (anterior)
Jd55	Premaxilla (anterior)?
6E12-74	Premaxilla (medium)
6F13-104	Premaxilla (posterior)
6F13-107	Premaxilla (posterior)
6E13.	Premaxilla (posterior)
6F12	Premaxilla (posterior)
Hc111	Premaxilla (posterior)
6E14.	Maxilla (anterior)
6E14.	Maxilla (anterior)
6F12	Maxilla (anterior)
6E13.	Maxilla (anterior)
A003	Maxilla (anterior)
A005	Maxilla (anterior)

A006	Maxilla (anterior)
A008	Maxilla (anterior)
NO ID	Maxilla (anterior)
6G12	Maxilla (posterior)
6E12.	Maxilla (posterior)
6E9-3	Maxilla (posterior)
NO ID	Maxilla (posterior)
Fb88c	Maxilla (posterior)
Gb16	Maxilla (posterior)
Hb3a	Maxilla (posterior)
Hc3	Maxilla (posterior)
Jd38	Maxilla (posterior)
Jd54	Maxilla (posterior)
A012	-
Hb3	-
Hc1 3rd tooth	Mandible
Hc1 4th tooth	Mandible
Hc1 11th tooth	Mandible
Hc1 36th tooth	Mandible
Hc112	8th cervical
Da10	Dorsal vertebra
6E+F12	Dorsal vertebra
Eb9a	Dorsal spine
Eb9b	Dorsal centrum
6E14.	Sacral
Gc51	3rd caudal
Fa42	4th caudal

130	6th caudal	142	Partial	Fb33	Phalanx
131	7th caudal	Ja117	Partial	6E13-54	Phalanx
132	8th caudal	Gc34	Partial	6F13	Phalanx
6E11-44	10th caudal	Ea67	Partial	Fa59	Phalanx
Hb4	Posterior caudal	58	Partial	Fa40	Phalanx
NOID	Posterior-last caudal	Gb95a	Partial	135	Phalanx
Kb123	Cervical rib	128	Partial	Ca13	Phalanx
Fa98	Cervical rib	Hc75c	Partial	Kc108	Morphotype 1
Kd106	Dorsal rib	Ea65	Partial	Gb95e	Morphotype 1
129	Dorsal rib	138	Partial	6E12.	Morphotype 1
Kb125	Dorsal rib	Jd65	Partial	NOID	Morphotype 1
Ea83	Dorsal rib	140	Partial	Fa26	Morphotype 1
Fb29a	Dorsal rib	137	Partial	Fa24	Morphotype 1
Gb95a	Dorsal rib	126	Partial	Jc74	Morphotype 1
Ea79	Dorsal rib	Kc122e	Partial	Fa81	Morphotype 1
Ea84	Dorsal rib	NOID	Interclavicle	Gb71	Morphotype 1
Eb66	Dorsal rib	Fa82	Interclavicle	Jd56	Morphotype 2
Hc75b	Dorsal rib	Fb31	Interclavicle	Fb45	Morphotype 2
Ea96	Dorsal rib	Gb21	Clavicle?	Hb103	Morphotype 2
Hb115	Gastralia	Hc75a	Right coracoid	Jc70	Morphotype 2
Gb30	Gastralia	136	Left coracoid	Da90	Morphotype 3
127	Gastralia	Gb39	"Baby" scapula	Eb73	Morphotype 3
Kc122d	Gastralia	Fa85	Left humerus	Ha118	Morphotype 3
Gb7	Gastralia	Ga116	Left humerus	NOID	Morphotype 4
Fb32	Gastralia	Gc6	Right humerus	6E12-81	Morphotype 4
Da68	Gastralia	6E13-54	Right ulna	6E13-70	Morphotype 4
Gc35	Gastralia	Jd57	Right ulna		
Kb129	Gastralia	113	Right radius		
Ea61	Gastralia	134	Left femur		
141	Partial	Hc74a	Left tibia		
Hc75d	Partial	6E12-54	Left fibula		
		Gc36	Phalanx		

SYSTEMATICS PALEONTOLOGY

PHYTOSAURIA Jaeger, 1828

Definition: *Rutiodon carolinensis* and all taxa more closely related to it than *Aetosaurus ferratus, Rauisuchus tiradentes, Prestosuchus chiniquensis, Ornithosuchus woodwardi* or *Crocodylus niloticus* (Jones & Butler, 2018)

Diagnosis (list of synapomorphies based on Ezcurra, 2016: p.300): Strongly dorsoventrally compressed skull with mainly dorsally facing antorbital fenestrae and orbits; dorsal orbital margin of the frontal elevated above skull table; external naris non-terminal, considerably posteriorly displaced, but posterior rim of the naris well anterior to the anterior border of the orbit; external naris dorsally directed; orbit without or with incipient elevated rim; antorbital length versus total length of the

skull = 0.70–0.76; snout transversely broader than or as broad as dorsoventrally tall at the level of the anterior border of the orbit; 10 or more tooth positions in the premaxilla; maxilla extends anterior to the nasal; alveolar margin of the maxilla sigmoid, anteriorly concave and posteriorly convex, in lateral view; posterior extension of the maxilla level with or anterior to anterior orbital border in mature individuals; number of maxillary tooth positions 15–22; lower temporal bar with a concave ventral margin in lateral view, though nowhere dorsal to tooth row; length of the posterior process of the jugal versus the height of its base = 4.07–5.37; posterior process of the jugal lies ventral to the anterior process of the quadratojugal; ventral process of the postorbital ends close to or at the ventral border of the orbit; neomorphic bone as a separate ossification anterior to nasals and surrounded by the premaxilla on the dorsal surface of the snout; dorsal head of the quadrate has a sutural contact with the paroccipital process of the opisthotic; palatine with a single anterior process forming the posterior border of the choana; foramina for the entrance of the cerebral branches of the internal carotid artery leading to the pituitary fossa posterolaterally placed on the parabasisphenoid; mandibular symphysis present along one-third of the lower jaw; tooth-bearing portion of the dentary mostly straight; dorsal margin of the anterior portion of the dentary dorsally expanded compared to the dorsal margin of the posterior portion; posteriormost dentary teeth placed on the posterior half of lower jaw; distal edge of the posterior maxillary tooth crowns with a distinct different morphology from those of the anterior tooth crowns, with the posterior edge usually convex in labial view; scapula with an acromion process in about the same plane as the ventral edge of the scapula; coracoid with a distinctly hooked anterior border in lateral view; coracoid without or small biceps process on the lateral surface; humerus with a strongly developed entepicondyle in mature individuals; pubic shaft rod-like and straight in lateral view; and osteoderms with sculpture on their external surface.

PARASUCHIDAE Lydekker, 1885

Definition: *Wannia scurriensis, Parasuchus hislopi, Mystriosuchus planirostris* and all descendants of their most recent common ancestor. (Kammerer et al, 2015)
Diagnosis (list of synapomorphies based on Jones & Butler, 2018: supplementary material, node 2, p.85): Narial openings B directed dorsally; antorbital fossa present but reduced lacrimal, jugal and maxillary fossae in contact dorsally but not ventrally.

MYSTRIOSUCHINAE von Huene, 1915

Definition: *Mystriosuchus planirostris, Angistorhinus grandis* and all descendants of their most recent common ancestor. (Kammerer et al, 2015)
Diagnosis (list of synapomorphies based on Jones & Butler, 2018: supplementary material, node 7, p.86): Suture between maxilla, premaxilla and nasal dorsally convex lobe; position of nares non-terminal, posterior rim of nares behind anterior rim of antorbital fenestra; posterior border of the nares and anterior border of orbits dip down into a concavity in interorbital nasal area lateral view; small elongate depression posterior rim of postorbital may create a small flange behind orbit; lateral ridge from postorbital/squamosal bar absent; length of posterior process of squamosal in relation to postorbital length 3.60 to 4.99; anterior border of parabasisphenoid contribution to basitubera, basitubera connected tubera form a sharp ridge along their anterior border; length of interpterygoid vacuity tiny oval indentation at posterior rim of conjoined pterygoids; anterior extent of the palatine, tip extends forward beyond the anterior rim of choana; septomaxillae separate

distinctly anterior of the anterior narial border; shape of antorbital fenestra approximately triangular.

LEPTOSUCHOMORPHA Stocker, 2010

Definition: *Leptosuchus studeri, Machaeroprosopus pristinus* and all descendants of their most recent common ancestor (Jones & Butler, 2018).

Diagnosis (list of synapomorphies based on Jones & Butler, 2018: supplementary material, node 13, p.87): Transverse width of the rostrum between the antorbital fenestrae in dorsal view greater than or equal to 1.60; narial outlets absent; length of antorbital fenestra greater than or equal to 1.9 times naris length; dorsal edge of squamosal expanded medially; medial extent of squamosal enters base of supraoccipital shelf wedged between parietal and supraoccipital; orientation of supratemporal fenestra partially depressed parietal process of squamosal below level of skull roof; visibility of supratemporal fenestrae in dorsal view, mostly visible, posterolateral portions of supratemporal fenestrae covered in dorsal view; dorsal edge of parietal/squamosal bar gently sloping; proximal section of postorbital descending process where posterior border of orbit meets skull roof, posterior border of orbit remains thin until it reaches skull roof.

MYSTRIOSUCHINI von Huene, 1915

Definition: *Mystriosuchus planirostris, Machaeroprosopus jablonskiae, Machaeroprosopus buceros* and all descendants of their most recent common ancestor (Jones & Butler, 2018)

Diagnosis (list of synapomorphies based on Jones & Butler, 2018: supplementary material, node 24, p.89): preinfratemporal shelf present; length of free postorbital/squamosal bar less than 2.90; width of squamosal lessor equal to 3.80; palatal ridge prominent, sharp ventrally to ventromedially directed crest; relative robusticity of the jugal 7.30-8.40, or greater than 8.40.

Mystriosuchus Fraas, 1896.

Diagnosis (list of synapomorphies based on Jones & Butler, 2018: supplementary material, node 26, p.89): interpremaxillary fossa present, narrow slit; interorbital nasal area cross section dorsally curved in cross section.

Mystriosuchus sp.

Autapomorphic characters: shape of retroarticular process in lateral view distally rounded or blunt; degree of heterodonty tripartite upper dentition.

Main material: NHMD-Hc1 (nearly complete left mandible) in display at GeoCenter Monsklint, Denmark.

Referred material: teeth, cranial and post-cranial bones from at least four individuals of different ontogenetical ages, all from the same site. See complete list in "material and methods" section.

Horizon, locality and age

In Mateus Quarry (N 71º 15.584' W 22º 31.798', 171m asl ±3m), at Lepidopteris Elv locality, Jameson Land Basin, East Greenland. In the middle of Malmros Klint Formation, Fleming Fjord Group (82m, Clemmensen et al., 2020). Late Norian (~211-210 Ma), Late Triassic.

DESCRIPTION

1. Skull and mandible

A total of 14 bones referred to the skull and mandible (Fig.3) have been collected. All the measurements in Table 2 are taken in millimeters.
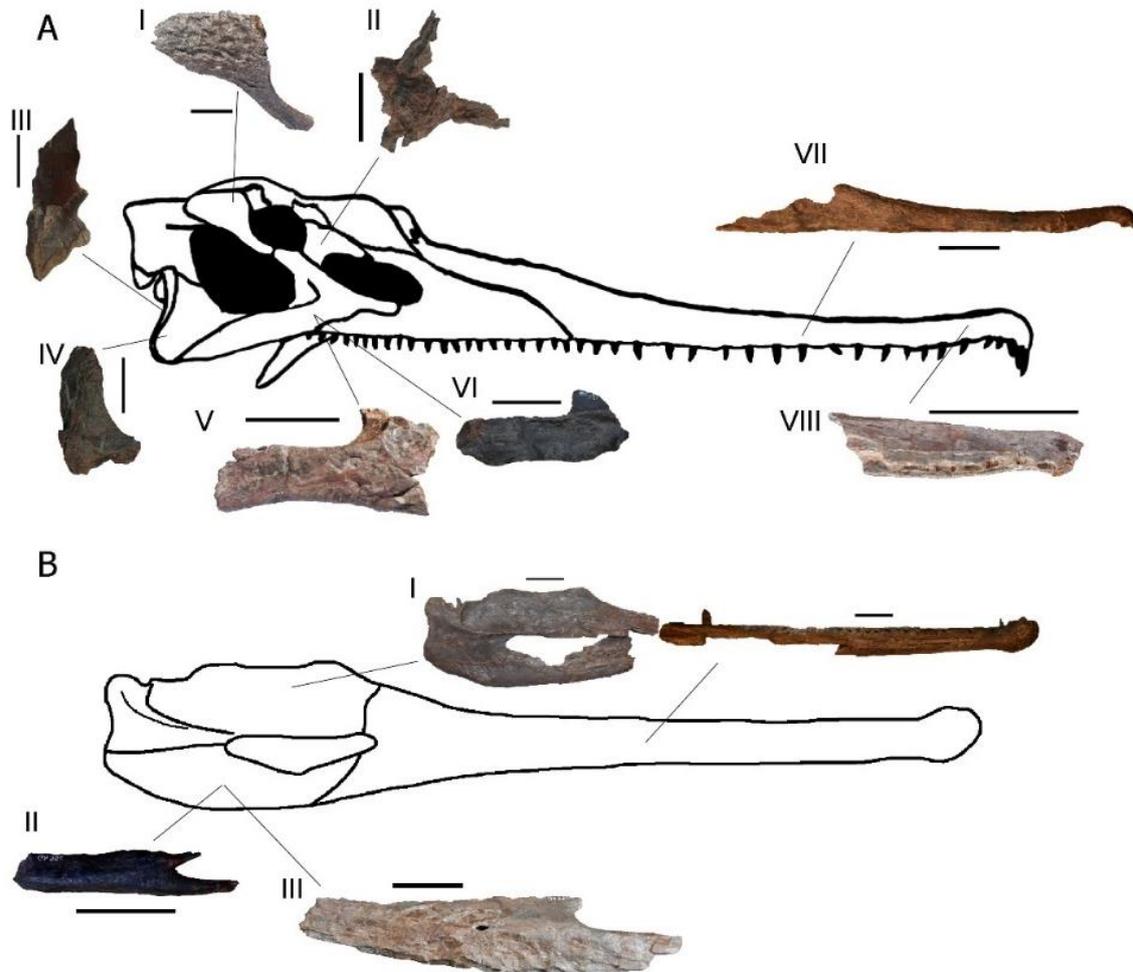
Figure 3. Relative position of the best preserved bones over the reconstruction of A. the skull, and B, the mandible of *Mystriosuchus* sp. from Greenland (modified from the skull of *M.planirostris* of Hungerbühler, 2002). A. I. Postorbital NHMD-Jc72 (mirror image); II. Lacrimal NHMD-6E13-92 (mirror image); III. Quadrate NHMD-Hc47b; IV. Quadratojugal NHMD-6E14; V. Jugal NHMD-Hc87; VI. Jugal NHMD-Kc121 (mirror image); VII. Partial rostrum NHMD-126a; VIII. Premaxilla NHMD-Gb8 (mirror image); B. I. Almost complete mandible NHMD-Hc1 (mirror image); II. Angular NHMD-Gb95c (mirror image); III. Angular NHMD-Jd53 (mirror image). Scales = 4cm. The schematic skull and mandible are not at scale.

Table 2. Measurements of *Mystriosuchus* sp., skull bones.

Field number	Bone	Length (mm)	Anterior Width (mm)	Posterior Width (mm)	Anterior Height (mm)	Posterior Height (mm)
NHMD-Gb8	Left premaxilla	67.1	8.3	7.6	12.6	15.4
NHMD-126a	Right premaxilla +maxilla	275	9.1	16.5	13	30.9
NHMD-Kc121	Right jugal	98.7	-	-	20.7	43.2
NHMD-Hc87	Left jugal	95.8	9.6	3	26.8	46.6

10

NHMD-6E12-84	Left ectopterygoid	100.2	25.4	48	-	-
NHMD-6E13-92	Left lacrimal	84.5	-	-	11.4	52.3
NHMD-Jc72	Left postorbital	176.3	20	25.3	19.8	64.4
NHMD-6E14	Right quadratojugal	56.5	13.7	27.2	26.8	93.1
NHMD-Hc47b	Right quadrate	123.8	34	52	-	-
NHMD-6D2/3 - FCT-UNL	Mandible	287.4	-	-	10.1	38.4
NHMD-Hc1	Mandible (dentary)	397.6	24.6	18.6	35.5	31
NHMD-Hc1	Mandible (posterior)	250.6	21.8	54.2	65.8	105.6
NHMD-Gb95c	Angular	90	17.7	15.4	14.5	18.2
NHMD-Jd53	Angular	214.5	13.3	14.4	24.6	43.6

NHMD-Gb8 anterior part of the left premaxilla (Fig.4A) has been preserved as a slender bone. There are eight alveoli, that vary from subcircular to elliptic from most anterior to posterior ones. Three of them can be seen in the terminal rosette region that in ventral and lateral views. The ventrolateral edges appear scalloped in lateral view. In ventral and dorsal view, the fossil has a rectangular shape, constricted at the end of the terminal rosette. In the anterior part, the terminal rosette is bowed ventrally, allowing to clearly distinguish the limit with the rest of the rostrum.

NHMD-126a (Fig.4B) is the anterior half of the rostrum, displayed by the right premaxilla and partial right maxilla. Both bones are fused and the limits between them are difficult to distinguish.
NHMD-126a is a long slender bone, thicker posteriorly than anteriorly, with a total of 36 teeth alveoli. The terminal rosette of the premaxilla is constricted between the fourth and fifth teeth, and with the anteriormost part ventrally turned. The partial maxilla is thicker ventrally than dorsally. There is a semi-circular shape at middle shaft of its dorsal surface that would form part of the anteroventral border of the antorbital fenestra. Posteriorly, the maxilla has a triangular shape that would continue and contact the jugal.
The labial surface of the maxilla is slightly hollowed, in contrast with the smooth and straight labial surface of the premaxilla. Lingually, the interpremaxillary fossa is preserved as a smoother and concave region that extends from the fifth tooth until the posterior and dorsal borders of the maxilla.

From the two jugals NHMD-Hc87 and NHMD-Kc121 (right and left respectively; Figs.5A-B) the main body is preserved, with both anterior and posterior processes partly broken. They have a rectangular shape with a weak concave curvature in their ventral edge (less marked in NHMD-Kc121, due to that part is broken). Part of the anterior ascending process is also preserved, which would contact dorsally with the ventral border of the lacrimal and anteriorly with the posterior maxilla. The contact with the maxilla can be found in NHMD-Hc87 as a scar in its anteroventral region in the labial surface. Its posterior and dorsal edges make a concave curve, being part of the anteroventral region of the laterotemporal fenestra. In NHMD-Hc87, the anterior edge has a smooth anterior concave surface similar to the posterodorsal edges.
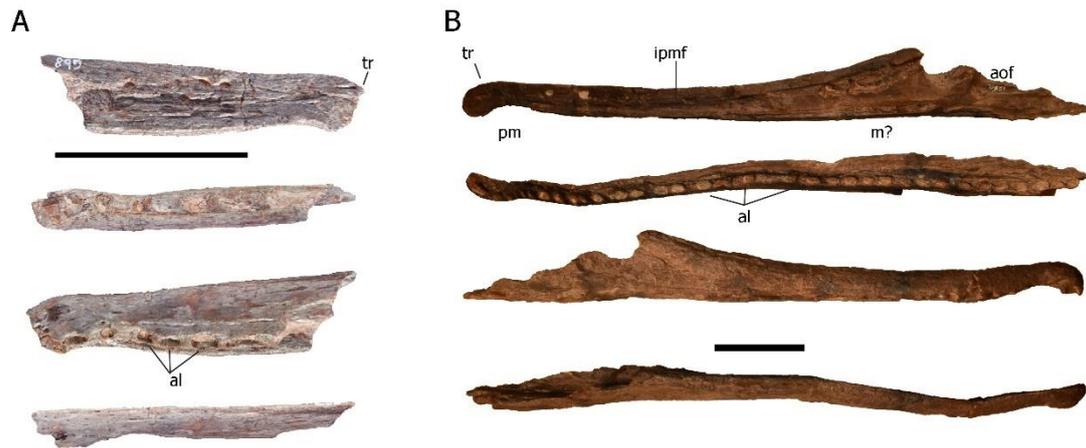
Figure 4. Rostrum material of *Mystriosuchus* sp. from Greenland. A. Left premaxilla NHMD-Gb8; B. Right partial rostrum NHMD-126. Scales = 4 cm. From top to bottom the views are medial, ventral, lateral, and dorsal. Abbreviations: al – alveolus, aof – anterior orbital fenestra, ipmf. – interpremaxillay fossa, m? – maxilla?, pm – premaxilla, tr – terminal rosette.

Figure 5. Jugals of *Mystriosuchus* sp. from Greenland. A. Right jugal NHMD-Hc87 (top views: dorsal, ventral; bottom views: labial, lingual, posterior); B. Left jugal NHMD-Kc121 (top view: labial; bottom view: lingual). Scales = 4 cm. Abbreviations: aof – anterior orbital fenestra, ltf – laterotemporal fenestra.

NHMD-6E12-84 (Fig.6A) is a flat broken bone. Its posterior region is wider than the anterior. Its medial edge is slightly medially bowed. Ventrally, the surface is rugose, flat and with no ornamentation. Dorsally, the lateral edge has a convex surface that turns into a flatter surface. In the medial dorsal surface, there is a slight depression, posteromedially expanded, giving a triangular shape in the posterior end.

This bone is here identified as a partial posterior left ectopterygoid. The medial surface depression is identified as a contact surface with other bone, in this case with the pterygoid. In this case then, the lateral edge would be the posterolateral edge of the left choana.

NHMD-6E13-92 (Fig.6B) pitting ornamentation in its central dorsal area, in contrast with the ventral area, suggests it is a broken bone from the dorsal region of the skull. The bone has a sub-triangular shape, with three processes. It exhibits a long thin rectangular bone attached in its medial edge, but it is a different bone, as it overlaps the main bone and does not connect with it.

The anterior process, the longest and thinnest, has a concave lateral surface in its ventral region. The posterior process is thicker in its medial surface and its ventral region displays also a concave lateral surface. The middle process, shorter, has soft concave surfaces in both

anterior and posterior edges. The continuity between the lateral surfaces of anterior and posterior processes indicates that they are the edges of two different fenestrae.

This bone is here classified as a partial left lacrimal. The fenestra between the anterior lateral edge and the anterior middle processes is the posterior region of the antorbital fenestra, while the posterior fenestra is the anterior region of the orbit.

The left postorbital NHMD-Jc72 (Fig.6C) preserves the descending process that contacts with the lacrimal dorsally. It forms part of the posterior border of the orbit, and the anterior border of the laterotemporal fenestra. The descending process is slender and expands anteroventrally, with a weak sigmoid curvature. The dorsal surface is ornamented with pitting structures, while the ventral surface is smooth.
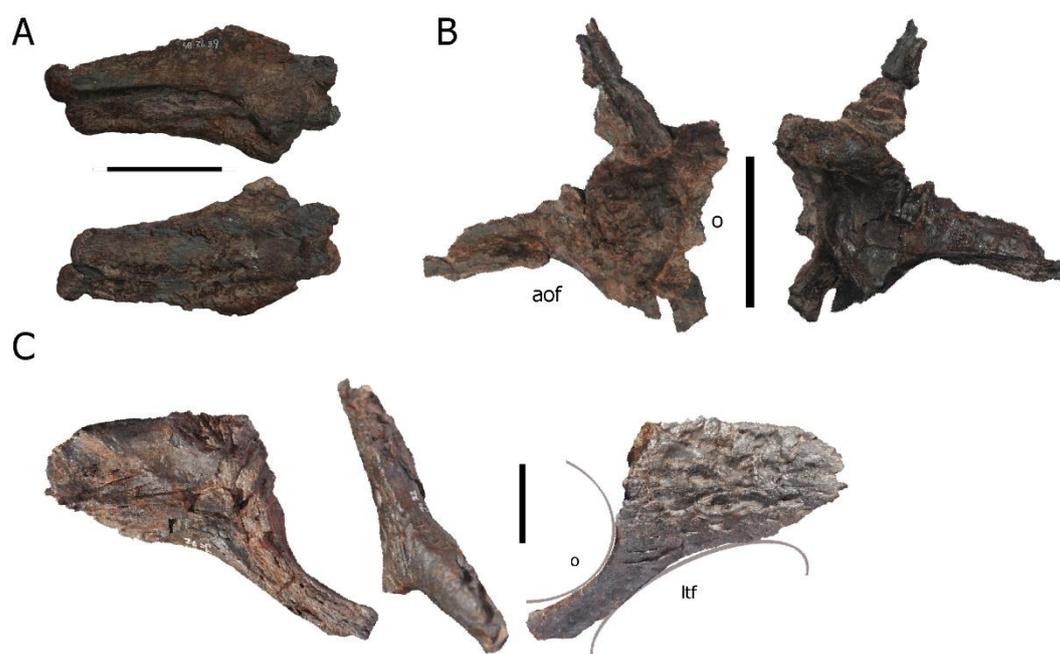
Figure 6. Bones of the palate and skull roof region of *Mystriosuchus* sp. from Greenland. A. Left ectopterygoid NHMD-6E12-84; B. Left lacrimal NHMD-6E13-92; C. Left postorbital NHMD-Jc72. Scales = 4cm. Abbreviations: aof – anterior orbital fenestra, o – orbit, stf – laterotemporal fenestra.

NHMD-6E14 (Fig.7A) is a broken skull bone. The bone is mediolaterally compressed, posteriorly thickened, and anteriorly bowed. The dorsal lateral edge displays a rough surface, interpreted as an articular facet. The anterior surface is faintly anteriorly bent, resembling to a fenestra edge. The anteroventral process is short and broken. The posterior surface is concave and soft laterally, while is medially rough and with a broken posteroventral process beginning. Although the dorsal region is broken, its medial surface has a concave region, maybe for the insertion of a bone.

This partial bone is identified as the anterior region of the right quadratojugal. The slight curve in its anterior margin can be referred as the posteroventral border of the subtemporal fenestra, making a smooth edge (as seen in Ezcurra et al., 2016). The dorsal margin would connect with the ventral squamosal, following the subtemporal fenestra border. The dorsal region would connect with the quadrate.

The partial left quadrate NHMD-Hc47b (Fig.7B) is preserved most of the medial portion. The ventral surface is softer in anterior that posterior view. In posterior view, the ventral surface

has an articular facet with other bone (the articular). The lateral condyle expanded more laterally, giving a triangular shape, than the medial condyle, more rounded.

The medial surface of the quadrate has a middle bulge dividing the dorsal region, that would contact the pterygoid, from the ventral region, opened to the interior of the mouth region without contacting any bone.
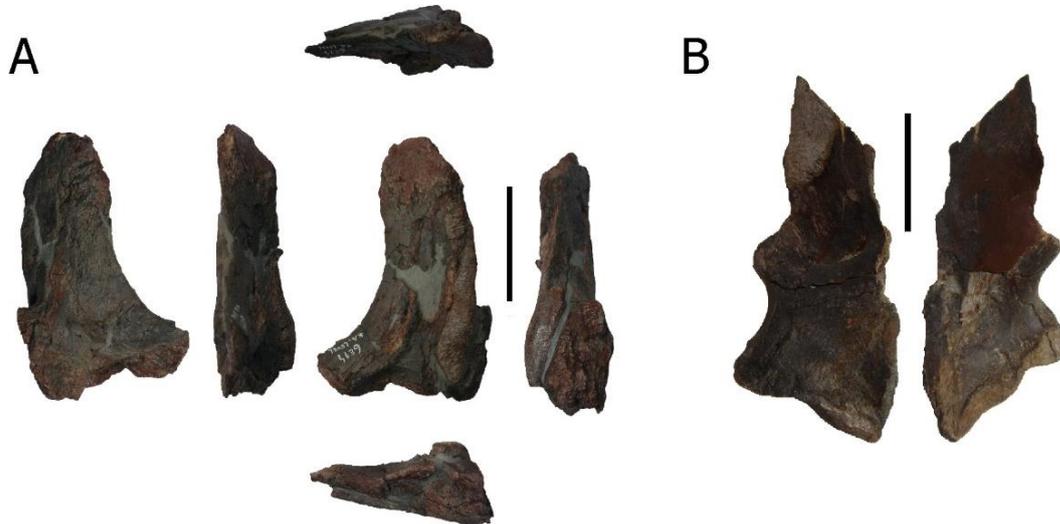
Figure 7. Posterior skull bones of *Mystriosuchus* sp. from Greenland. A. Right quadratojugal NHMD-6E14; B. Left quadrate NHMD-Hc47b. Scales = 4cm.

NHMD-Hc1 (Fig.8) is an almost entire left mandible. It is broken in the posterior dentary, dividing it into the almost entire dentary with a total of 42 alveoli (Fig.8A; and four teeth still attached, see *Teeth section*), and the posterior body (Fig.8B). However, it lacks the splenial, the ventral region between the 21st tooth and the anterior angular. The dentary is a long, straight and robust bone, that displays a faintly sigmoideal shape in dorsal view. The dentary is straight until the 22nd alveoli tooth, where it becomes thicker posterolingually. It has a terminal rosette with four teeth, and a constriction between the fourth and fifth teeth (as in the premaxilla NHMD-126a and NHMD-Gb8). The terminal rosette also displays a pitting pattern in its surface. The lingual surface is smoother than the labial.

The posterior mandible (Fig.7B) is displayed by an incomplete dentary, the surangular, the articular and a partial angular. The dentary preserved the last three alveoli of the tooth row, contacts posterolaterally with the anterior surangular, which makes an anterodorsal concave curve transition. The surangular is a short, rectangular bone that contributes to the posterodorsal border of the external mandibular fenestra. It exhibits two dorsal "condyle-like" expansion: anteriorly near the contact with the dentary, and another posteriorly. The articular expands medially, and remains below the surangular dorsal edge level. The dorsal angular surface forms part of the posteroventral border of the external mandibular fenestra. Medially, the angular has a lined-up circular pitting that starts near the posterior border of the fenestra, which extends posteriorly without reaching the articular. The retroarticular process in the posteroventral edge of the angular has a round shape.
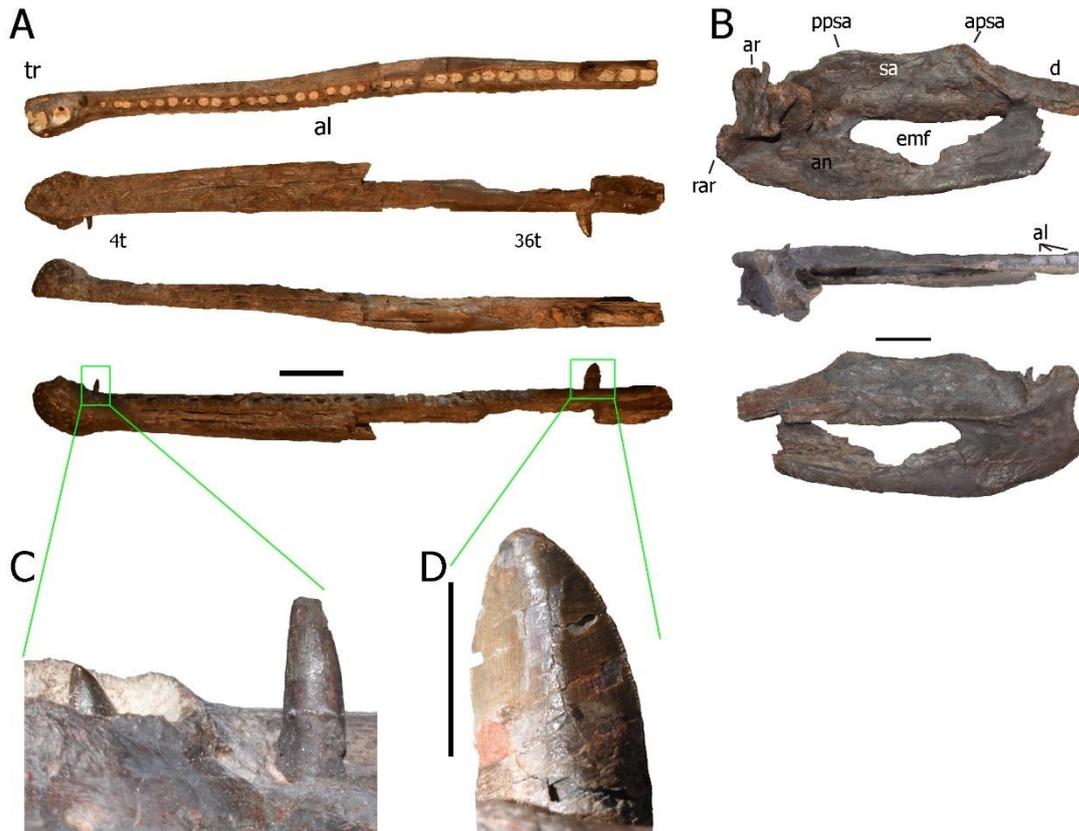
Figure 8. Mandible of *Mystriosuchus* sp. from Greenland. A. Dentary of the mandible NHMD-Hc1 (from top to bottom, the views are dorsal, medial, ventral, and lateral); B. Posterior body of the mandible NHMD-Hc1 (from top to bottom, the views are medial, dorsal, and lateral); C. Closer look to the third and fourth mandibular teeth; D. Closer look to the 36th mandibular teeth. Scales A-B = 4 cm, C-D = 1 cm. Abbreviatures: al – alveolus, an – angular, apsa – anterior projection of the surangular, ar – articular, d – dentary, emf – external mandibular fenestra, ppsa. – posterior projection of the surangular, rar – retroarticular, sa – surangular, tr – terminal rosette, 4t – forth dentary tooth, 36t – 36th dentary tooth.

The partial preserved posterior mandible NHMD-6D2/3 (Fig.9A) is conserved as a thin portion of the posterior dentary, with its last tooth, and the surangular. The posterior surangular edge is eroded, and part of the posterior edge has been removed, only the limits imprint remains.

The angulars NHMD-Jd53 and NHMD-Gb95c (Fig.9B-C) are both broken posterior regions, with the body medially concave. NHMD-Jd53 has the ventral surface also broken, which gives it a convex ventral shape, in contrast with NHMD-Gb95c, that has a straight rectangular shape. The anterior edge has an anteriorly concave surface that forms part of the posterior mandibular fenestra.

15
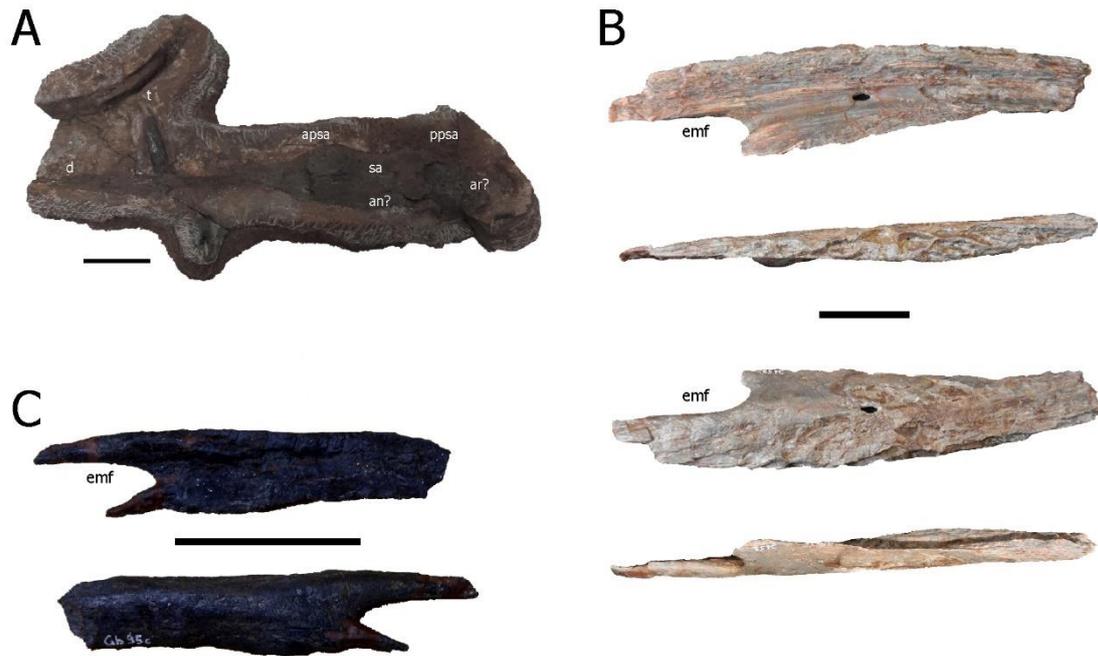
Figure 9. Partial mandible remains of *Mystriosuchus* sp. from Greenland. A. Partial posterior mandible NHMD-6D2/3 in labial view; B. Angular NHMD-Jd53 (from top to bottom, the views are lingual, ventral, labial, and dorsal); C. Angular NHMD-Gb95c (in labial and lingual views). Scales = 4 cm. Abbreviatures: an? – angular?, apsa – anterior projection of the surangular, ar? – articular?, d – dentary, emf – external mandibular fenestra, ppsa – posterior projection of the surangular, sa – surangular, t – teeth.

2. Teeth

A total of 62 isolated teeth were recovered, of which only 50 of them could have been accurately described (Figs.11-13). The measurements (Table 3; Fig.10) were taken following Hungerbühler (2000).

Table 3. Measurements of *Mystriosuchus* sp. teeth. Abbreviations: AL – Apical length, CBL – Length of crown-base, CBW – Width of crown-base, TCH –Tooth crown height, SD – Serration density (number of denticles per millimeter).

Field number	Position	TCH	AL	CBL	CBW	Root	SD
NHMD-6G12	Premaxilla (snout)	27	26	8	-	-	HIDDEN IN MATRIX
NHMD-6F12	Premaxilla (snout)	22	22	7	5	-	0
NHMD-A011	Premaxilla (snout)	30,4	30,2	10,9	8,5	-	?
NHMD-NO ID	Premaxilla (anterior)	24	25	7	-	-	0
NHMD-6E12-59	Premaxilla (anterior)	10	11	4	-	-	0
NHMD-6E12	Premaxilla (anterior)	11	11	5	-	-	0
NHMD-6C14	Premaxilla (anterior)	8	9	5	-	-	0
NHMD-6E11	Premaxilla (anterior)	10	11	4	-	16	0
NHMD-A000	Premaxilla (anterior)?	31,08	30,75	8,6	-	-	0
NHMD-A001	Premaxilla (anterior)?	23,18	22,95	9,58	-	-	0
NHMD-A002	Premaxilla (anterior)?	9,5	9,38	4,65	3,5	-	?
NHMD-A004	Premaxilla (anterior)	-	-	6,4	7	-	0
NHMD-A009	Premaxilla (anterior)	6,5	7,5	3,5	3,2	-	0

NHMD-A010	Premaxilla (anterior)	9,5	9,1	4,6	4,4	-	0
NHMD-Gb93a	Premaxilla (anterior)	38	38,5	11	9,1	-	0
NHMD-Hc2	Premaxilla (anterior)	46,2	45,5	13,4	13,9	-	0
NHMD-Hc49	Premaxilla (anterior)	12,55	12,1	7,05	6,8	-	5
NHMD-Hc78	Premaxilla (anterior)	11,4	12,8	4,47	5	-	0
NHMD-Jd55	Premaxilla (anterior)?	20,3	21,45	7,3	7,7	-	?
NHMD-6E12-74	Premaxilla (media)	29	30	8	-	-	5
NHMD-6F13-104	Premaxilla (posterior)	31	32	9	-	-	3
NHMD-6F13-107	Premaxilla (posterior)	33	34	10	9	-	3,-
NHMD-6E13	Premaxilla (posterior)	21	21	9	6	-	5
NHMD-6F12	Premaxilla (posterior)	24	23	10	-	-	3,5
NHMD-Hc111	Premaxilla (posterior)	27	26,6	10,3	8,5	-	5
NHMD-6E14	Maxilla (anterior)	15	15	8	-	-	4,--5
NHMD-6E14	Maxilla (anterior)	35	36	10	7	-	3-3,5
NHMD-6F12	Maxilla (anterior)	14	14	7	-	-	5
NHMD-6E13	Maxilla (anterior)	-	-	-	-	-	2,5-3
NHMD-A003	Maxilla (anterior)	6	6	6,7	4,8	-	4
NHMD-A005	Maxilla (anterior)	10,9	9,6	6,9	6,8	-	4,5
NHMD-A006	Maxilla (anterior)	15,3	15,4	6,1	4,9	-	4
NHMD-A008	Maxilla (anterior)	13,2	13,7	5,7	3,2	-	?
NHMD-NO ID	Maxilla (anterior)	17	19	10	-	-	4,-
NHMD-6G12	Maxilla (posterior)	19	18	15	-	-	3,5
NHMD-6E12	Maxilla (posterior)	19	20	16	6	-	3?
NHMD-6E9-3	Maxilla (posterior)	11	12	5	-	-	4
NHMD-NO ID	Maxilla (posterior)	12	12	9	-	-	3,2-3,8
NHMD-Fb88c	Maxilla (posterior)	12,2	12,1	7,9	5,1	-	4
NHMD-Gb16	Maxilla (posterior)	9,3	10,1	7	5,5	-	?
NHMD-Hb3a	Maxilla (posterior)	15,23	14,76	11,88	7,2	-	?
NHMD-Hc3	Maxilla (posterior)	17,5	15,2	11,2	8,3	25,45	3,5
NHMD-Jd38	Maxilla (posterior)	12,8	11,5	10,8	6,7	-	?
NHMD-Jd54	Maxilla (posterior)	14,6	13	9,9	8,4	-	4
NHMD-A012	-	-	-	9	8,5	-	?
NHMD-Hb3	-	14,4	13,83	7,5	-	-	?
NHMD-Hc1 3rd tooth	Mandible	4,8	4,3	3,4	4	-	-
NHMD-Hc1 4th tooth	Mandible	10,6	10,2	3,8	4,3	-	-
NHMD-Hc1 11th tooth	Mandible	-	-	-	-	-	-
NHMD-Hc1 36th tooth	Mandible	19	18,2	9,8	7,6	-	5
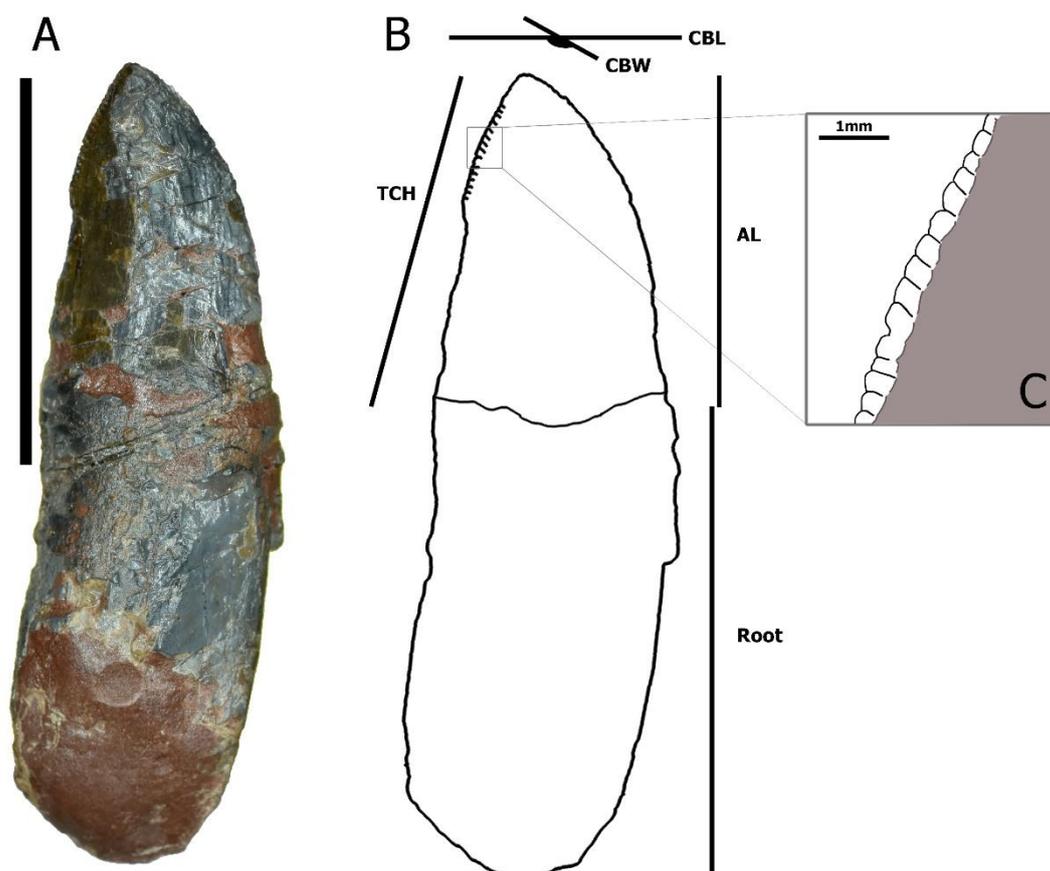
Figure 10. Measurements made on the teeth of *Mystriosuchus* sp. from Greenland. A. Tooth NHMD-Hc3; B. Outline from NHMD-Hc3 to show the measurements; C. Zoom into the serrated area of the tooth. Abbreviations: AL – Apical length, CBL – Length of crown-base, CBW – Width of crown-base, TCH –Tooth crown height. Scale in A = 2 cm.

Tip of the snout set. Teeth NHMD-A011, NHMD-6F12, and NHMD-6G12 (Fig.11A-C respectively) preserved only the crown region, with a conical shape, straight and almost circular in cross-section. There is no serration in NHMD-6F12, while the serration measurements could not be taken in NHMD-A011 and NHMD-6G12. In NHMD-A011 the anterior and posterior borders are partly preserved; and in the case of NHMD-6G12, its posterior surface is still covered by the matrix.

Anterior premaxilla set. Teeth NHMD-6E12-59, NHMD-6E12, NHMD-6C14, NHMD-6E11, NHMD-A002, NHMD-A009, NHMD-Gb93a, NHMD-Hc2, NHMD-Hc49, NHMD-Hc78 (Fig.11D-M respectively), NHMD-A000, NHMD-A001, NHMD-A004, NHMD-A010, NHMD-Jd55, and NHMD-NOID (Fig.13A-F respectively) preserved mostly the crown, while NHMD-6E11 preserved the root as well, and NHMD-Gb93a and NHMD-Hc49 partly preserved the root. These teeth have circular basal cross-section, which become more oval toward the apex (except in NHMD-NOID, for half of the apical crown is broken). The teeth are strongly curved lingually, except NHMD-A000, NHMD-A001, NHMD-A002, NHMD-Jd55, which are straight. However, these teeth are broken, and are considered as part of the anterior premaxilla due to the lack of serration.
A carina is present only in NHMD-6C14 NOID, which suggests that NHMD-6E12-59, NHMD-6E12b and NHMD-6E11 are more anteriorly located in the tooth row.

Posterior premaxilla set. Teeth NHMD-A007, NHMD-Hc111, NHMD-6F13-107, NHMD-6E13, NHMD-6F12 (Fig.11N-R respectively), NHMD-6E12-74 and NHMD-6F13-104 (Fig.13G-H respectively) are complete crowns. They have a circular cross section, which starts to flatten lingually near the base, becoming asymmetrical with a D-shape, in contrast to the anterior premaxilla teeth. The teeth change from lingually curved (NHMD-6E12-74, NHMD-6F13-104, NHMD-6F12) to straight in both lingual and labial faces (NHMD-6F13-107, NHMD-6E13).

Mesial and distal carinae are present and fully serrated on the entire height of the crown. Although some of the carinae are partly broken (NHMD-6E12-74, NHMD-6F13-104, NHMD-6F13-107, NHMD-A007, NHMD-Hc111), it can be assessed they are fully serrated. The serration starts to appear in the tooth row from the apex and goes to base, so if these teeth have both mesial and distal basal carinae serrated, the crowns should be as well. The SD of the portions that were visible was between 3-5 denticles per millimeter.

Anterior maxilla set. Teeth NHMD-A008, NHMD-A003, NHMD-6E14, NHMD-A005, NHMD-6E14, NHMD-NOID (Fig.12A-F respectively), NHMD-6F12, NHMD-6E13, and NHMD-A006 (Fig.13I-K respectively) are broken crowns.

Most of them, in exception of NHMD-A006 and NHMD-A005, have D-shape cross section, flattened and faintly curved lingually. Although the apex is broken in some, all of them have the entire crown carinae fully serrated mesially and distally, with a SD between 3-5 denticles per millimeter. These features are characteristics for anterior maxillary teeth posteriorly located in the tooth row.

In NHMD-A005, NHMD-A006 and NHMD-A008 cases, because of the flanges are broken, only partial marks of denticles remain. Therefore, their position is difficult to enclose in the set.

Posterior maxilla set. Teeth NHMD-Jd54, NHMD-Fb88c, NHMD-Jd38, NHMD-Hc3, NHMD-6G12, NHMD-6E9-3 (Fig.12G-L respectively), NHMD-6E12, NHMD-NOID, NHMD-Gb16, NHMD-Hb3a (Fig.13L-P respectively) preserved the crown, while NHMD-Hc3 preserved the root as well. They are labiolingually flattened, with a D-shape (NHMD-NOID, NHMD-Gb16, NHMD-Hc3, NHMD-Jd38, NHMD-Jd54) or oval-flattened cross-section (NHMD-6G12, NHMD-6E9-3, NHMD-6E12, NHMD-Fb88, NHMD-Hb3a).

The crowns distal and mesial carinae are fully serrated, with a SD between 3-4 denticles per millimeter. The oval-flattened cross-section and the mesial and distal expanded carinae give the appearance of a flat tooth in the case of NHMD-6E9-3, less pronounced in NHMD-6G12 and NHMD-6E12.

The tooth NHMD-NOID has a morphology that resembles more the anterior position in comparison with the other three. However, it is more flattened that anterior maxillary teeth. NHMD-Gb16, NHMD-Hb3a, and NHMD-Jd38 have their flanges broken and badly preserved, so the SD could not be measured.
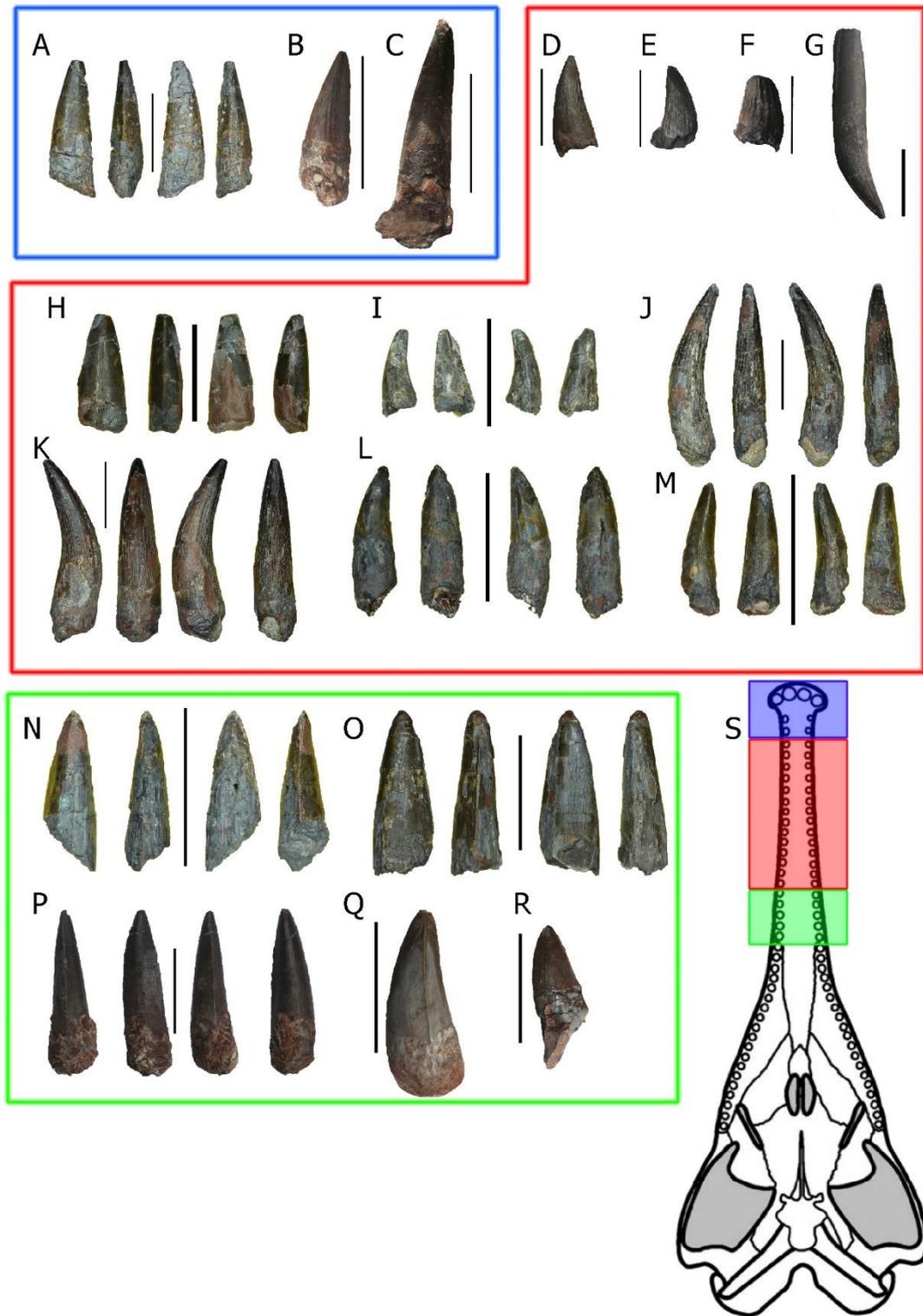
Figure 11. Premaxillary teeth of *Mystriosuchus* sp. from Greenland. A-C. Tip of the snout set teeth. D-M. Anterior premaxillary teeth. N-R. Posterior premaxilla teeth. A. NHMD-A011; B. NHMD-6F12; C. NHMD-6G12; D. NHMD-6E12-59; E. NHMD-6E12; F. NHMD-6C14; G. NHMD-6E11; H. NHMD-A002; I. NHMD-A009; J. NHMD-Gb93a; K. NHMD-Hc2; L. NHMD-Hc49; M. NHMD-Hc78; N. NHMD-A007; O. NHMD-Hc111; P. NHMD-6F13-107: Q. NHMD-6E13; R. NHMD-6F12; S. Relative position of the teeth set in the skull of *Angistorhinus* (modified from Datta et al., 2019b). Scales D-G, I = 1cm; A-C, H, J-R = 2 cm.

Mandibular set. The four mandible teeth found in NHMD-Hc1 (Fig.8A) can be related to their counterparts of the premaxilla and maxilla.

The third and fourth teeth are conical and faintly lingually curved, have rounded cross-section, and the carinae are not serrated. However, the third tooth is smaller than the alveolus, which could mean it is a new tooth to replace the older one. These teeth are the counterparts of the "Tip of the snout" set.

The eleventh tooth has its apex broken. It is, like the third tooth, smaller than the alveolus, which could mean it is a new one. However, it slightly curves lingually, and it is the counterpart of the "anterior premaxilla" set.

The 36th tooth is more robust than the previous. It has a D-shape cross-section, and both carinae are fully serrated, with a SD of 5 denticles per millimeter. This tooth would be the counterpart of the posterior "anterior maxilla" set.
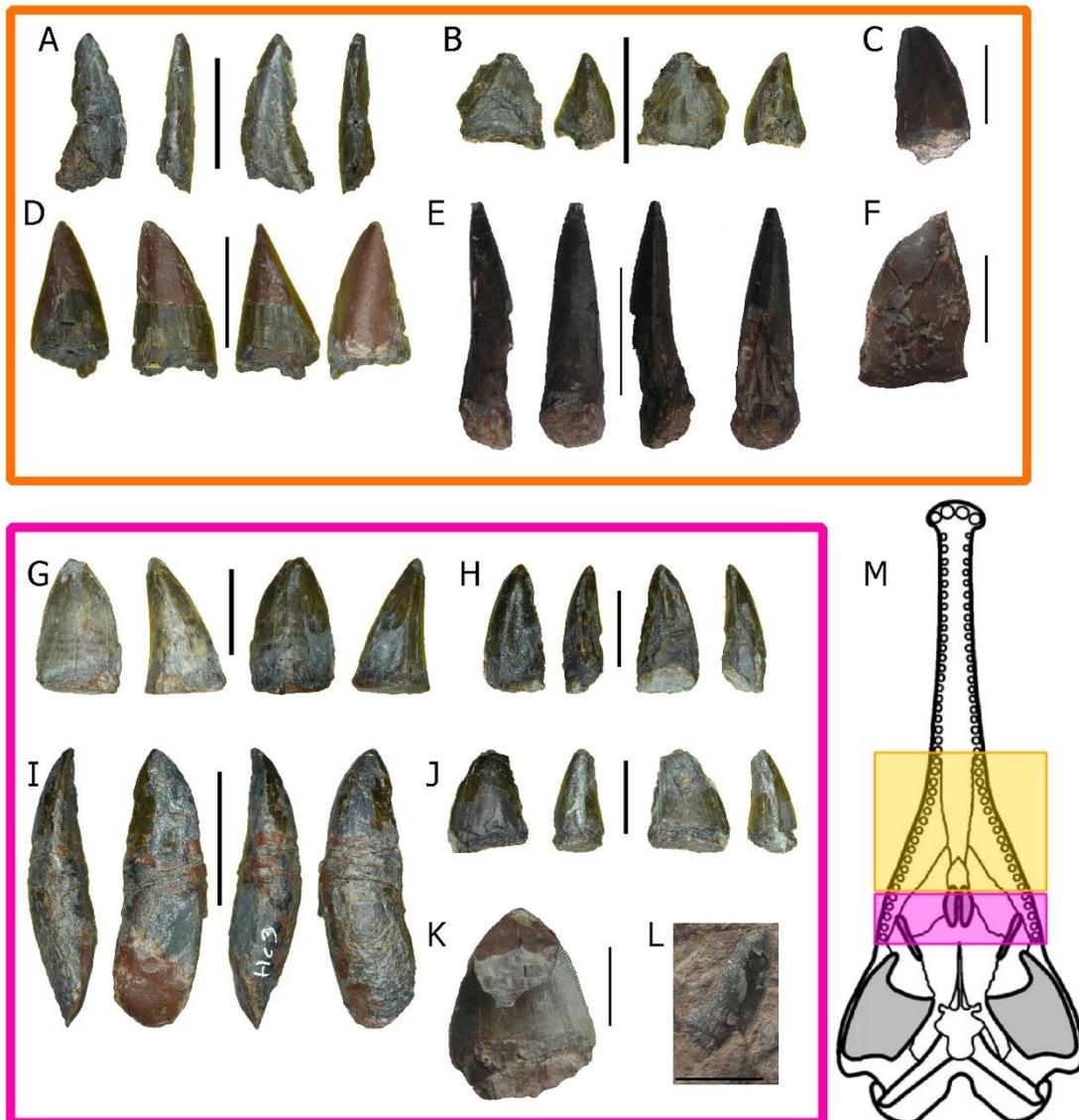
Figure 12. Maxillary teeth of *Mystriosuchus* sp. from Greenland. A-F. Anterior maxillary teeth, G-L. Posterior maxillary teeth. A. NHMD-A008; B. NHMD-A003; C. NHMD-6E14; D. NHMD-A005; E. NHMD-6E14; F. NHMD-NOID; G. NHMD-Jd54; H. NHMD-Fb88c; I. NHMD-Hc3; J. NHMD- Jd38; K. NHMD-6G12; L. NHMD-6E9-3; M. Relative position of the teeth set in the skull of *Angistorhinus* (modified from Datta et al., 2019b). Scales A-D, F-H, J-L = 1cm; E, I = 2cm.
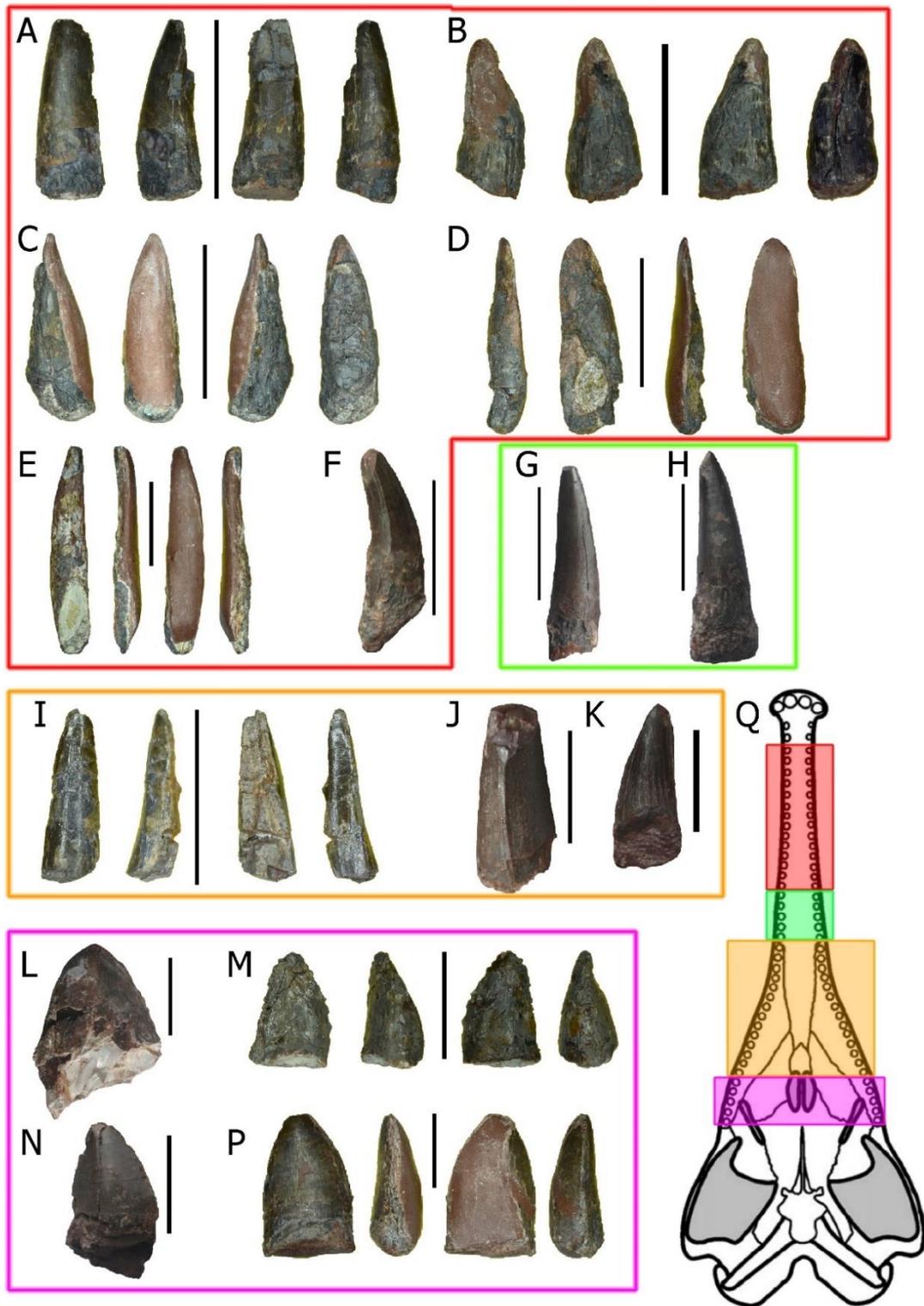
Figure 13. Premaxillary and maxillary teeth of *Mystriosuchus* sp. from Greenland. A-F. Anterior premaxillary teeth, G-H. Posterior premaxillary teeth, I-K. Anterior maxillary teeth, L-P. Posterior maxillary teeth. A. Anterior premaxillary tooth NHMD-A004; B. Anterior premaxillary tooth NHMD-A010; C. Anterior premaxillary tooth NHMD-Jd55; D. Anterior premaxillary tooth NHMD-A001; E. Anterior premaxillary tooth NHMD-A000; F. Anterior premaxillary tooth NHMD-NOID; G. Posterior premaxillary tooth NHMD-6E12-74; H. Posterior premaxillary tooth NHMD-6F13-104; I. Anterior maxillary tooth NHMD-A006; J. Anterior maxillary tooth NHMD-6F12; K. Anterior maxillary tooth NHMD-6E13; L. Posterior maxillary tooth NHMD-6E12; M. Posterior maxillary tooth NHMD-Gb16; N. Posterior maxillary tooth NHMD-NOID; P. Posterior maxillary tooth NHMD-Hb3a; Q. Relative position of the teeth set in the skull of *Angistorhinus* (modified from Datta et al., 2019b). Scales A, C-I = 2 cm: B, J-P = 1 cm.

3. Vertebrae

A total of 14 vertebrae from the cervical, dorsal and caudal region have been collected. All the measurements are in millimeters in the Table 4. All the bones parts are referred in Fig.14.

Table 4. Measurements of *Mystriosuchus* sp. vertebrae.

Field number	Bone	Length	Total height	Heigth (Neural arch)	Heigth (centrum)	Width (Neural arch)	Width (centrum)	Length (diapophysis)
NHMD-Hc112	8th cervical	84.7	101.6	101.6	-	46.8	-	37.9
NHMD-Da10	Dorsal vertebra	53.1	69	69	-	35.9	-	28.3
NHMD-6E+F12	Dorsal vertebra	41.5	63.8	63.8	-	-	-	-
NHMD-Eb9a	Dorsal spine	32.5	71.2	71.2	-	35.1	-	-
NHMD-Eb9b	Dorsal centrum	34.3	-	-	28.3	-	24.4	-
NHMD-6E14	Sacral	43	38.9	38.9	-	-	-	-
NHMD-Gc51	3rd caudal	60.8	129.5	129.5	-	22.3	-	-
NHMD-Fa42	4th caudal	73.7	177.3	131.1	49.6	38.8	51.1	-
NHMD-130	6th caudal	59.8	-	~114.1	42.9	41.7	49.3	40.2
NHMD-131	7th caudal	75.2	177.9	133.4	44.5	33.6	43.4	33.9
NHMD-132	8th caudal	58.8	157.2	112.5	42.1	35.2	40.9	34
NHMD-6E11-44	10th caudal	44.8	155.6	118.4	36.3	25.9	26.9	-
NHMD-Hb4	Posterior caudal	37.3	46.5	24	24.5	21.8	~19.6	-
NHMD-NOID	Posterior-last caudal	16.5	15.2	-	15.2	-	12.2	-
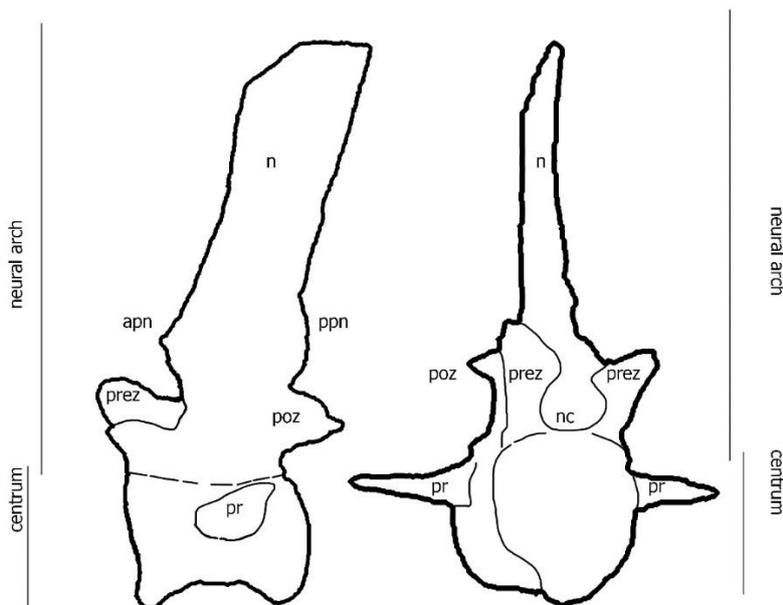
Figure 14. *Mystriosuchus* sp. anterior caudal vertebrae outline with referred morphological characters. Abbreviations: apn – anterior projection of the neural spine, n – neural spine, nc – neural canal, ppn – posterior projection of the neural spine, poz – postzygapophysis, pr – proximal portion of the rib, prez – prezygapophysis.

Cervical

The cervical vertebra NHMD-Hc112 (Fig.15) is an almost complete neural arch, missing the ventral region of the neural canal. The neural spine is 66.2 mm, vertically oriented, transversally compressed. The anterior border of the neural spine is almost vertical, while the posterior border is expanded posteriorly and fused to the postzygapophysis, giving a triangular shape to the neural spine. The prezygapophyses are anteriorly expanded, with the facets dorsally oriented, making an open V outline. The postzygapophyses are oriented ventrally and laterally. The diapohyses appear ventrally to the prezygapophyses, perpendicular to the neural arch, and oriented posteroventrally, getting wider distally. The neural canal has a round shape.

Figure 15. Cervical vertebra NHMD-Hc112 of *Mystriosuchus* sp. from Greenland. Scale = 5cm. Views are dorsal, left, frontal, right, and ventral, respectively.

Dorsal

The dorsal vertebra NHMD-Da10 (Fig.16A) is an almost complete neural arch, except for the ventral region of the neural canal. The neural spine is 30 mm, vertically directed, slightly tilted posteriorly, transversally compressed, with the anterior and posterior edges sub-parallels. The apex of the neural spine is transversally expanded. The base of the neural spine has an anterior bump anteriorly directed. The neural spine suffered a taphonomical alteration, as suggested by the tilt. The prezygapophyses are anteriorly expanded, dorsally oriented making an almost horizontal facet. The postzygapophyses are ventrally oriented, with the facets making a widely open V. The neural canal remains almost complete, missing the ventral region; it is deep with a round-shape. The diapophyses are perpendicular to the neural arch. The parapophyses are in the anterior region of the neural arch, between the diapophyses and the prezygapophyses, ventrally to both.

The dorsal vertebra NHMD-6F+F12 (Fig.16B) is an almost complete neural arch, like NHMD-Da10. However, it is still in the matrix and only the lateral view is visible, and the lateral portion of the neural canal is broken. The neural spine is 47.2 mm, slightly tilted posteriorly,

with the anterior and posterior margins sub-parallels, transversally compressed. The apex of the neural spine is round and is not transversally expanded. The prezygapophyses is damaged, but its facet is almost horizontal and dorsally oriented. The postzygapophyses is more damaged and difficult to see its facet.

The dorsal vertebra NHMD-Eb9a and NHMD-Eb9b (Fig.16C-D) are the centrum and neural arch isolated from the same vertebra, respectively. Both vertebra parts were found near one to the other, and the suture limit can be seen in both. The neural spine NHMD-Eb9b is 48.4 mm, vertically directed, elliptical-shaped, transversally compressed. The apex of the neural spine is convex, transversally expanded, making a rectangular outline in anterior view. The prezygapophyses are anteriorly projected, with the facets dorsally oriented making an open U (it is more open, with the central meeting point between the zygapophyses more curved than the open V found in other vertebrae, like in the cervical vertebra NHMD-Da10 or the caudal vertebra NHMD-131). The postzygapophyses are complete, shorter than the prezygapophyses and ventrally oriented. The neural canal is round and deep. The rib facet appears in the base of the neural arch, ventrally to the neural canal.

The centrum NHMD-Eb9a is slightly amphicoelous, with a rectangular-shape in lateral view, and sub-elliptical in anterior and posterior views. The dorsal surface is broken with contact facet scars remains. The ventral surface is slightly concave.
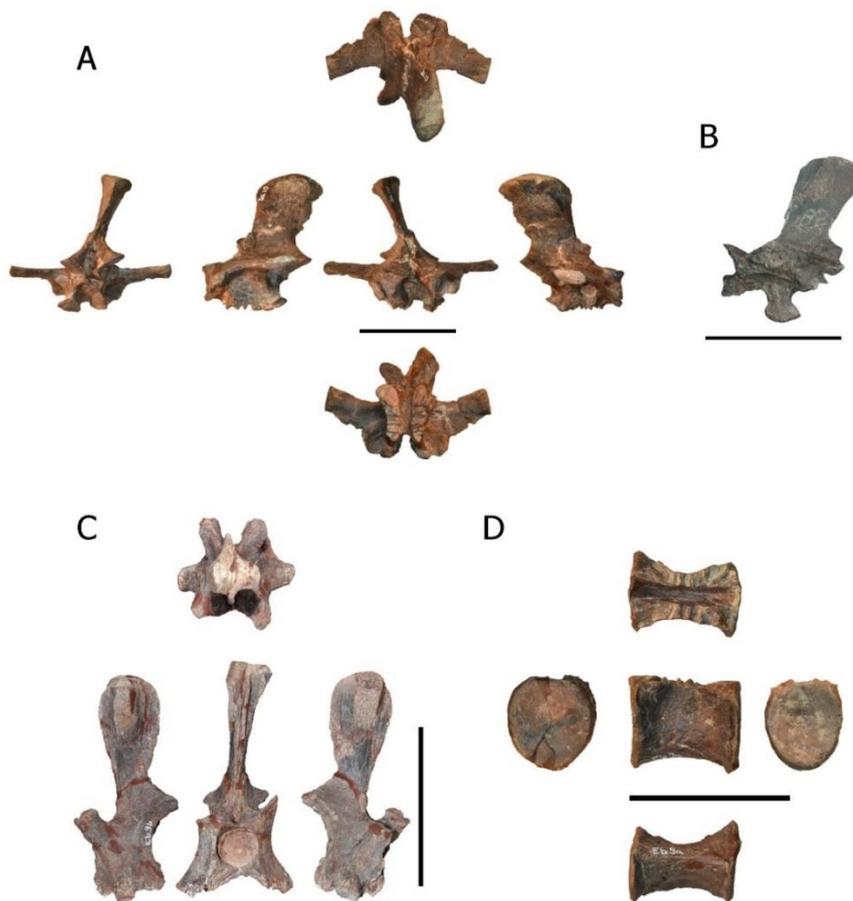
Figure 16. Dorsal vertebrae of *Mystriosuchus* sp*.* from Greenland. A. Dorsal vertebra NHMD-Da10 (dorsal, posterior, left, anterior, right, ventral views, respectively); B. Dorsal vertebra NHMD-6F+12 (left view); C. Dorsal vertebra NHMD-Eb9a (dorsal, left, anterior and right views, respectively); Dorsal vertebra NHMD-Eb9b (dorsal, posterior, right, anterior, ventral views, respectively). Scales = 5 cm.

Sacral

The two sacral vertebrae NHMD-6E14 (Fig.17) are partially preserved and still in the matrix. Their centrums are fused, as well as their proximal diapophyses. The pre-zygapophyses and post- zygapophyses are difficult to delimit because of the conservation.
The neural spines are separated and tilted posteriorly.

Figure 17. Sacral vertebrae of *Mystriosuchus* sp*.* from Greenland. NHMD-6E14 in left view. Scale = 1 cm.

Caudal

The caudal vertebrae from *Mystriosuchus* sp*.* from Greenland are the most complete vertebrae found.

The caudal vertebra NHMD-Gc51 (Fig.18A) is a nearly complete neural arch, except for the left anterior neural canal portion and left prezygapophyses. The neural spine is 109.7 mm tall, with a vertically directed blade shape, transversally compressed, and anterior and posterior margins sub-parallels. The apex of the neural spine is sub-horizontal, slightly tilted anteriorly, with no transversal expansion. The anterior edge of the neural spine base has a slight bump anteriorly projected. The prezygapophyses are projected anteriorly, making a deep curve with the neural spine. The postzygapophyses are almost complete, with a triangular shape and their facet facing almost horizontally ventral.

The caudal vertebra NHMD-130 (Fig.18B) is complete centrum and partial neural arch, preserving only the neural canal, postzygapophyses and upper-most of the neural spine. The partial neural spine has a blade-like shape transversally compressed, with the anterior and posterior margins sub-parallel. Its apex is sub-horizontal, slightly tilted anteriorly, with no transversal expansion. The postzygapophyses are robust and facing ventrally, however, their position is taphonomical altered into a more lateral right position. The neural canal is round and deep. The centrum is amphicoelous and bigger posteriorly. The ribs are fused ventrally to the suture of the centrum and the neural arch. The ribs are almost perpendicular to the centrum, slightly ventrally oriented.

The caudal vertebra NHMD-6E11-44 (Fig.18C) is nearly complete, except for postero-lateral left part of the centrum and postzygapophyses. The entire vertebra is 155.6 mm tall, from which 102.4 mm composes the neural spine. The neural spine is directed vertically, blade-like, transversally compressed, and anterior and posterior margins are sub-parallels. The apex of the neural spine is sub-horizontal giving a rectangular outline in lateral view, not expanded transversally. The anterior rim at the base of the neural spine forms a round bump that projects anteriorly. The prezygapophyses are simple and their facets made an open V. The

inter prezygapophysal vacuity is deep. The prezygapophyses only projects slightly anterior to the anterior rim of the centrum. The neural canal is round and three times the width of the pedicels. In the middle of the base of the neural spine, there is a discrete lateral vertical crest. The centrum is procealous. The rib is broken, so only the base is preserved.

The broken condition of the centrum allows to pick the interior structure of it in this phytosaur. The bone is mainly spongy with no visible pleurocoel.

The fused neural central suture is located anteriorly to the rib, being unclear if it runs ventrally or through the rib facet. In Renesto (2008) MCSNB 10.087 specimen, the neural central suture is dorsally to the rib facet.

The caudal vertebra NHMD-131 (Fig.18D) is completely preserved, with the suture line between neural arch and centrum. The entire vertebra is 177.9 mm, from which 111 mm composes the neural spine. The neural spine is directed postero-vertically, with a blade-like shape, transversally compressed, and anterior and posterior margins are sub-parallels. The half-anterior margin of the apex of the neural spine is tilted, while the half-posterior margin is horizontal. The apex of the neural spine is not expanded transversally. The base of the neural spine has anteriorly and posteriorly directed bumps, dorsally to the zygapophyseis. The prezygapophyses have their facets dorsally oriented, making an open V, while the postzygapophyses have their facets ventrally oriented. The inter prezygapophysal and inter postzygapophysal vacuity are deep. The neural canal is round-shape and deep. The centrum is amphicoelous, with a deep concave ventral surface. The ribs are fused between the suture of the centrum and neural arch. The right rib is ventrally oriented, while the left rib is dorsally oriented due to taphonomic alterations. Both ribs are fused ventrally to the neural arch and centrum suture

The caudal vertebra NHMD-Fa42 (Fig.18E) is completely preserved, except for the partially broken postzygapophyses and posterior centrum base. The entire vertebra is 177.3 mm, from which 102.1 mm composes the neural spine. The neural spine is directed vertically, slightly bowed, blade-like shape, transversally compressed, with anterior and posterior margins sub-parallels. The neural spine apex is not expanded transversally, with a sub-horizontal margin. The prezygapophyses are robust and facing dorsally, making an open V shape. The prezygapophyses are anteriorly expanded, surpassing the centrum anterior margin, making a smooth 90º angle with the neural spine. The left postzygapophyses is nearly complete, facing ventrally. The postzygapophyses are broken are not surpass the posterior margin of the centrum. The neural canal has a round shape anteriorly, and elliptical posteriorly. The centrum is amphicoelous, with a ventral concavity. The ribs are broken, only the base is preserved. The rib base is between the suture of the neural arch and the centrum.

The caudal vertebra NHMD-132 (Fig.18F) is a complete preserved vertebra, except for the apex of the neural spine. The entire vertebra is 157.2 mm, from which 100.3 mm composes the neural spine. The neural spine is directed vertically, with the anterior and posterior margins sub-parallels, transversally compressed. The neural spine apex is broken, however, there are no signs of a transversal expansion. The base of the neural spine has an anteriorly and posteriorly directed bump expansions. The anterior bump is more expanded anteriorly than the posterior bump posteriorly. The prezygapophyses are robust and make an open V facet dorsally oriented, while the postzygapophyses are facing almost horizontally ventral. The inter prezygapophysal and inter postzygapophysal vacuity are deep. The neural canal is deep, and round-shaped anteriorly, while more elliptical-shaped posteriorly. The centrum is amphicoelous and has a concavity in its ventral surface. The ribs are fused, short, and perpendicular to the centrum. The ribs are fused ventrally to the neural arch and centrum suture.

The distal caudal vertebra NHMD-Hb4 (Fig.18G) is a broken vertebra, with the neural spine preserved and the left half posterior centrum. The neural spine is short, posteriorly located and posteriorly tilted, compressed transversally. The postzygapophyses are short and facing ventrally. The neural canal is round shape and deep. The centrum is broken, at least procealous. The left rib is short and perpendicular to the centrum, fused ventrally to the neural arch and centrum suture.

The vertebra NHMD-NOID (Fig.18H) is a small centrum preserved. The centrum is procealous, with the ventral surface concave. It still has the contact surfaces in both anterior and posterior ventral margins for the chevrons.
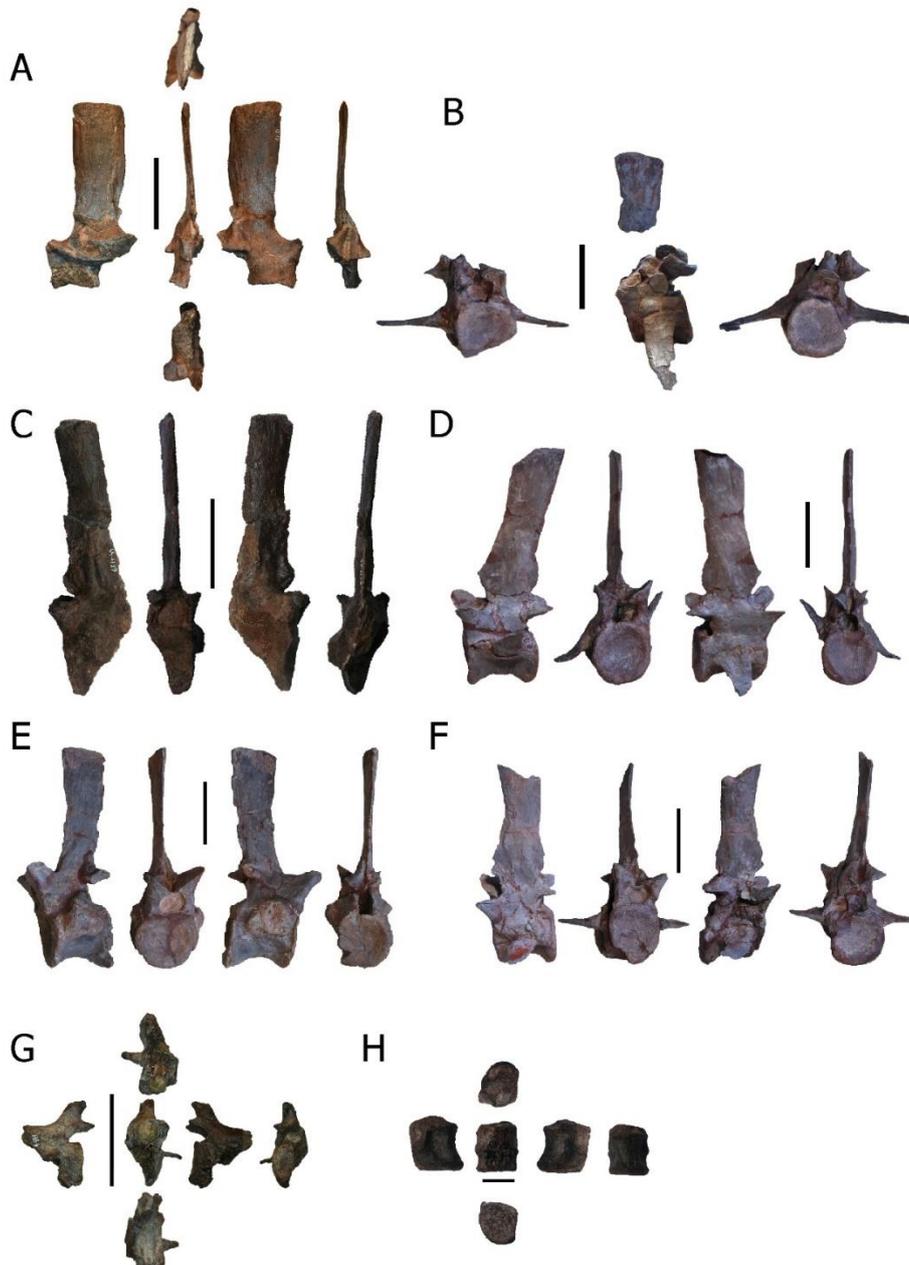
Figure 18. Caudal vertebrae of *Mystriosuchus* sp*.* from Greenland. A. Caudal vertebra NHMD-Gc51; B. Caudal vertebra NHMD-130; C. Caudal vertebra NHMD-6E11-44; D. Caudal vertebra NHMD-131; E. Caudal vertebra NHMD-Fa42; F. Caudal vertebra NHMD-132; G. Caudal vertebra NHMD-Hb4; H. Caudal vertebra NHMD-NOID. Views in A, C, D-G: left, anterior, right, posterior; in B: anterior, left, posterior; in H: left, ventral, right, dorsal, anterior, posterior. Scales A-G = 5cm, H = 1cm.

4. Ribs

A total of 40 ribs (Figs.19-21) were collected and can be divided into three morphotypes. Only the most complete, 23 of them, were measured and appear in Table 5 are in millimeters.

Table 5. Measurements of *Mystriosuchus* sp. ribs

Field number	Bone	Length	Width (head)	Width (posterior)
NHMD-Kb123	Cervical rib	54.6	14.3	5.5
NHMD-Fa98	Cervical rib	66.7	22.4	3
NHMD-Kd106	Dorsal rib	181.7	23.9	5
NHMD-129	Dorsal rib	103	20.3	3.1
NHMD-Kb125	Dorsal rib	246.4	67	7.9
NHMD-Ea83	Dorsal rib	167.5	52.9	7.9
NHMD-Fb29a	Dorsal rib	239.2	11	9.1
NHMD-Gb95a	Dorsal rib	218.9	9,5	8.8
NHMD-Ea79	Dorsal rib	301	26.2	13.1
NHMD-Ea84	Dorsal rib	338.5	58.8	10.3
NHMD-Eb66	Dorsal rib	272.8	35.7	10.7
NHMD-Hc75b	Dorsal rib	328.4	58.8	14.1
NHMD-Ea96	Dorsal rib	256.5	36	26.3
NHMD-Hb115	Gastralia	193.5	11.8	7.2
NHMD-Gb30	Gastralia	132	5.5	4.7
NHMD-127	Gastralia	145.1	8.4	7.3
NHMD-Kc122d	Gastralia	260	5.6	5
NHMD-Gb7	Gastralia	206	12.2	8.6
NHMD-Fb32	Gastralia	150.7	51.3	2.7
NHMD-Da68	Gastralia	176.6	13.7	5
NHMD-Gc35	Gastralia	218.5	5.3	5.1
NHMD-Kb129	Gastralia	186.	6	5.2
NHMD-Ea61	Gastralia	160.7	8.3	5.3

The cervical ribs NHMD-Kb123 (Fig.20A) and NHMD-Fa98 (Fig.20B) are small and short, with double headed proximal end dorsoventrally flattened. However, the proximal surface is shallow concave, in contrast with the dorsal.

The dorsal ribs NHMD-Kd106, NHMD-129, NHMD-Kb125, NHMD-Ea83, NHMD-Fb29a, NHMD-Gb95a, NHMD-Ea79, NHMD-Ea84, NHMD-Eb66, NHMD-Hc75b, and NHMD-Ea96 (Fig.19A-K. respectively) share a long, slender, straight to bowed shape. The proximal end is double headed (partly broken in NHMD-Kd106, NHMD-Fb29a and NHMD-Gb95a), with the proximal condyle larger than the distal. The proximal end is dorsoventrally flattened, with a deep concave surface. The rib gets thicker distally, changing from a flat to a circular cross-section that extends until the distal end. In the case of NHMD-Fb29a and NHMD-Eb66, the head had smaller condyles, almost similar in size. In NHMD-Gb95a, the head is broken and lack one of the condyles, indicated by the scar. In NHMD-Kd106, NHMD-Kb125 and NHMD-Ea83, the head and the body are straighter.

The gastralia ribs NHMD-Hb115, NHMD-Gb30, NHMD-127, NHMD-Kc122d, NHMD-Gb7, NHMD-Fb32, NHMD-Da68, NHMD-Gc35, NHMD-Kb129, NHMD-Ea61 (Fig.20C-L, respectively)

have a long and slender body shape, strongly curved with a prominent vertex in the middle of the body (in the case of NHMD-6E13-6G, only this vertex remains). The ends are broken and sharp in all of them, in exception of NHMD-Gb7.

There are also partial remains of broken distal ends (NHMD-141, NHMD-Hc75, NHMD-142, NHMD-Ja117, NHMD-Gc34, NHMD-Ea67, NHMD-58, NHMD-Gb95; Fig.20A-H) and middle bowed parts (NHMD-128, NHMD-Hc75c, NHMD-Ea65, NHMD-138, NHMD-Jd65, NHMD-140, NHMD-137, NHMD-126, and NHMD-Kc122e; Fig20I-Q) that cannot be enclosed into any of the previous morphotype.
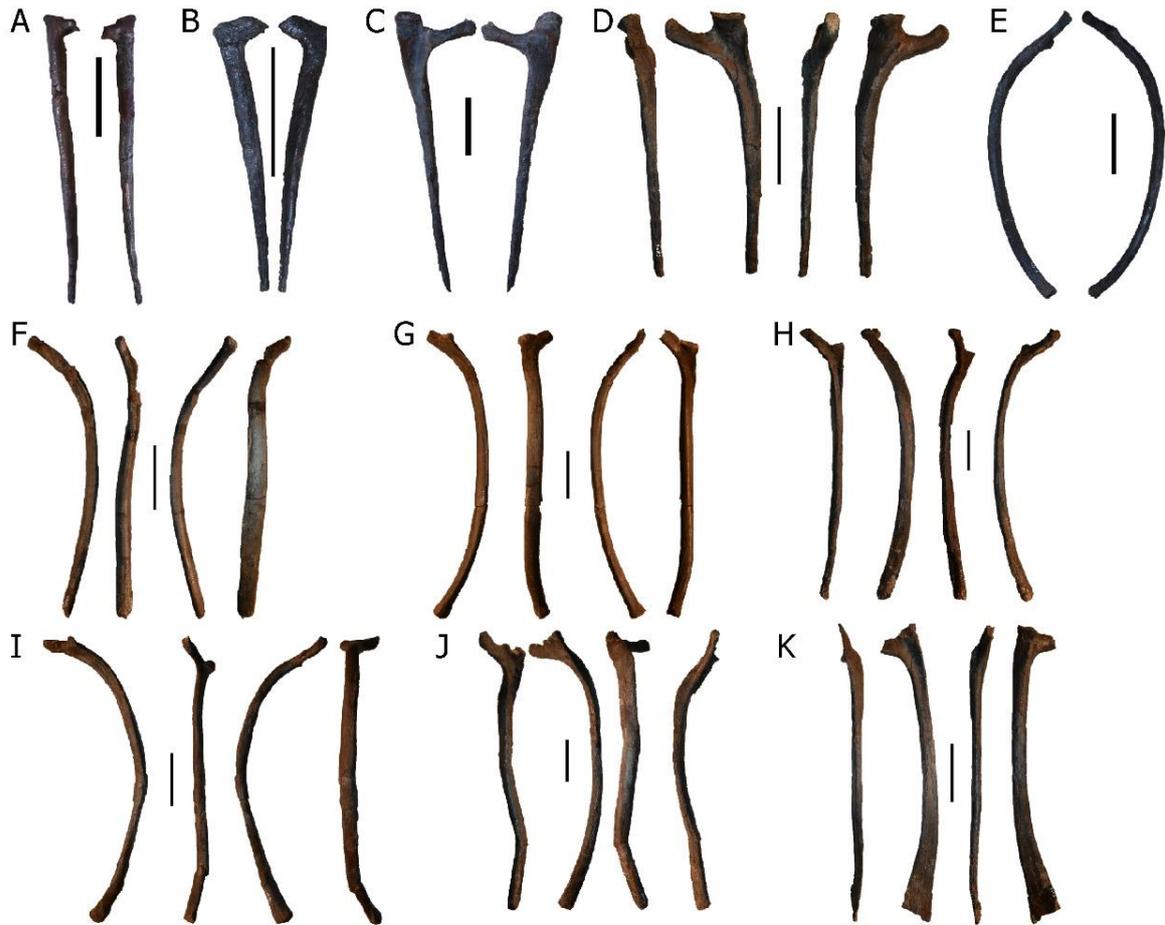
Figure 19. Dorsal ribs of *Mystriosuchus* sp. from Greenland. A. NHMD-Kd106; B. NHMD-129; C. NHMD-Kb125; D. NHMD-Ea83; E. NHMD-Fb29a; F. NHMD-Gb95a; G. NHMD-Ea79; H. NHMD-Ea84; I. NHMD-Eb66; J. NHMD-Hc75b; K. NHMD-Ea96. Scales = 5 cm.

Figure 20. Cervical ribs (A-B) and gastralia (C-L) of *Mystriosuchus* sp. from Greenland. A. NHMD-Kb123; B. NHMD-Fa98; C. NHMD-Hb115; D. NHMD-Gb30; E. NHMD-127; F. NHMD-Kc122d; G. NHMD-Gb7; H. NHMD-Fb32; I. NHMD-Da68; J. NHMD-Gc35; K. NHMD-Kb129; L. NHMD-Ea61. Scales A-B = 4 cm; C-L = 5 cm.
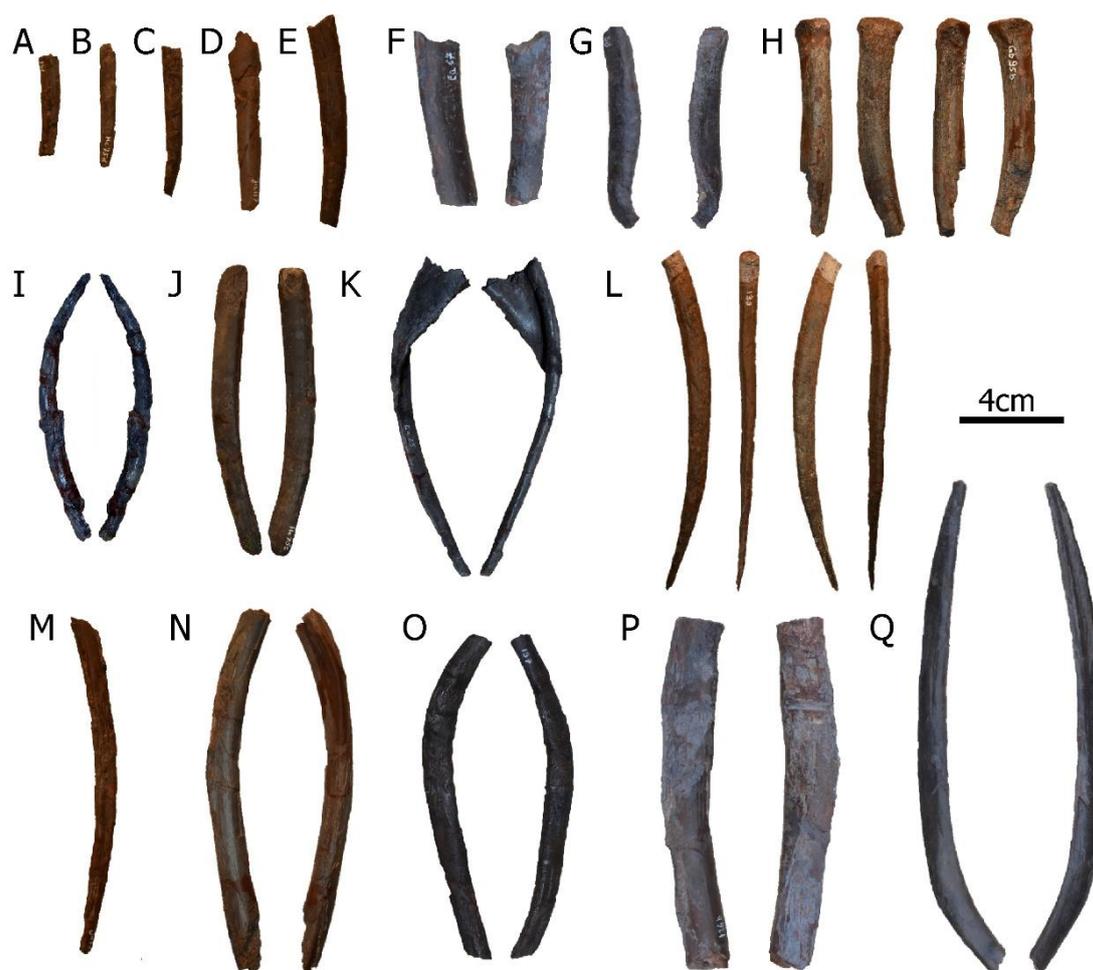
Figure 21. Partial ribs of *Mystriosuchus* sp*.* from Greenland. A. NHMD-141; B. NHMD-Hc75d; c. NHMD-142; D. NHMD-Ja117; E. NHMD-Gc34; F. NHMD-Ea67; G. NHMD-58; H. NHMD-Gb95; I. NHMD-128; J. NHMD-Hc75c; K. NHMD-Ea65; L. NHMD-138; M. NHMD-Jd65; N. NHMD-140; O. NHMD-137; P. NHMD-126; 1. NHMD-Kc122e. Scale = 4 cm.

5. Pectoral girdle

A total of six disarticulated bones referred to the pectoral girdle were recovered. The measurements in Table 6 are in millimeters.

Table 6. Measurements of *Mystriosuchus* sp. pectoral girdle bones.

Label	Bone	Length	Width (anterior)	Width (posterior)
NHMD-NOID	Interclavicle	91.3	48.6	24.7
NHMD-Fa82	Interclavicle	99.6	~55.5	~24.5
NHMD-Fb31	Interclavicle	225.5	38.1	48
NHMD-Gb21	Clavicle?	83	23.5	14
NHMD-Hc75a	Right coracoid	170	52.2	16.5
NHMD-136	Left coracoid	-	-	-
NHMD-Hd48	Left ischium	174	41.3	18.2
NHMD-Gb39	"Baby" scapula	33.8	13.9	11.2

The interclavicle NHMD-NOID (Fig.22A) anterior body is thin with the dorsal anteriormost portion region still covered in matrix. The anteriormost region has a rhomboid shape with short lateral processes, that is gradually reduced and reaches the connection with the interclavicle body. The interclavicle body has two middle ventral ridges near the connection with the interclavicle head.

The interclavicle NHMD-Fa82 (Fig.22B) preserved only the half anteriormost body. The remaining lateral process expands laterally, displaying a triangular shape. The posterior region is thinner and smoother than the anterior. There is a convex ridge in the middle shaft, between the lateral processes.

The partial body of the interclavicle NHMD-Fb31 (Fig.22C) is a thin sub-elliptical bone. In the anterior region, the contact with the interclavicle head is broken. There are two central ridges that run through the middle body. These ridges start sub-parallels and separate distally.

The partial scapula NHMD-Gb39 (Fig.22D) has a sub-rectangular shape, posteriorly bowed, with the distal end more posteriorly projected than the proximal end. The distal end ventral surface has a triangular shape, which would contact the coracoid.

The right coracoid NHMD-Hc75a (Fig.22D) has a convex blade-like shape in its medial surface which broadens anteriorly. The glenoid process is laterally oriented, perpendicular to the blade, with a thick neck connection, and a sub-elliptic surface.

From the left coracoid NHMD-136 (Fig.22E) only the anterior portion of the blade region and the posterior portion of the glenoid process is preserved. The anterior portion of the blade-like region is thin, with a sharp anterior edge. The glenoid process has a concavity that would contact the scapula.

The clavicle (NHMD-Gb21; Fig.22G) is a short, anteriorly bowed, broken bone, medially concave. Its dorsal surface is concave, while the ventral is straight and smooth. It gets wider medially, and the anterior edge expands more than the posterior. The antero and postero medial surfaces make a square-shape that would surround the interclavicle left lateral process.

6. Forelimbs

A total of seven forelimb bones were collected. All the measurements in Table 7 are in millimeters.

Table 7. Measurements of *Mystriosuchus* sp. forelimb bones.

Field number	Bone	Length	Width (anterior)	Width (posterior)
NHMD-Fa85	Left humerus	259.3	94.2	86.2
NHMD-Ga116	Left humerus	261	89.3	79.9
NHMD-Gc6	Right humerus	275.7	99.5	90.1
NHMD-6E13-54	Right ulna	143.2	39.6	45.4
NHMD-Jd57	Right ulna	216.4	55.8	36
NHMD-113	Right radius	172.4	26.3	27.8
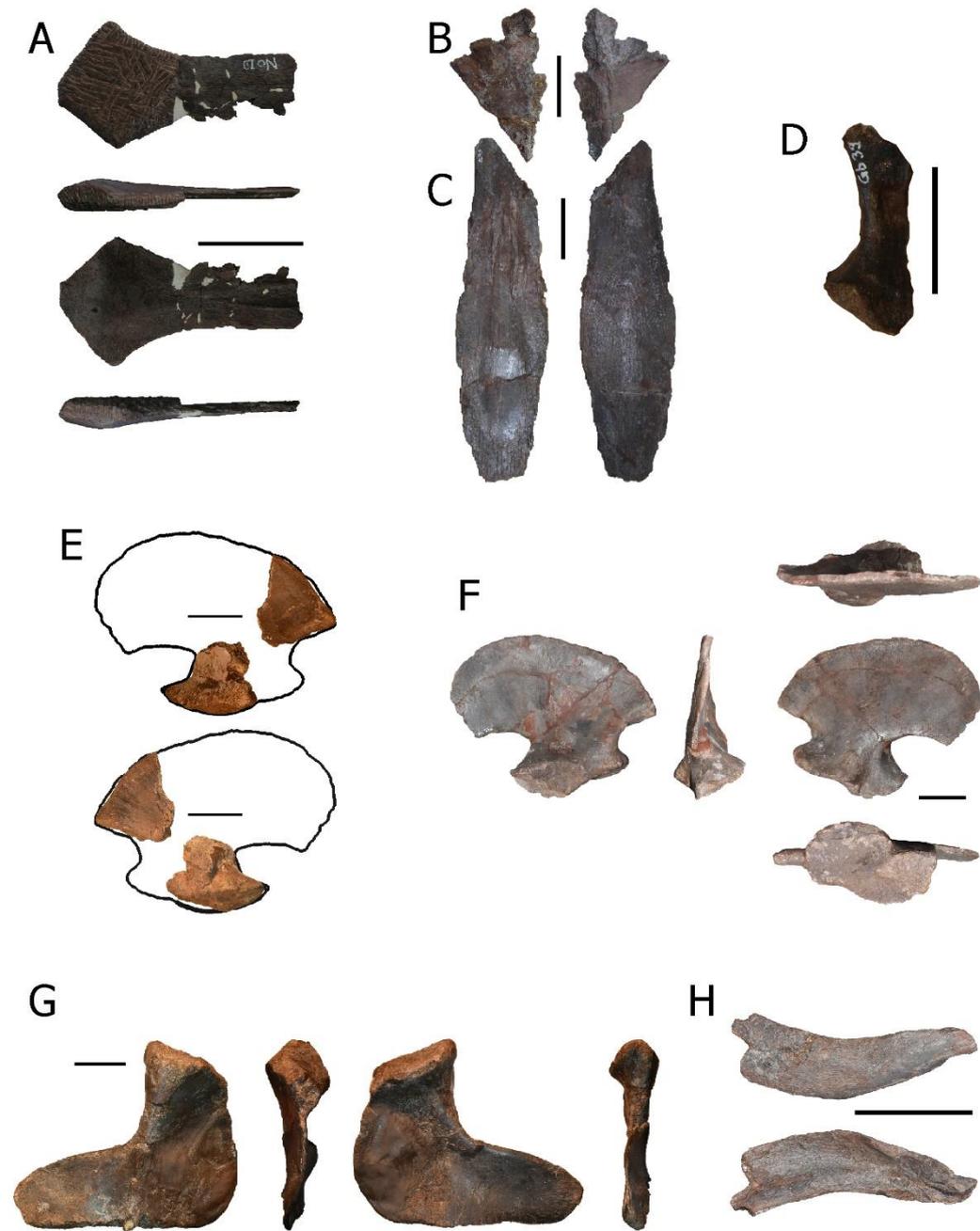
Figure 22. Pectoral and pelvic girdle bones of *Mystriosuchus sp.* from Greenland. A. Interclavicle NHMD-NOID (left, ventral, right, dorsal views, respectively); B. Partial interclavicle NHMD-Fa82 (dorsal, ventral views, respectively); C. Partial interclavicle NHMD-Fb31 (ventral, dorsal views, respectively); D. "Baby" scapula NHMD-Gb39; E. Left coracoid NHMD-136 (left, right views, respectively); F. Right coracoid NHMD-Hc75a (left, anterior, right, dorsal, ventral views, respectively); G. Left ischium NHMD-Hd48 (right, posterior, left, anterior views, respectively); H. Left clavicle NHMD-Gb21 (ventral, dorsal views, respectively). Scales A-C, E-H = 4cm, B = 2cm.

Complete left (NHMD-Fa85 and NHMD-Ga116; Fig.23A-B) and right humerus (NHMD-Gc6; Fig.23C) display a robust, ventrally bowed body shape.

In NHMD-Gc6, NHMD-Fa85, and NHMD-Ga116, the proximal end is dorsoventrally flattened, with a rugose convex surface. The condyles are flat, the medial condyle being more expanded medially than proximally. The deltoic crest appears along the lateral margin of the ventral surface (105 mm in NHMD-Fa85, 114 mm in NHMD-Ga116, and 126 mm in NHMD-Gc6), almost reaching the middle part of the body. The distal end is dorsoventrally flattened, with broad condyle expansions. In contrast with the proximal surface, the distal surface is gently concave and soft. The radio-condylar groove is located above the laterodistal condyle, lateroventrally expanded, extending the laterodistal condyle edge.

The partial right ulna NHMD-6E13-86 (Fig.23E) has a subrectangular, medially bowed, dorsoventrally flattened, faintly ventrally concave body shape. The proximal end becomes medially broad, while the distal end is broader laterally than medially, with a smooth surface. In the dorsal surface there is a dorsally expanded sigmoideal relief running along the diaphysis midshaft.

The partial right ulna NHMD-Jd57 (Fig.23F) is a long dorsoventrally flattened bone bowed medially and ventrally, faintly ventrally concave, and distally thinner. The proximal end is proximally wide, with a circular shape. It has a ventral expansion of the medial border, over the radius. On the medial side, the olecranon has a soft concave surface. Although the distal end is broken, the remaining portion has a concave ventral surface, surrounding the radius dorsal surface.

The right radius NHMD-113 (Fig.23F) is a straight sub-cylindrical bone, bowed ventrally but less than the ulna. The proximal end exhibits a flattened elliptical surface, more expanded laterally than medially. The distal end also exhibits a flattened surface, but the shape is more circular than the proximal surface.

7. Pelvic girdle

Only one ischium was found. The measurements are in Table 4.

The well-preserved left ischium NHMD-Hd48 (Fig.20G) has a blade-like ventral process, mediolaterally flattened and posteriorly slimed down, with the posterodorsal region thicker than the anteroventral. The dorsal surface is smooth, laterally tilted.

8. Hindlimbs

A total of four hindlimb bones were collected. All the measurements are in Table 8 in millimeters.

Table 8. Measurements of *Mystriosuchus* sp. hindlimbs bones.

Field number	Bone	Length	Width (anterior)	Width (posterior)
NHMD-134	Left femur	301.3	68.5	59.3
NHMD-Hc74a	Left tibia	192.5	67.9	49
NHMD-6E12-54	Left fibula	100.8	15.8	19.3

The left femur NHMD-134 (Fig.24A) displays a long, slender, sigmoideal shape, medially bowed. The proximal end is dorsoventrally flattened, anteriorly expanded, with a rugose convex surface. The medial and lateral condyles are posteriorly oriented, with the medial condyle more expanded medially. The ventral surface is convex and smooth, larger in the medial condyle. The intercondylar grooves appear in both anterior and posterior surfaces, deeper in the posterior surface.

There left fibula NHMD-6E12-54 (Fig.24B) is a long bone, dorsoventrally flattened, with a gentle sigmoid curvature. The proximal end has a smooth surface, and the lateral condyle looks swollen over the medial. The diaphysis exhibits an iliofibularis trochanter over the middle shaft of the body. The distal end displays an ellipsoid smooth surface, and is dorsoventrally flattened, in contrast with the proximal end, with a dorsal groove extending toward the middle diaphysis.

The left tibia NHMD-Hc47a (Fig.24C) displays a robust, straight, medially bowed shape, with an oval cross-section. The proximal end is anteriorly projected, more medially expanded than the distal end, with a smooth convex surface. The distal end is anteromedially expanded, which is where the fibula contacts.

9. Phalanges

A total of eight phalanges were recovered. All the measurements are in millimeters in Table 9.

Table 9. Measurements of *Mystriosuchus* sp. phalanges bones.

Field number	Bone	Length	Width (anterior)	Width (posterior)
NHMD-Gc36	Phalanx	36.5	23.5	22.8
NHMD-Fb33	Phalanx	31.8	20.5	20.5
NHMD-6E13-54	Phalanx	27.3	15.7	14.2
NHMD-6F13	Phalanx	36.2	22.4	22.3
NHMD-Fa59	Phalanx	96.4	21.8	12.6
NHMD-Fa40	Phalanx	42.6	18	7.6
NHMD-135	Phalanx	43.3	18.4	17.7
NHMD-Ca13	Phalanx	28.3	16.1	15.5

Figure 23. Forelimb bones of *Mystriosuchus* sp. from Greenland. A. Left humerus NHMD-Fa85 (ventral, medial, and dorsal views, respectively); B. Left humerus NHMD-Ga116 (ventral, medial, dorsal, and lateral views, respectively); C. Right humerus NHMD-Gc6 (medial, dorsal, lateral, and ventral views, respectively); D. Right ulna NHMD-6E13-54 (medial, dorsal, lateral, and ventral views respectively); F. Right ulna NHMD-Jd57 (ventral, medial, dorsal, and lateral views, respectively) and right radius NHMD-113 (anterior, lateral, posterior, and medial views, respectively). Scales = 10 cm. Abbreviations: dc – deltoic crest, dmc – distal medial condyle, o – olecranon, pmc – proximal medial condyle, rcg – radio condylar groove, Ra – radius, Ul – ulna.

Figure 24. Hindlimb bones of *Mystriosuchus* sp*.* from Greenland. A. Left femur NHMD-134 (medial, dorsal, lateral, and ventral views, respectively); B. Left fibula NHMD-6E12-54 (dorsal, medial, ventral, and lateral views, respectively); C. Left tibia NHMD-Hc74a (lateral, dorsal, medial, and ventral views, respectively). Scales A = 10cm; B-C = 4cm. Abbreviations: c – condyle, fh – femur head, fc – fibula contact, gr – grove, p – process, tr – trochanter.

The isolated phalanges NHMD-Gc36, NHMD-Fb33, NHMD-6E13, NHMD-6F13, NHMD-Fa59, NHMD-Fa40, NHMD-135 and NHMD-Ca13 (Fig. 25A-H, respectively) are complete. However, since they are not associated neither articulated, most of them could not be attributed as carpals nor tarsals.

They have round smooth proximal surfaces (flat in NHMD-6E13 and NHMD-Ca13, dorsally concave in the other), while the distal surface is convex and flattened lateromedially, giving a square-shape in anterior view.

The ventral surface is smooth and straight in NHMD-6E13, NHMD-135, NHMD-Ca13, NHMD-Fa40 and NHMD-Fa59, and anteriorly concave in NHMD-6F13, NHMD-Fb33 and NHMD-Gc36, while the dorsal surface is slightly bowed. The anterior region is smaller than the posterior one, having a triangle-shape in medial and lateral views. The body of the phalanges is constricted in the center. The anterolateral condyle is projected laterally, making the lateral surface look more concave than the medial surface in the constricted area.

However, the phalanges NHMD-135, NHMD-Fa40 and NHMD-Fa59 can be enclosed as the first phalanges. These phalanges are longer (see Table 9) and more dorsoventrally flattened than the others.

10. Dermal armor

A total of 19 osteoderms were collected. All the measurements are in Table 10 in millimeters.

Table 10. Measurements of *Mystriosuchus* sp. osteoderms.

Field number	Morphotype	Length	Width
NHMD-Kc108	Morphotype 1	28.6	33.3
NHMD-Gb95e	Morphotype 1	26.3	27.5
NHMD-6E12	Morphotype 1	13.9	12.6
NHMD-NOID	Morphotype 1	22.4	19.1
NHMD-Fa26	Morphotype 1	56.6	45.9
NHMD-Fa24	Morphotype 1	52.5	29.8
NHMD-Jc74	Morphotype 1	71.8	50
NHMD-Fa81	Morphotype 1	50	85.9
NHMD-Gb71	Morphotype 1	38.7	25.2
NHMD-Jd56	Morphotype 2	69.6	76.4
NHMD-Fb45	Morphotype 2	51.8	25.6
NHMD-Hb103	Morphotype 2	55.7	36.4
NHMD-Jc70	Morphotype 2	73.3	62.3
NHMD-Da90	Morphotype 3	36.2	51.6
NHMD-Eb73	Morphotype 3	34.1	27.6
NHMD-Ha118	Morphotype 3	33.1	57.5
NHMD-NOID	Morphotype 4	43.5	58.5
NHMD-6E12-81	Morphotype 4	41.2	46.1
NHMD-6F13-102	Morphotype 4	41.7	33.8

Most of the isolated osteoderms found can be related to the lateral dorsal armor, because of the presence of pitting in their surface. However, some have lost their edges and are difficult to include in any morphology.

The first osteoderm morphotype (Fig.26A-I) includes NHMD-Kc108; NMHD-Gb95e, NHMD-6E12, NMHD-NOID, NHMD-Fa26, NHMD-Fa24, NHMD-Jc74, NHMD-Fa81 and NHMD-Gb71. These osteoderms have almost a longitudinal bilateral symmetry with a teardrop-shaped (except NHMD-Fa81 and NHMD-Hc50) and a mid-dorsal bar. The pitting appears in the dorsal region, in a rough convex surface, while the ventral region is smooth.

The second osteoderm morphotype (Fig.26J-M) includes NHMD-Jd56, NHMD-Fb45, NHMD-Hb103 and NHMD-Jc70. They present a sub-rectangular shape, with a dorsal bar near the anterior edge. The dorsal pitting and smooth ventral surface are similar to the previous morphotype.

A third morphotype (Fig.26N-P) NHMD-Da90, NHMD-Eb73 and NHMD-Ha118 exhibits a sub-circular shape with small spines in the edges

Figure 25. Phalanges of *Mystriosuchus* sp. from Greenland. A. NHMD-Gc36 (medial, dorsal, lateral, and ventral views, respectively); B. NHMD-Fb33 (medial, dorsal, lateral, and ventral views, respectively); C. NHMD-6E13 (ventral, lateral, dorsal, and medial views, respectively); D. NHMD-6F13 (lateral, dorsal, medial, and ventral views, respectively); E. NHMD-Fa59 (lateral, and medial views, respectively); F. NHMD-Fa40 (lateral, dorsal, medial, and ventral views, respectively); G. NHMD-135 (lateral, dorsal, and medial views, respectively); H. NHMD-Ca13 (dorsal, medial, ventral, and lateral views, respectively). Scales A-B, E-G = 3cm; C-D = 2cm; H = 1cm.

Other morphotype of osteoderms found (Fig.26Q-S), such as NHMD-NOID, NHMD-6E12-81 and NHMD-6F13-102, in contrast with the previous ones, are ornamented with small ridges interconnected, similar to *Ginkgo biloba* leaves. These osteoderms are still in the matrix, so only one of the surfaces can be seen.
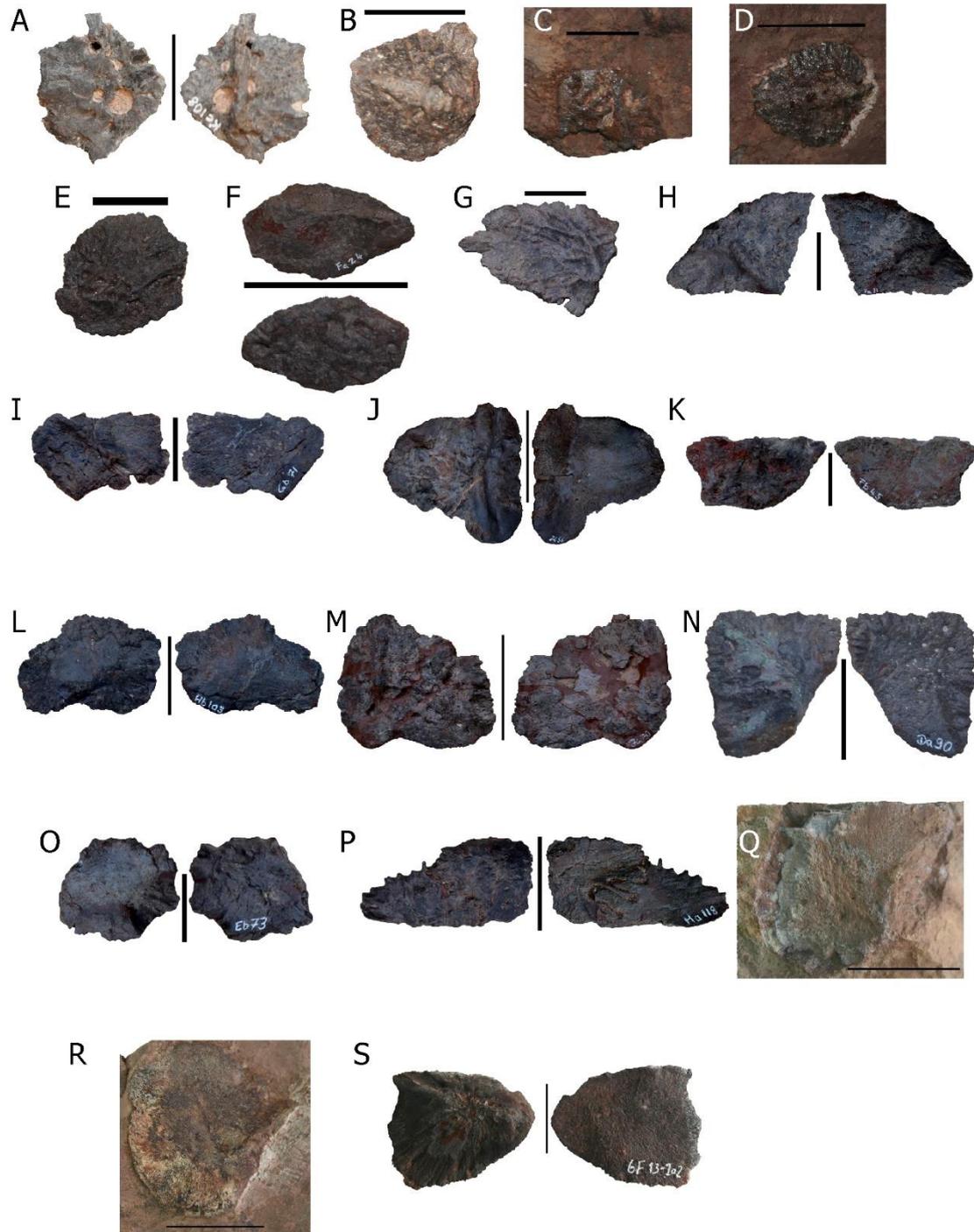
Figure 26. Osteoderms of *Mystriosuchus* sp. from Greenland. A NHMD-Kc108; B. NHMD-Gb95e; C. NHMD-6E12; D. NHMD-NOID; E. NHMD-Fa26; F. NHMD-Fa24; G. NHMD-Jc74; H. NHMD-Fa81; I. NHMD-Gb71; J. NHMD-Jd56; K. NHMD-Fb45; L. NHMD-Hb103; M. NHMD-Jc70; N. NHMD-Da90; O. NHMD-Eb73; P. NHMD-Ha118; Q. NHMD-NOID; R. NHMD-6E12-81; S. NHMD-6F13-102; T. NHMD-6F11-16*. A-I. First osteoderms morphotype; J-M. Second osteoderm morphotype; N-P. Third osteoderm morphotype; Q-S. "Ginkgo-like" morphotype. Scales A-B, D, I, K, O, S = 2cm; C = 1cm; E, G-H, L, N, P-R = 3cm; F, J, M = 5cm.

11. Bones with problematic identification

Here there is an approach of some fossil descriptions that, due to their preservation and partial conservation, were not able be accurately described without doubts. These bones will need further study and a comparison with complete phytosaur remains. Their measurements are in the Table 11 in millimeters.

Table 11. Measurements of *Mystriosuchus* sp. problematic bones.

Field number	Bone	Length	Width (anterior)	Width (posterior)
NHMD-6C4-36	?	104.3	16.8	29
NHMD-6F12	?	38.7	10.7	13

NHMD-6C4-36 and NHMD-6F12 (Fig.27A-B) are two straight, slender broken bones, posteriorly wider. These bones have ornamentation typical from dorsal skull bones. In the case of NHMD-6C4-36 (Fig.27A), it also has a smooth concave surface in one of its lateral edges, which could mean it is part of a fenestra region.

NHMD-2016 NOID is a broken terminal end of a long bone. It has a rectangular shape, dorsoventrally flattened, laterally convex, and slightly anteriorly bowed.
The anterior half edge of the terminal end slightly expands ventrally. The concave surface of the end has a sub-elliptical shape. The lateral and medial surfaces have no condyles, and the width along the bone is constant.
It is described here as a partial radius because of its lateral surface curvature, lack of condyles and constant width.
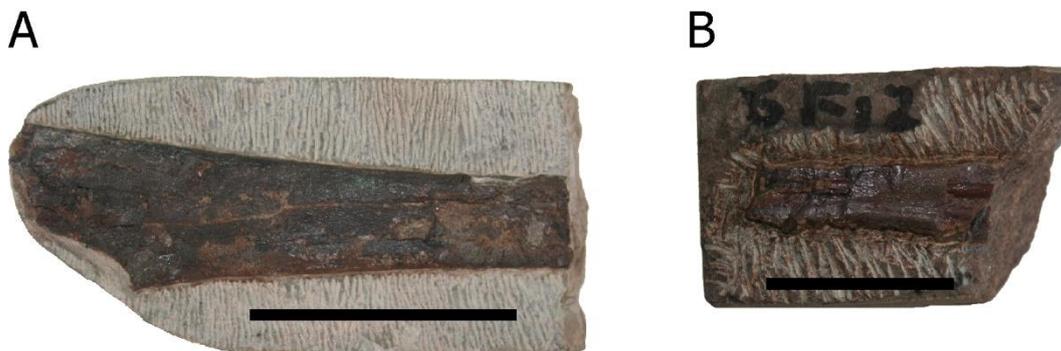
Figure 27. Problematic bones of *Mystriosuchus* sp. from Greenland. A. NHMD-6C4-36; B. NHMD-6F12. Scales = 5cm.

DISCUSSION AND COMPARISONS

The Greenland phytosaur fossils were in a bonebed with at least 6 individuals, however, most bones were nor in anatomical articulation. There are no significant morphological differences in the bones that indicate more than one species of phytosaur, even there are at least remains of four individuals. There is not much bone duplication (premaxilla, humeri, fibulae), and the anatomy remains consistent from one to another. Therefore, in this study, these fossils were treated as a single species, but with different individuals. This research makes

the first phylogenetic approach of the Greenland phytosaur, preserved mostly in post-cranial remains, which makes this approach as important as difficult.

The different degree of heterodonty was previously studied only in *Nicrosaurus kapffi* by Hungerbühler (2000) and an isolated teeth from India (Datta et al., 2019a), so the only comparison with a Laurassian phytosaur that can be made is with the *N.kapffi*. Since then, the degree of heterodonty has been poorly studied afterwards in phytosaurs and not used in phylogenetic neither morphometric studies, in contrast with dinosaurs (Larson, 2008; Hendrickx & Mateus, 2014; Isasmendi et al., 2020).
The number of denticles is superior in the tip of snout and anterior premaxilla of *N.kapffi*, while it is higher in the posterior premaxilla and the maxilla of the Greenland phytosaur. The difference between the SD of the *N.kapffi* from Hungerbühler (2000) and the Greenland phytosaur (here described as a phytosaur with as well tripartite dentition) needs further study and comparison with other Laurasian phytosaurs to corroborate that the character "Degree of heterodonty" has significant taxonomic value.

In the rostrum NHMD-126a, in comparison with other phytosaurs and other archosauriformes, such as *Proterochampsa*, *Proterosuchus* and *Eurparkeria* (Ewer, 1965; Rossman et al., 2005; Dilkes & Arcucci, 2012), the premaxilla never reaches the antorbital fenestra. The suture between premaxilla and maxilla is almost inexistent. However, between teeth number 20-21, there is a faint suture that goes dorsally, and posteriorly while reaching the dorsal part, that could be the limit between premaxilla and maxilla. With this idea, the tooth row would be divided in almost half of them as premaxillary (20 premaxillary teeth) and the other maxillary (at least 16 premaxillary, due to the maxilla is broken posteriorly). This almost half premaxillary-half maxillary teeth number can be seen in other phytosaurs such as *Nicrosaurus kapffi* (Hungerbühler, 2000), *Parasuchus hislopi* (Chaterjee, 1978), or *Angistorhinus grandis* (Mehl, 1915).
The beginning of the interpremaxillary fossa from the fifth tooth is also found in *Machaeroprosopus lottorum* TTU-P10076 (Hungerbühler et al., 2013). However, the fossa from the Greenland *Mystriosuchus* sp. is not totally bottom-flat posteriorly as it is slightly bowed dorsally in the bottom of the maxilla.

In both jugals, the anterior edge has a smooth anterior concave surface similar to the posterior and dorsal edges. This smooth concave surface could mean that the anterior region of the jugal was part of the anteorbital fenestra, like in *Mystriosuchus planirostris* and *M.westphali* (Hungerbühler, 2002).

The premaxilla NHMD-Gb8 is similar in morphology and alveoli shape to *Protome batalaria* (Stocker, 2012) and *Angistorhinus grandis* (Mehl, 1915), with the terminal rosette that in medial and lateral views looks downturned.

The surangular has two dorsal projections: one right after the dentary, and another one right before the articular. These dorsal projections have a similar position in NHMD-Hc1 and NHMD-6D2/3. When compared to other phytosaur species, the position and distance between these two dorsal projections differs among them (Fig.28) and could be used as a character to differentiate them in future researches.

The prezygapophyses and postzygapophyses in the cervical vertebra NHMD-Hc112 are, as seen by Lucas et al. (2002) in *Angisthorinus grandis*, above the neural canal. While the diapophyses of the Greenland specimen are located between the middle and ventral region of the neural canal, in contrast with *A.grandis*.

There is no centrum remain in the cervical vertebra; however, taking the zygapophyses as limits for the centrum to have an idea of the length, the centrum should be short, in contrast with the ones from *Rutiodon* (Romer, 1956), but more similar to *Angistorhinus grandis* (Lucas et al., 2002). Here, the cervical vertebra is enclosed as the mid-last cervical vertebrae, the eighth one.

The dorsal vertebrae are similar to the ones from *Parasuchus* (Chaterjee, 1978) and *Angistorhinus* (Lucas et al., 2002), with the transversa expansion of the neural spine apex, and the short square-shaped amphicoelous, not keeled, centrum.
The sacral vertebrae neural spines are thinner that the ones from *Parasuchus* (Chaterjee, 1978) and *Angistorhinus* (Lucas et al., 2002).

The anterior caudal vertebrae (NHMD-130, NHMD-131, NHMD-132, NHMD-6E11-44, NHMD-Fa42, NHMD-Gc51) have, as seen in *Parasuchus* (Chaterjee, 1978) and *Rutiodon* (Romer, 1956), their centrum taller than wider in comparison with the dorsal vertebra. All the caudal vertebrae from *Mystriosuchus* sp. share a feature that is not found either in cervical, dorsal or sacral vertebrae, and it is the basis neural spine bumps. All of them have anteriorly projected anterior bumps at the basis of the neural spine, and some of them (NHMD-131 and NHMD-132) also have posterior bumps posteriorly projected. This feature is shared with other *Mystriosuchus* (McGregor, 1906; Gozzi & Renesto, 2003), but it is not found in other phytosaur, because of the lack of description on post-cranial material (Gozzi & Renesto, 2003; Griffin et al., 2017). The positions enclosed here are NHMD-Gc51 as the third (even the centrum is missing, the bump is less projected than in other caudal vertebrae and could be referred as a more cranial position), NHMD-Fa42 as fourth, NHMD-130 as sixth, NHMD-131 as seventh, NHMD-132 as eighth, NHMD-6E11-44 maybe the as tenth (due to the centrum ventral region for the chevron is missing).

The difference of size and morphology between the distal caudal vertebrae could mean that NHMD-NOID is in a more posterior position than NHMD-Hb4, and it should be one of the last distal caudal vertebrae (Fig.29).

In the pectoral girdle, the interclavicle NHMD-NOID has no notch in its anterior margin like the ones that appear in *Parasuchus* (Ezcurra, 2016) or *Mystriosuchus* (Gozzi & Renesto, 2003), and the lateral process is really short in comparison with *Parasuchus* (Ezcurra, 2016). However, the partial interclavicle NHMD-Fa82 is longer anteriorly, which gives the look of the notch that NHMD-NOID lacks. It could be a difference in ontogenic level, as is reposted a range of variation in the morphology in *Mystriosuchus* genus (Kimmig, 2009).

Dermal armour remains found are usually from the dorsal region (Lucas et al., 2002; Gozzi & Renesto, 2003; Zeigler et al., 2003). While the ventral armour is not often well preserved (McGregor, 1906), the throat osteoderms or "gular shield" is typical from phytosaurs and different among archosauriforms (Holloway, 2018; Stocker & Butler, 2013). Here, the isolated osteoderms can all be referred as dorsal armor, with the exception of NHMD-6F11-16* with the skin pattern, that could be referred as ventral armor.
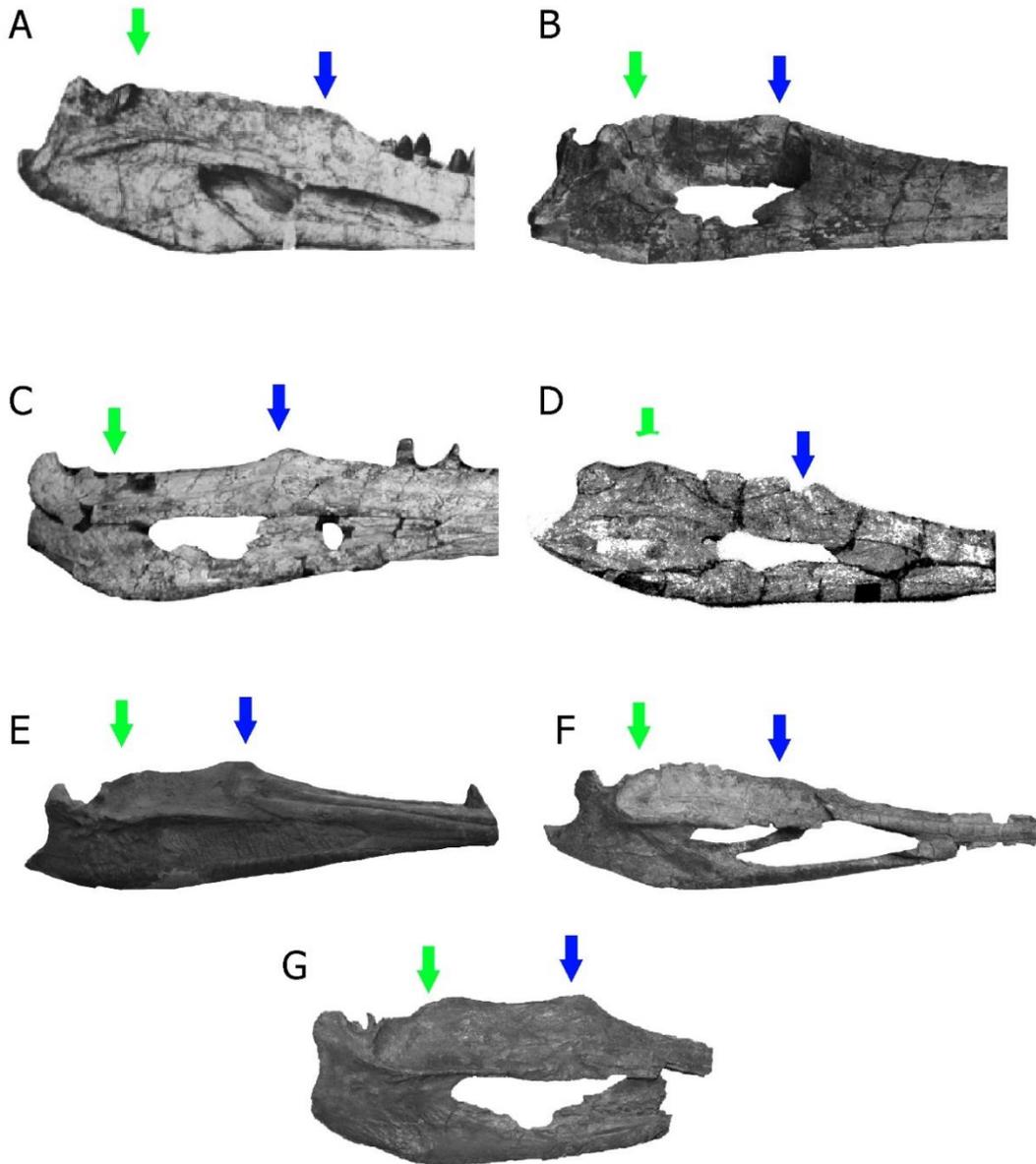
Figure 28. Position of the anterior (blue) and posterior (green) dorsal projections structures in the surangular of the mandibles of A. *Brachysuchus* (modified from Case, 1930); B. *Protome* (modified from Stocker, 2012); C. *Machaeroprosopus* (modified from Hunt et al., 2006); D. *Angistorhinus* (modified from Lucas et al., 2002); E. *Mystriosuchus planirostris* SMNS 91574 (photography took by Octavio Mateus); F. *Phytosauria* indet. from Portugal (modified from Mateus et al., 2014a); and G. *Mystriosuchus* sp. from Greenland (mirror image). Specimens are not in scale.
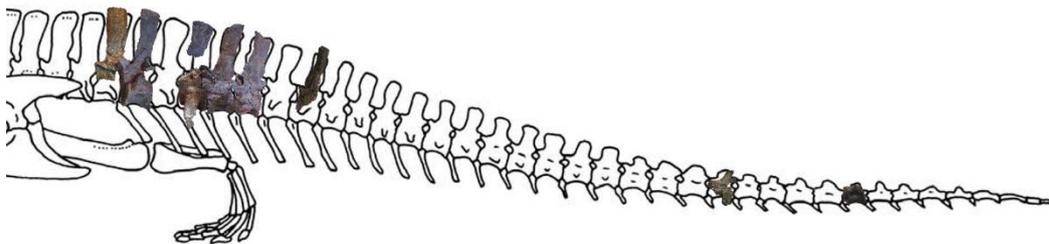
Figure 29. Relative position of the *Mystriosuchus* sp. caudal vertebrae NHMD-Gc51, NHMD-Fa42, NHMD-130, NHMD-131, NHMD-132, NHMD-6E11-44, NHMD-Hc4, and NHMD-NOID, over the reconstruction of *Rutiodon* skeleton (Witzman et al., 2014). Specimens are not in scale.

PHYLOGENETIC POSITION

The analysis (Appendix 1) recovered a total of 30 trees, with tree length of 348 steps, and the consensus of them with a tree length of 367 steps, with a Consistency Index of 0.391 and Retention Index of 0.698.

The results of the analysis are similar to the ones from Jones & Butler (2018) on "discrete character", with no continuous characters introduced. The continuous characters where not introduced because most of them are referred to the narial region, the width of the skull, or a relation between two of them and, in most cases, were not found or, in the best case, broken (as the premaxilla and maxilla). The main difference are the polytomies in the most basal phytosaurs (*Diandongosuchus fuyuanensis, Wannia scurriensis, Paleorhinus parvus, P. sawini, Parasuchus angustifrons,* and *Ebracosuchus neukami*). However, the Mystriosuchinae clade remains almost the same.

Here, the "Greenland phytosaur" appears within the genus *Mystriosuchus* (Fig.30) due to the possession of an interpremaxillary fossa narrow slit (Ch.2=2), and in a tricomy with *M. westphali* and *M. planirostris* due to the proximal section of postorbital descending process where posterior border of orbit meets skull roof, the posterior border of orbit remains thin until it reaches skull roof (Ch.88=1). *M. steinbergeri* has another state of the previous character (Ch.88=0: the postorbital descending process flares anteroposteriorly creating a wide triangular connection) and has two autapomorphies (Ch.22=1: antorbital fossa present but reduced lacrimal, jugal and maxillary fossae in contact dorsally but not ventrally; Ch.73=1: suborbital foramen elongated, slit-like).

The *Mystriosuchus* from Greenland has two potential autapomorphies that differentiates it from *M. planirostris* and *M. westphali*, with which shares a polytomic position (Ch.78=1: shape of retroarticular process in lateral view distally rounded or blunt, Fig.31; Ch.95=2: degree of heterodonty, tripartite upper dentition).

In comparison with other bones, such as the premaxilla and maxilla, the shape of the rostrum is flatter than in *Mystriosuchus westphali*, without the bump in the middle dorsal region of the premaxilla, more similar to *M. planirostris* (Fig.32).
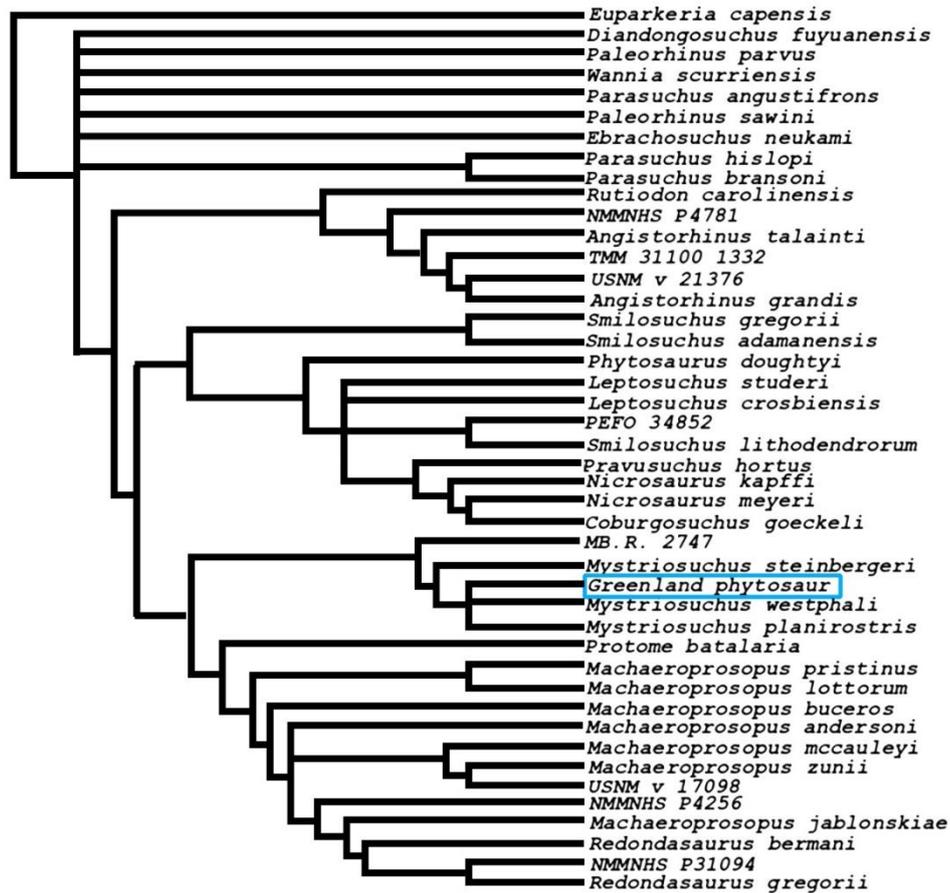
Figure 30. Strict consensus, showing the Bremer supports, resulting from the 30 phylogenetic trees from the analysis of discrete characters scoring, based on Jones & Butler (2018). The Consistency index of the characters is equal to 0.391, and the Retention index is 0.698.

Figure 31. Lateral view of the posterior mandible in A. *Mystriosuchus planirostris* (SMNS 91574) and B. *Mystriosuchus* sp. from Greenland. Red squares mark the retroarticular region.
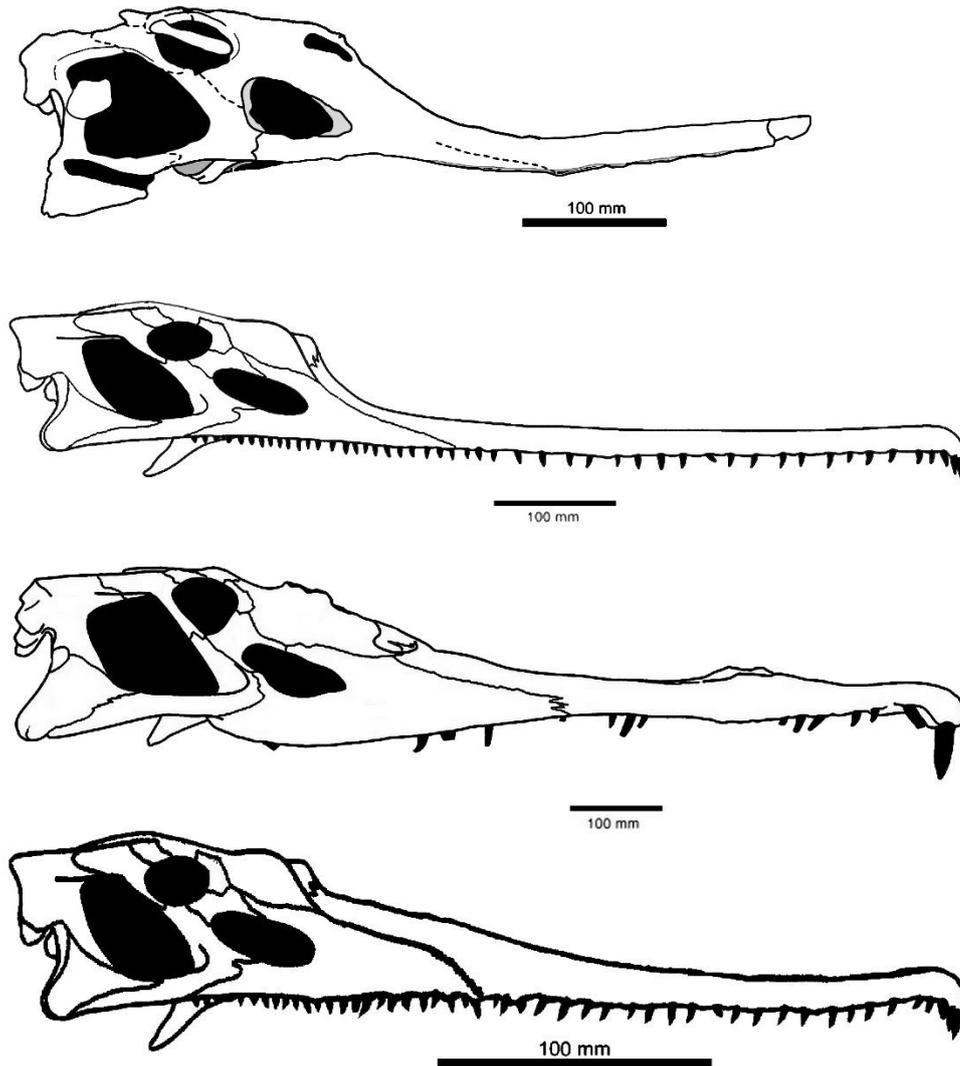
Figure 32. Skulls in *Mystriosuchus* clade. A. *Mystriosuchus planirostris* (modified from Hungerbühler, 2002); B. *Mystriosuchus westphali* (modified from Hungerbühler, 2002); C. *Mystriosuchus steinbergeri* (modified from Butler et al., 2019); D. Reconstruction of *Mystriosuchus* sp. from Greenland, modified from *M.planirostris* skull.

The character 95 (Degree of heterodonty) was introduced to better clarify the difference between the basal and more derived phytosaurs. As seen in Hungerbühler (2000), the three sets dentition of the Greenland phytosaur is shared by *Nicrosaurus, Leptosuchus, Smilosuchus* and *Machaeroprosopus*, more derived phytosaurs englobed in the clade Leptosuchomorpha (Jones & Butler, 2018). However, *Mystriosuchus* and *Redondasaurus* exhibits the two sets dentition, while being enclosed in Leptosuchomorpha too.

As Hungerbühler (2000) indicated, isolated teeth cannot be used to indicate a taxon, due to the needs for further studies. In the Greenland phytosaur, most of the teeth studied were isolated and could not be used following the previous indication. However, in the mandible NHMD-Hc1 were still attached teeth. And as explained in Hungerbühler (2000), the mandibular teeth follow the same features as their upper jaw counterpart, so we found teeth attached in the mandible related with their counterparts (snout, premaxilla and maxilla), and these teeth can be used to provide the statement "3 set dentition" to the character 95.

The post-cranial material among phytosaurs is poorly studied. In phylogenetic analysis such as in Ezcurra (2016) and Nesbitt (2011), the phytosaur are more studied to know their relationship with other archosauriformes. However, the diagnosis of phytosaurs has only six post-cranial features out of the total 30. It has been discussed that some phytosaurs, like *Mystriosuchus steinbergeri*, could have lived in a marine ecosystem (Butler et al., 2019). The adaptations to a more aquatic lifestyle would imply some changes in its body and more differential features among phytosaurs, not only in the skull and mandibles, but also in the post-cranial bones. Here, a common character among *Mystriosuchus* caudal vertebrae was found (the anterior and posterior projections in the basis of the neural spine, Figs.17-18), while not described in other researches, despite its potential diagnostic feature. Because of this, further studies need to be made focused into the post-cranial material of phytosaurs to better understand the relationship and evolution among them.

IMPLICATIONS

The *Mystriosuchus* sp. found in Greenland gives us a series of implications to understand better the Malmros Klint Formation chronology and geography, and the taxonomy and ontogeny of the Greenland remains.

Chronologically, Greenland *Mystriosuchus* sp. is from the Norian. The other species of *Mystriosuchus* clade (*M. planirostris*, *M. westphali*, and *M. steinbergeri*) are restricted to the Alaunian and Sevatian (Middle to Late Norian; Hungerbühler, 2002; Butler et al., 2019), while the North American phytosaurs, such as *Angistorhinus* and *Machaeroprosopus*, are restricted to Carnian-Norian (Lucas et al., 2002) and Norian-Rhaetian (Hunt & Lucas, 1993; Parker et al., 2013), respectively. Even though the three clades appear in the Norian, the short range of the *Mystriosuchus* clade reinforces the range of the Greenland Triassic layers to the Norian age.

Geographically, the Greenland phytosaur reinforce the previous concept of the European faunal influence between East Greenland and Europe by Late Triassic suggested by Clemmensen et al. (1998), and later supported by other researchers (Sulej et al., 2014; Marzola et al., 2017b), with common species in stem mammals as *Brachyzostrodon* (Jenkins et al., 1994;), amphibians as *Cyclotosaurus* (Sigogneau-Russell, 1983; Jenkins et al., 1994) and archosaurs as *Plateosaurus* (Jaekel, 1910a; Jenkins et al., 1994) or *Aetosaurus* (Jenkins et al., 1994; Schoch, 2007). Moreover, this is the northernmost species of *Mystriosuchus* species ever found. North America and Europe-Greenland was separated by an arid and dry environmental belt (Benton, 2016), that can be placed nearly the North Hadley Cell range (Fig.33), which can be an explanation of the separation between the North American and European-Greenland faunas at the end of the Triassic.
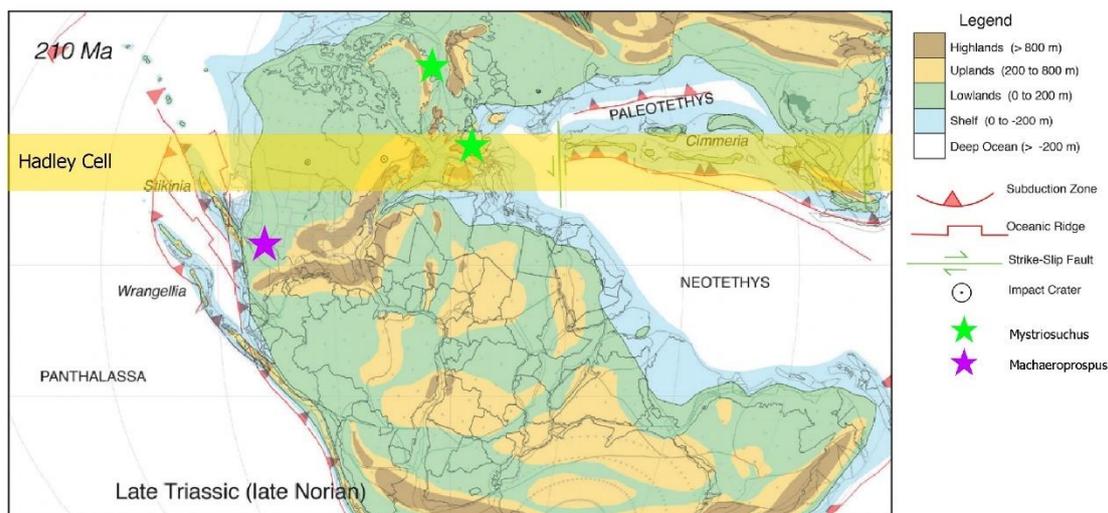
Figure 33. Map of the Late Triassic (modified from Scotese, 2018). The stars mark the position where *Machaeroprosopus* (purple) and *Mystriosuchus* (green) appear.

Taxonomically, the phytosaur reported in Greenland has the potential to be a new species of the genus *Mystriosuchus*. However, there is a polytomy with *Mystriosuchus planirostris* and *M. westphali* due to the lack from cranial material of the Greenland phytosaur.

Ontogenically, even there can be referred at least four individuals, the remains were isolated and only a few bones are doubled (humeri, premaxilla, jugals, fibulae), so the ontogenetic variation is difficult to determine. Following some ontogenetic studies done in crocodilians (Brochu, 1996), there can be more ontogenetical features in the Greenland phytosaur. Such as in some vertebrae, where the centrum and neural arch have the suture between them (NHMD-131) or are isolated one from the other following the suture (NHMD-Eb9a, NHMD-Eb9b). The appearance of the suture is a juvenile feature, while the adults have centrum and neural arch totally fused, with no suture remain (Brochu, 1996). However, as the researcher explains, it can be conditioned also by sexual dimorphism. Another example of ontogenetic difference is the juvenile scapula (NHMD-Gb39), which is different in shape and size with the adult humerus found.

However, the Greenland *Mystriosuchus* sp. opens a series of questions. The phylogeny suggest it could be a new species, even with low cranial material found. There are characters found in the cranial region (projections of the surangular in the mandible) and in the post-cranial region (the anterior and posterior projections in the base of the neural spine of the caudal vertebrae) that require better study to improve a phylogeny based also in post-cranial material.

Finding at least four individuals of different ontogeny also opens some questions: if they were gregarious or from the same family population, or if the more juveniles were from the same family population as the adult.

CONCLUSIONS

- The Mateus Quarry in Lepidopteris Elv (East Greenland) provided nearly 150 bones of phytosaurs, which are the first undisputed phytosaurs reported from Greenland.
- The bone assemblage is from a bone bed with at least four individuals of three age ranges (very juvenile – the "baby" scapula –, juvenile and adult).
- Based on the anatomy of all the bones, there is no sign of intraspecific variation between the phytosaurs in the Quarry, which therefore are identified as one species only.
- The bones are attributed to *Mystriosuchus* based Jones & Butler (2018)'s on character 2 (interpremaxillary fossa, narrow slit) and character 88 (proximal section of postorbital descending process where posterior border of orbit meets skull roof, posterior border of orbit remains thin until it reaches the skull roof).
- The Greenland phytosaur represents a species of *Mystriosuchus* with the unique characters 78 (shape of retroarticular process in lateral view distally rounded or blunt) and 95 (degree of heterodonty, tripartite upper dentition). Besides that, there were found potential *Mystriosuchus* common features, as the anterior and posterior projections of the basis of the neural spine in the caudal vertebrae, plus the potential unique feature of the dorsally anterior and posterior projections of the angular.
- Due to the Middle-Late Norian range of *Mystriosuchus* clade, it is here used as a potential fossil indicator of those periods to narrow the age range of the Greenland layers where the Greenland phytosaur was found.
- Moreover, this is the first *Mystriosuchus* outside Europe. It reinforces the European affinity of Triassic Greenland vertebrate fauna, despite the fact the closer geographic proximity to North American mainland. The arid latitudinal band that resulted from the north limb of the Hadley shell may have played a role as a geographic barrier that prevented crossing by aquatic animals, such as phytosaurs.

BIBLIOGRAPHY CITED

Ballew, K. L. (1989). A phylogenetic analysis of Phytosauria (Reptilia: Archosauria) from the Late Triassic of the western United States. In Lucas, S. G. & Hunt, A. P. (eds) Dawn of the age of dinosaurs in the American Southwest, 309–39. Albuquerque: New Mexico Museum of Natural History and Science.

Barrett, P. M., Sciscio, L., Viglietti, P. A., Broderick, T. J., Suarez, C. A., Sharman, G. R., Jones, A. S., Munyikwa, D., Edwards, S. F., Chapelle, K. E. J., Dolman, K. N., Zondo, M., & Choiniere, J. N. (2020). The age of the Tashinga Formation (Karoo Supergroup) in the Mid-Zambezi Basin, Zimbabwe and the first phytosaur from sub-Saharan Africa. Gondwana Research.

Benton, M. J. (2016). The Triassic. Current Biology, 26(23), R1214-R1218.

Brochu, C. A. (1996). Closure of neurocentral sutures during crocodilian ontogeny: implications for maturity assessment in fossil archosaurs. Journal of Vertebrate Paleontology, 16(1), 49-62.

Broom, R. (1913). Note on *Mesosuchus browni*, Watson, and on a new South African Triassic pseudosuchian (*Euparkeria capensis*). Records of the Albany Museum, 2, 394-396.

Brusatte, S. L., Butler, R. J., Niedzwiedzki, G., Sulej, T., Bronowicz, R., & Satkūnas, J (2013). First record of Mesozoic terrestrial vertebrates from Lithuania: phytosaurs (Diapsida: Archosauriformes) of probable Late Triassic age, with a review of phytosaur biogeography. Geological Magazine, 150(1), 110-122.

Buffetaut, E., & Ingavat, R. (1982). Phytosaur remains (Reptilia, Thecodontia) from the Upper Triassic of North-Eastern Thailand. Géobios, 15(1), 7-17.

Buffetaut, E., Martin, M., & Monod, O. (1988). Phytosaur remains from the Cenger Formation of the Lycian Taurus (Western Turkey): Stratigraphical implications. Géobios, 21(2), 237-243.

Burmeister, K. C., Flynn, J. J., Parrish, J. M., & Wyss, A. R. (2006). Paleogeographic and liostratigraphic implications of new Early Mesozoic vertebrates from Poamay, central Morondava Basin, Madagascar. New Mexico Museum of Natural History and Science Bulletin, 37, 457-475.

Butler, R. J., Jones, A. S., Buffetaut, E., Mandl, G. W., Scheyer, T. M., & Schultz, O. (2019). Description and phylogenetic placement of a new marine species of phytosaur (Archosauriformes: Phytosauria) from the Late Triassic of Austria. Zoological Journal of the Linnean Society, 187(1), 198-228.

Case, E. C. (1922). New reptiles and stegocephalians from the upper Triassic of western Texas. Carnegie Institution of Washington, 321, 1–84.

Case, E. C. (1930). On the lower jaw of *Brachysuchus megalodon*. Contributions from the Museum of Paleontology, University of Michigan, 3(8), 155-161.

Chaterjee, S. (1978). A primitive Parasuchid (Phytosaur) reptile from the Upper Triassic Maleri Formation of India. Paleontology, 21(1), 83-127.

Clemmensen, L. B. (1979). Triassic lacustrine red-beds and palaeoclimate: The „Buntsandstein" of Helgoland and the malmros Klint member of East Greenland. Geologische Rundschau, 68(2), 748-774.

Clemmensen, L. B., Kent, D. V., & Jenkins Jr., F. A. (1998). A Late Triassic lake system in East Greenland: facies, depositional cycles and palaeoclimate. Palaeogeography, Palaeoclimatology, Palaeoecology, 140, 135–159.

Clemmensen, L. B., Mila, J., Adolfssen, J. A. N. S., Estrup, E. J., Frobøse, N., Klein, N., Mateus, O., & Wings, O. (2015). The vertebrate-bearing Late Triassic Fleming Fjord Formation of central East Greenland revisited: stratigraphy, palaeoclimate and new palaeontological data. In: Kear, B.P., Lindgren, J., Hurum, J.H., Milàn, J. & Vajda, V. (eds) Mesozoic Biotas of Scandinavia and its Arctic Territories. Geological Society, London, Special Publications, 434.

Clemmensen, L.B., Kent, D.V., Mau, M., Mateus, O. & Milàn, J. (2020). Triassic lithostratigraphy of the Jameson Land basin (central East Greenland), with emphasis on the new Fleming Fjord Group. Bulletin of the Geological Society of Denmark, vol. 68.

Colbert, E. H. (1947). Studies of the phytosaurs *Machaeroprosopus* and *Rutiodon*. Bulletin of the AMNH, 88(2), 53-96.

Cope, E. D. (1881). *Belodon* in New Mexico. The American Naturalist 15, 922–23.

Datta, D., Kumar, N., & Ray, S. (2019a). Taxonomic identification of isolated phytosaur (Diapsida, Archosauria) teeth from the Upper Triassic of India and their significances. Historical Biology, 1-11.

Datta, D., Ray, S., & Bandyopadhyay, S. (2019b). Cranial morphology of a new phytosaur (Diapsida, Archosauria) from the Upper Triassic of India: implications for phytosaur phylogeny and biostratigraphy. Papers in Paleontology, 1-34.

Dilkes, D., & Arcucci, A. (2012). Proterochampsa barrionuevoi (Archosauriformes: Proterochampsia) from the Late Triassic (Carnian) of Argentina and a phylogenetic analysis of Proterochampsia. Palaeontology, 55(4), 853-885.

Dutuit, J. M. (1977). Description du crâne de *Angistorhinus talainti* n. sp: un nouveau Phytosaure du Trias atlasique marocain. Muséum national d'histoire naturelle.

Dzik, J. (2001): A new Paleorhinus fauna in the Early Late Triassic of Poland, Journal of Vertebrate Paleontology, 21:3, 625-627

Emmons, E. (1856). Geological report on the Midland Counties of North Carolina. George P. Putnam and Co., New York, XX + 352 pp

Erwin, D. H. (1994). The Permo–Triassic extinction. Nature, 367(6460), 231.

Ewer, R. F. (1965). The anatomy of the thecodont reptile *Euparkeria capensis* Broom. Philosophical Transactions of the Royal Society of London. Series B, Biological Sciences, 248(751), 379-435.

Ezcurra M. D. (2016). The phylogenetic relationships of basal archosauromorphs, with an emphasis on the systematics of proterosuchian archosauriforms. PeerJ 4:e1778.

Fraas, E. (1866). Vor der Sündfluth. Eine Geschichte der Urwelt. Hoffmann, Stuttgart, 512 pp.

Fraas, E. (1896). Die schwäbischen Trias – Saurier nach dem Material der Kgl. Naturalien-Sammlung in Stuttgart zusammengestellt. Stuttgart: Schweizerbart.

Godefroit, P., Cuny, G., Delsate, D., & Roche, M. (1998). Late Triassic Vertebrates from Syren (Luxembourg). Neues Jahrbuch Fur Geologie und Palaontologie Abhandlungen, 210, 305-343.

Goloboff, P. A., & Catalano, S. A. (2016). TNT version 1.5, including a full implementation of phylogenetic morphometrics. Cladistics, 32(3), 221-238.

Golonka, J. (2007). Late Triassic and Early Jurassic palaeogeography of the world. Palaeogeography, Palaeoclimatology, Palaeoecology, 244, 297–307.

Gozzi, E., & Renesto, S. (2003). A complete specimen of *Mystriosuchus* (Reptilia, Phytosauria) from the Norian (Late Triassic) of Lombardy (Northern Italy). Rivista Italiana di Paleontologia e Stratigrafia (Research In PaleontologyandStratigraphy), 109(3).

Griffin, C. T., Stefanic, C. M., Parker, W. G., Hungerbühler, A., & Stocker, M. R. (2017). Sacral anatomy of the phytosaur *Smilosuchus adamanensis*, with implications for pelvic girdle evolution among Archosauriformes. Journal of Anatomy, 231(6), 886-905.

Guarnieri, P., Brethes, A., and Rasmussen, T. M. (2017). Geometry and kinematics of the Triassic rift basin in Jameson Land (East Greenland). Tectonics, 36, 602–614,

Hendrickx, C., & Mateus, O. (2014). *Torvosaurus gurneyi* n. sp., the Largest Terrestrial Predator from Europe, and a Proposed Terminology of the Maxilla Anatomy in Nonavian Theropods. PLOS ONE 9(3): e88905.

Holloway, W. L. (2018). Comparative Cranial Ecomorphology and Functional Morphology of Semiaquatic Faunivorous Crurotarsans (Doctoral dissertation, Ohio University).

Huene, F. B. D. Sc. (1908). XXXIII.–On Phytosaurian remains from the magnesian Conglomerate of Bristol (Rileyaplatyodon), Annals and Magazine of Natural History: Series 8, 1(3), 228-230.

Hungerbühler, A. (2000). Heterodonty in the European phytosaur *Nicrosaurus kapffi* and its implications for the taxonomic utility and functional morphology of phytosaur dentitions. Journal of Vertebrate Paleontology, 20(1), 31-48.

Hungerbühler, A. (2002). The Late Triassic phytosaur *Mystriosuchus westphali*, with a revision of the genus. Palaeontology, 45(2), 377-418.

Hungerbühler, A., & Hunt, A P. (2000). Two new phytosaur species (Archosauria, Crurotarsi) from the Upper Triassic of southwest Germany: Neues Jahrbuch fur PaUiontologie Monatshefte, v. 2000, p. 467- 484.

Hungerbühler, A., Mueller, B., Chatterjee, S., & Cunningham, D. P. (2013). Cranial anatomy of the Late Triassic phytosaur *Machaeroprosopus*, with the description of a new species from West Texas. Earth and Environmental Science Transactions of the Royal Society of Edinburgh, 103, 269-312.

Hunt, A. P., Lucas, S. G., & Spielmann, J. A. (2006). Sexual dimorphism in a large brachyrostral phytosaur (Archosauria: Crurotarsi) from the Late Triassic of western North America. New Mexico Museum of Natural History and Science Bulletin, 37, 563-567.

Hunt, A.P., & Lucas, S.G. (1993). A new phytosaur (Reptilia: Archosauria) genus from the uppermost Triassic of the western United States and its biochronological significance. New Mexico Museum of Natural History and Science Bulletin, 3, 193-196.

Isasmendi, E., Sáez-Benito, P., Torices, A., Navarro-Lorbés, P., & Pereda Suberbiola, X. (2020). New insights about theropod palaeobiodiversity in the Iberian Peninsula and Europe: Spinosaurid teeth (Theropoda, Megalosauroidea) from the Early Cretaceous of La Rioja (Spain). Cretaceous Research.

Jaeger, G. (1828). Uber die fossile Reptilien, welche in Württemberg aufgefunden worden sind: Stuttgart, Metzler, 48.

Jaekel, O. (1910a). Die Fußstellung und Lebensweise der großen Dinosaurier. Zeitschrift der Deutschen Geologischen Gesellschaft, 270-277.

Jaekel, O. (1910b). Über einen neuen Belodonten aus dem Buntsandstein von Bernburg. Sitzungsberichte der Gesellschaft naturforschender Freunde zu Berlin 5, 197–229.

Jenkins, F. A. Jr., Shubin, N. H., Amarel, W. W., Gatesy, S. M., Schaff, C. R., Clemmensen, L. B., Downs, W. R., Davidson, A. R., Bonde, N. C., & Osbaeck, F. (1994). Late Triassic continental vertebrates and depositional environments of the Fleming Fjord Formation, Jameson Land, east Greenland. Meddelelser om Grønland, Geoscience, (32), 1-25.

Jones, A. S., & Butler, R. J. (2018). A new phylogenetic analysis of Phytosauria (Archosauria: Pseudosuchia) with the application of continuous and geometric morphometric character coding. PeerJ,6:e5901.

Kammerer, C. F., Butler, R. J., Bandyopadhyay, S., & Stocker, M. R. (2015). Relationships of the Indian phytosaur *Parasuchus hislopi* Lydekker, 1885. Papers in Palaeontology, 2(1), 1–23.

Kimmig, J. (2009). Functional morphology and systematic palaeontology of the Phytosauria (Archosauria; Crurotarsi) and the development of their Late Triassic habitats (Doctoral dissertation, Department of Life Sciences and the Natural History Museum, Imperial College London).

Kimmig, J., & Arp, G. (2010). Phytosaur remains from the Norian Arnstadt Formation (Leine Valley, Germany), with reference to European phytosaur habitats. Paleodiversity, 3, 215-224.

Kischlat, E. E., & Lucas, S. G. (2003). A phytosaur from the Upper Triassic of Brazil. Journal of Vertebrate Paleontology, 23(2), 464-467.

Kuhn, O. (1936). Weitere Parasuchier und Labyrinthodonten aus dem Blasensandstein des mittleren Keuper von Ebrach. Palaeontographica Abteilung A 83: 61–98.

Lagnaoui, A., Klein, H., Saber, H., Fekkak, A., Belahmira, A., & Schneider, J. W. (2016). New discoveries of archosaur and other tetrapod footprints from the Timezgadiouine Formation (Irohalene Member, Upper Triassic) of the Argana Basin, western High Atlas, Morocco–Ichnotaxonomic implications. Palaeogeography, palaeoclimatology, palaeoecology, 453, 1-9.

Larson, D. W. (2008). Diversity and variation of theropod dinosaur teeth from the uppermost Santonian Milk River Formation (Upper Cretaceous), Alberta: a quantitative method supporting identification of the oldest dinosaur tooth assemblage in Canada. Canadian Journal of Earth Sciences, 45(12), 1455-1468.

Li, C., Wu, X. C., Zhao, L. J., Sato, T., & Wang, L. T. (2012). A new archosaur (Diapsida, Archosauriformes) from the marine Triassic of China. Journal of Vertebrate Paleontology, 32(5), 1064-1081.

Long, R. A., & Murray, P. A. (1995). Chapter 4 - The Phytosaurs of the Southwestern Triassic, with comments on the classification and relationships of the Parasuchia. In: Late Triassic (Carnian and Norian) Tetrapods from the Southwestern United States. Bulletin 4(4). New Mexico Museum of Natural History and Science.

Lucas, S. G., Heckert, A. B., & Kahle, R. (2002). Postcranial anatomy of *Angistorhinus*, a Late Triassic phytosaur from West Texas. Upper Triassic Stratigraphy and Paleontology, New Mexico Museum of Natural History and Science Bulletin, 21.

Lydekker R. (1885). The Reptilia and Amphibia of the Maleri and Denwa groups. Palaeontologia Indica, 1 1(1), 1–38.

Maisch, M. W., & Kapitzke, M. (2010): A presumably marine phytosaur (Reptilia: Archosauria) from the pre-planorbis beds (Hettangian) of England Neues Jahrbuch für Geologie und Paläontologie - Abhandlungen, 257: 373-379; Stuttgart.

Manspeizer, W. (1988). Triassic–Jurassic rifting and opening of the Atlantic: an overview. In Developments in Geotectonics, 22, 41-79. Elsevier.

Marzola, M. (2019). The Late Triassic vertebrate fauna of the Jameson Land Basin, East Greenland: description, phylogeny, and paleoenvironmental implications. PhD Thesis. UNL, 260 pp.

Marzola, M., Mateus, O., Milàn, J., & Clemmensen, L. B. (2017a). The 2016 Dinosaur Expedition to the Late Triassic of the Jameson Land Basin, East Greenland, p. 249-253. In: Barrios de Pedro, S.; Blanco Moreno, C.; de Celis, A;, Colmenar, J.; Cuesta, E.; García-Martínez, D.; Gascó, F.; Jacinto, A.; Malafaia, E.; Martín Jiménez, M.; de Miguel Chaves, C.; Mocho, P.; Pais V.; Páramo Blázquez, A.; Pereira, S.; Serrano Martínez, A.; Vidal, D.(Eds), A Glimpse of the Past. Abstractbookofthe XV Encuentro de Jóvenes Investigadores en Paleontología/XV Encontro de Jovens Investigadores em Paleontologia, Lisboa.

Marzola, M., Mateus, O., Shubin, N. H., Clemmensen, L. B. (2017b). *Cyclotosaurus naraserluki*, sp. nov., a new Late Triassic cycloosaurid (Amphibia, Temnospondyli) from the Fleming Fjord Formation of the Jameson Basin (East Greenland). Journal of Vertebrate Paleontology, 37(2), e1303501.

Mateus, O., Butler, R. J., Brusatte, S. L., Whiteside, J. H., & Steyer, J. S. (2014a). The first phytosaur (Diapsida, Archosauriformes) from the Late Triassic of the Iberian Peninsula. Journal of Vertebrate Paleontology, 34(4), 970-975.

Mateus, O., Clemmensen, L. B, Klein, N., Wings, O., Frobøse, N., Milàn, J., Adolfssen, J. S., & Estrup, E. (2014b). The Late Triassic of Jameson Land revisited: new vertebrate findings and the first phytosaur from Greenland. In: Maxwell, E. & Miller-Camp, J. (eds) Society of Vertebrate Paleontology, 74th Meeting, Program and Abstracts, 5–8 November 2014, Berlin, Germany. Society of Vertebrate Paleontology, Bethesda, MD, 182.

McGregor, J. H. (1906). The Phytosauria, With Especial Reference to *Mystriosuchus* and *Rhytidodon* (Vol. 9). American Museum of Natural History.

Mehl, M. G. (1913). *Angistorhinus*, a new genus of Phytosauria from the Trias of Wyoming. The Journal of Geology, 21(2), 186-191.

Mehl, M. G. (1915). The Phytosauria of the Trias. The Journal of Geology, 23(2), 129-165.

Mehl, M. G., & Branson, E. B. (1928). *Pseudopalatus pristinus*: a new genus and species of phytosaurs from Arizona (Vol. 3, No. 1-4). University of Missouri.

Mehl, M. G. (1928). The Phytosauria of the Wyoming Triassic. Denison University Bulletin, Journal of the Scientific Laboratories 23, 141– 72. Granville, Ohio: Denison University.

Meyer, H. (1863). Der Schädel des Belodon aus dem Stubensandstein des oberen Keupers. – Palaeontographica, 10: 227–246

Nesbitt, S. J. (2011). The early evolution of archosaurs: relationships and the origin of major clades. Bulletin of the American Museum of Natural History, 2011(352), 1-292.

Nesbitt, S. J., Smith, N. D., Irmis, R. B., Turner, A. H., Downs, A., & Norell, M. A. (2009). A complete skeleton of a Late Triassic saurischian and the early evolution of dinosaurs. Science, 326(5959), 1530-1533.

Nøttved, A., Johannessen, E. P., & Surlyk, F. (2008). The Mesozoic of Western Scandinavia and East Greenland. Episodes, 31(1), 59.

Owen, R. (1859). On the orders of fossil and recent Reptilia and their distribution in time. Report of the British Association for the Advancement of Science, 153-166.

Parker, W. G., Hungerbühler, A., & Martz, J. W. (2013). The taxonomic status of the phytosaurs (Archosauriformes) *Machaeroprosopus* and *Pseudopalatus* from the Late Triassic of the western United States. Earth and Environmental Science Transactions of the Royal Society of Edinburgh, 103(3-4), 265-268.

Renesto, S. (2008). Remains of a juvenile phytosaur from the Late Triassic of Northern Italy. Rivista Italiana di Paleontologia e Stratigrafia. 114 (1), 155-160.

Romer, A. S. (1956). Chapter 6: The axial skeleton. In: The Osteology of the Reptiles. The University of Chicago Press, Chicago, 218-297.

Rossmann, T., Witzel, U., & Preuschoft, H. (2005). Mechanical stress as the main factor in skull design of the fossil reptile *Proterosuchus* (Archosauria). In Bionik (pp. 517-528). Springer, Berlin, Heidelberg.

Sahney, S., & Benton, M. J. (2008). Recovery from the most profound mass extinction of all time. Proceedings of the Royal Society B: Biological Sciences, 275, 759-765.

Schoch, R. R. (2007). Osteology of the small archosaur *Aetosaurus* from the Upper Triassic of Germany. Neues Jahrbuch für Geologie und Paläontologie-Abhandlungen, 246(1), 1-35.

Schubert, J. K., & Bottjer, D. J. (1995). Aftermath of the Permian-Triassic mass extinction event: Paleoecology of Lower Triassic carbonates in the western USA. Paleogeography, Paleoclimatology, Paleoecology, 116, 1-39.

Scotese, C. (2018, November). The Triassic world: plate tectonics, paleogeography, paleoclimate & paleobiogeography. In GSA Annual Meeting in Indianapolis, Indiana, USA-2018. GSA.

Sereno, P. C. (1991). Basal archosaurs: phylogenetic relationships and functional implications. Journal of Vertebrate Paleontology, 11(S4), 1-53.

Sigogneau-Russell, D. (1983). Nouveaux taxons de Mammifères rhétiens. Acta Palaeontologica Polonica, 28(1-2).

Spielmann, J. A., & Lucas, S. G. (2012). Tetrapod Fauna of the Upper Triassic Redona Formation East-central New Mexico: The Characteristic Assemblage of the Apachean Land-vertebrate Faunachron, New Mexico Museum of Natural History and Science Bulletin, 55.

Stocker, M. R. (2010). A new taxon of phytosaur (Archosauria, Pseudosuchia) from the Late Triassic (Norian) Sonsela Member (Chinle Formation) in Arizona, and a critical reevaluation of Leptosuchus Case, 1922. Palaeontoloy, 53(5), 997-1022.

Stocker, M. R. (2012). A new phytosaur (Archosauriformes, Phytosauria) from the Lot's Wifebeds (Sonsela Member) within the Chinle Formation (Upper Triassic) of Petrified Forest National Park, Arizona, Journal of Vertebrate Paleontology, 32:3, 573-586.

Stocker, M. R., & Butler, R. J. (2013). Phytosauria. Geological Society, London, Special Publications, 379.

Stocker, M. R., Zhao, L. J., Nesbitt, S. J., Wu, X. C., & Li, C. (2017). A short-snouted, Middle Triassic phytosaur and its implications for the morphological evolution and biogeography of Phytosauria. Scientific reports, 7, 46028.

Sulej, T., Woniewicz, A., Bonde, N., Blazejowski, B., Niedzwiedzki, G., & Talanda, M. (2014). New perspectives on the Late Triassic vertebrates of East Greenland: preliminary results of a Polish–Danish palaeontological expedition. Polish Polar Research, 35 (4), 541-552.

Tong, J., Zhang, S., Zuo, J., & Xiong, X. (2007). Events during Early Triassic recovery from the end-Permian extinction. Global and Planetary Change, 55(1-3), 66-80.

Turner, A. H., & Nesbitt, S. J. (2013). Body size evolution during the Triassic archosauriform radiation. Geological Society, London, Special Publications, 379(1), 573-597.

von Huene, F. (1915). On reptiles of the New Mexican Trias in the Cope Collection. Bulletin of the American Museum of Natural History, 34, 485-507.

von Huene, F. (1922) Neue Beiträge zur Kenntnis der Parasuchier. Jb Preuss Geol Landesanst 42: 59–160.

von Meyer, H., & Plieninger, T. (1844). Beiträge zur Paläontologie Württemberg's: enthaltend die fossilen wirbelthierreste aus den triasgebilden mit besonderer rücksicht auf die Labyrinthodonten des Keupers. E. Schweizerbart., 132, 12 pls.

Witzmann, F., Schwarz-Wings, D., Hampe, O., Fritsch, G., & Asbach, P. (2014). Evidence of Spondyloarthropathy in the Spine of a Phytosaur (Reptilia: Archosauriformes) from the Late Triassic of Halberstadt, Germany. PLoS ONE, 9(1): e85511.

Zeigler, K. E., Heckert, A. B., & Lucas, S. G. (2003). An illustrated atlas of the phytosaur (Archosauria: Parasuchidae) postcrania from the Upper Triassic Snyder Quarry (Petrified Forest Formation, Chinle Group). Paleontology and Geology of the Upper Triassic (Revueltian) Snyder Quarry, New Mexico: Bulletin 24, 24, 89.

Zerfass, H., Lavina, E. L., Schutz, C. L., Garcia, A. J. V., Faccini, U. F., & Chemale Jr., F. (2003). Sequence stratigraphy of continental Triassic strata of Southernmost Brazil: a contribution to Southwestern Gondwana palaeogeography and palaeoclimate. Sedimentary Geology, 161, 85–105.

Ziegler, P. A. (1988). Post-Hercynian plate reorganization in the Tethys and Arctic–North Atlantic domains. In Developments in Geotectonics, Elsevier, 22, 711-755.

APPENDIX

APPENDIX 1 – TnT MATRIX

nstates 8 ;
xread 'Data saved from TNT'
95 44
&[num]
Angistorhinus_grandis
11001010??1112?1101101?1000???10?10?????0??0????0???2??10100??0?01?11??????0??0120?????????1?01
Angistorhinus_talainti
?100101000?0121100110101000121100100021?01[12]0110?0111211101000?1?00012011?201??01200??0010001??1
Coburgosuchus_goeckeli
????1????????????01??????00?1021?0031?1021?100210?1030201000100021?????????????????00010????
Ebrachosuchus_neukami
1??0000200201111010?020?010121100101?0??0020??0?000?20100001001?0?0210101100??00013??0201??0??1
Leptosuchus_crosbiensis
1100[01][01]4?1?[12]012?001[01]10301100[01]1110010002[01]?[01][01][12][01]?101[12]00?[12]1?0101?[02]01?00?12??11?0010[01]?10[03]??0[012][01]0[01]001?2
Leptosuchus_studeri
110011421110120001 01?2011000111001000?1?002?110011??2120101????00001????????
??11100??0000?00???
Machaeroprosopus_andersoni
111100421?1012?001100??10001?110????????????????20????????2120111??121?12201??1120????????00???
Machaeroprosopus_buceros
1100[01]0421?1012?0[01]1100201000010[01]02[12]11[01][12]2010[012]1011120[01]110?02022201[12]?02121?12211??11[12]000[01]0100100??1
Machaeroprosopus_jablonskiae
???????????1?????10?????000??102???0???100????020??00??2?22?0111???21?????????
????????0???????
Machaeroprosopus_lottorum
110000111010121111100201000[01]1010[02]211[01]3201001111[01]201[01]00002032201[12]102120112211??[01]120001?001100???
Machaeroprosopus_mccauleyi
1111102[12]1?[12]012?001[01]0030110001010211[01][01][23][12]110[012]1?[01][01]120[01]010?020222011[01]02120?1?2011??1[12]0[03][01]1[01][12]00[01]00102
Machaeroprosopus_pristinus
[01]10000[01][01]1?2012?[01][01]1[01]00[123]01[01]00[01][01]010211[01][01]12[01]10[012]1?1[01]120[01][01]1[01]?0202[12]20[01]11[01][02]12[01]?12211100120001[01]10110010
1
Mystriosuchus_planirostris
1?00001[01]0021121[01]00110201[01]00[01]01110110?0??10011?[01]02?11100010301021 02[02]1201122101001200101210?10111
Mystriosuchus_westphali
1200[01]202002[01]121[01]00110[23]01[01]0010011211[01]?0??100?1?[01]02?1110001030 [01]1[02]10201?0?1221???01200101210?10??1

61

Nicrosaurus_kapffi
11[01]01032[01]110121001011[23]0[01]1000011001[01]0021?102[01]010020??0030202100
20012110011210??11100010001100??2
Nicrosaurus_meyeri
1100000[12]0[01]10121[01]01011[23]0[01]1000[01]11001[01]0031?100?0100200?003020?
??0[12]0?0212011[12]2[01]01001[01]0001000[01]?00??1
Paleorhinus_sawini
110010000?0011?1010?030?10000110?001?0??0120??0?0?1121?10001001?02?1?????????
?0?000??001?000???
Parasuchus_angustifrons
0100000[01]010011110[01]0?0[01]1001[01][01][02]110000[12]?0??01[12][01]??0?0?0?[12]
110000100[01]?0001001[01]0100??00011??00[01]0?10???
Parasuchus_bransoni
[01]10000000?[01]011?1001?0[12]1?[01]1[02][01][012]110[01]001?0??01[12]0??0?01[01]1
21?00000001?0[01]01100?0100000000[01]??00[01]0000???
Parasuchus_hislopi
01?0000000001111000?0110011[01]111000[01]2?0??012?1?0?01??211000000?1??00110?
??????000011??0010010??1
Phytosaurus_doughtyi
????????????12??0?10?[012]???0001?100101120?1021?1?1[12]?0?21?0101?001??001????
????????????000010????
Pravusuchus_hortus
110[01]00221?1012?001011?011000001011[01][01]01[012]?10[12]??1[01][01]100?21?0101
0001??00120???2??????[12]00??0100[01]00???
Protome_batalaria
1100?01?0??01??0?1???????00?1?101????20?100??100?00?10?01011201?10??21????????
01?????????1?0?1?
Redondasaurus_bermani
1101002?1?0012??0?000?01?0011?10?11?131?1001??10201121?030322?011?012?????1?
???1203111200000??2
Redondasaurus_gregorii
110[01]002?1??012??0???00301000[01][12]?102111[01]31?1001?11[01]2011[02]0?0303220[
01]1110121????1???0120[03][01]11201000?02
Rutiodon_carolinensis
110000101?2012?[01]0[01]11[01]10100[01]1111[01]1100020?000??1??[01]0??21?000[01]0
0?0?00?120??2210?101[02]00??011?0?1??1
Smilosuchus_adamanensis
1100100?1??012?001100[23]0?1000[01]?101100030?102??000100?21?01011001?0021[12]
0??1?001001100??000?000?0?
Smilosuchus_gregorii
1111102[12]1?1012?0011[01]03011000[01]?[01]01100030?1021?[01]1[01]200?21?0101100
[01]?00212??112001[01]?1[12]0[03]??000000000?
Smilosuchus_lithodendrorum
111[01]102?1?1012?001010?01100[01]??1021[01]0?31?10[01]??10[01]??0?21?000?0????0
?012???????10?110[03]?1000010010?
Wannia_scurriensis
????0?0?0??011?100??01010?0????0??0000????????0?0??????0?00?001?000?00?00100??
00002????????0???
MB.R._2747
110000??????12??0?00??01?00???102?1?????10???????2????1?103?1?0?????20????????0
??0010??????????

TMM_31100_1332
11000010??2112?11011010?00011110?1000?0?012??1??001121?10100?00??10121???00
??0?200??0?1?0?1???
Mystriosuchus_steinbergeri
?2000?1?0??112?100010101?00?0?1?2110?0???0????002??????0?0???????2?????1?????
01200???2000?0?0?
NMMNHS_P31094
????1??21??012?001000?01000??0102211031?100??010200?00?03?32??011??1?????211?
??1200011201000???
NMMNHS_P4256
1111002?1?0012?00110?30100001010?101?31?1001?00120??10?020??2?????0?1????????1
0?1203011200000?0?
PEFO_34852
111010211?2012?001010?0?1001??102100021?101??101????21??1010??1?00?120???????
?11[12]00??0000100???
USNM_v_17098
1111104???1012?001?0020?10001?10?1?0020?100??010[12]???21?????????????120??221
110?1?00??0?0?0?01??
Euparkeria_capensis
000000?00?0?00??0?0?000110000100000002??0020??0?00???1?00001000?00000?000000
0???30????010?00??0
Machaeroprosopus_zunii
??????????????0?00??0??0000?102110010?10???011?00?2??????????????0?????????
??????0?0?0?????
NMMNHS_P4781
??????????????????0????1?????100??0?00??????0?0????1010??????????????????
??0??001?00????
Paleorhinus_parvus
1??0000?0??011?1????0??000
???????????0??1
USNM_v_21376
1100001?1??112?1101101???001??10?????0???????00??????010????????111????????
01?0????????01???
Diandongosuchus_fuyuanensis
0??000010?0001?0010?000000010110?00??0??012?01???01??1010000?0??0?0??????????0
1??011??001??1????
Greenland_phytosaur
120000?????????????????01????[01]???11
0??00??1?1??????2
;

Ccode
 -[/1 0   -[/1 1   -[/1 2   -[/1 3   -[/1 4
 -[/1 5   -[/1 6   +[/1 7   -[/1 8   -[/1 9
 +[/1 10   -[/1 11   -[/1 12   +[/1 13   -[/1 14
 -[/1 15   -[/1 16   -[/1 17   -[/1 18   -[/1 19
 -[/1 20   +[/1 21   -[/1 22   -[/1 23   +[/1 24
 -[/1 25   -[/1 26   -[/1 27   -[/1 28   -[/1 29
 -[/1 30   -[/1 31   -[/1 32   +[/1 33   -[/1 34
 -[/1 35   -[/1 36   +[/1 37   -[/1 38   -[/1 39
 -[/1 40   -[/1 41   +[/1 42   -[/1 43   -[/1 44

```
 -[/1 45    -[/1 46    -[/1 47    +[/1 48    -[/1 49
 -[/1 50    -[/1 51    -[/1 52    +[/1 53    -[/1 54
 -[/1 55    +[/1 56    -[/1 57    +[/1 58    +[/1 59
 -[/1 60    -[/1 61    -[/1 62    -[/1 63    -[/1 64
 -[/1 65    -[/1 66    -[/1 67    -[/1 68    -[/1 69
 -[/1 70    -[/1 71    -[/1 72    -[/1 73    -[/1 74
 -[/1 75    -[/1 76    -[/1 77    -[/1 78    -[/1 79
 -[/1 80    -[/1 81    -[/1 82    -[/1 83    -[/1 84
 -[/1 85    +[/1 86    -[/1 87    +[/1 88    -[/1 89
 -[/1 90    -[/1 91    -[/1 92    +[/1 93    -[/1 94
;
cnames
{0 Anterior_end_of_premaxillae;
{1 Interpremaxillary_fossa;
{2 Alveolar_ridges;
{3 Ventral_alveolar_bulge_between_premaxilla_and_maxilla;
{4 Alveolar_rim_of_maxilla;
{5 Premaxillary_crest;
{6 Rostral_crest;
{7 Transverse_width_of_the_rostrum_between_the_antorbital_fenestrae_in_dorsal_view;
{8 Suture_between_maxilla_and_premaxilla_and_nasal;
{9 Posterior_portion_of_maxilla_lateral_outline_in_dorsal_view;
{10 Ratio_of_rostral_to_narial_plus_post_narial_length;
{11 Narial_openings;
{12 Narial_openings_b;
{13 Position_of_nares;
{14 Anterior_extent_of_septomaxillae;
{15 Narial_outlets;
{16 Dorsal_rim_of_nares;
{17 Narial_wing;
{18 Interorbital_nasal_area_lateral_view;
{19 Interorbital_nasal_area_cross_section;
{20 Infranasal_recess;
{21 Antorbital_fossa;
{22 Discrete_row_of_anteroposteriorly_extending_nodes_on_the_lateral_surface_of_the_jugal;
{23 Jugal_and_AOF;
{24 Length_of_antorbital_fenestra;
{25 Broad_median_depression_on_dorsal_surface_of_frontals_near_border_with_nasals;
{26 Posterolateral_margins_of_nares;
{27 Pre_orbital_depression;
{28 Depression_and_flange_in_postorbital_bar;
{29 Jugal_and_orbit;
{30 Medial_margins_of_orbits;
{31 Deep_sculpture_of_the_skull_roof;
{32 Sutural_articulation_of_sq_and_po_in_dorsal_view;
{33 Most_anterior_extent_of_infratemporalfenestra;
{34 Pre_infratemporal_shelf;
{35 Lateral_ridge_from_po_sq_bar;
```

{36 Lateral_ridge_of_postorbital_squamosal_bar_continues_as_ridge_onto_posterior_process_of_squamosal;
{37 Length_of_posterior_process_of_squamosal_in_relation_to_postorbital_length;
{38 Posterior_process_of_squamosal;
{39 Terminal_knob;
{40 Dorsal_edge_of_sq;
{41 Dorsal_edge_of_sq_b;
{42 Length_of_free_postorbital_squamosal_bar;
{43 Medial_extent_of_squamosal;
{44 Cross_section_of_posterior_half_of_postorbito_squamosal_bar;
{45 Ventral_margin_of_sq;
{46 Subsidiary_opisthotic_process_of_sq;
{47 Extent_of_sq_fossa;
{48 Orientation_of_supratemporal_fenestrae;
{49 Mediolateral_expansion_of_posterior_process_of_squamosal;
{50 Face_of_medial_rim_of_squamosal_along_supratemporal_fenestra_and_posterior_process;
{51 Extent_of_squaring_of_the_squamosal_rim;
{52 Ridge_around_anterior_and_or_medial_edge_of_supratemporal_fenestra;
{53 Width_of_squamosal;
{54 Outline_of_medial_rim_of_squamosal_along_supratemporal_fenestra_and_posterior_process;
{55 Path_of_parietal_sq_bars;
{56 Visibility_of_supratemporal_fenestrae_in_dorsal_view;
{57 Parietal_squamosal_bars;
{58 Dorsal_edge_of_parieto_squamosal_bar;
{59 Parietal_ledge_ratio_of_width_to_length;
{60 Medial_half_of_parieto_squamosal_bar_lateral_wall_of_supraoccipital_shelf_;
{61 Lobate_extension_on_the_vertical_rim_of_the_squamosal_processes_of_the_parietal;
{62 Depth_and_shape_of_supraoccipital_shelf;
{63 Top_of_parieto_supraoccipital_complex_formed_by_squamosal_processes_of_parietals;
{64 Parietal_prongs;
{65 Posttemporal_fenestra;
{66 Lateral_border_of_posttemporal_fenestra;
{67 Shape_of_quadratojugal;
{68 Anterior_border_of_parabasisphenoid_contribution_to_basitubera;
{69 Morphology_of_basioccipital_between_tubera;
{70 Lateral_extent_of_basitubera_compared_to_basipterygoid_processes_in_ventral_view;
{71 Length_of_interpterygoid_vacuity;
{72 Suborbital_foramen;
{73 Anterior_extent_of_palatine;
{74 Palatal_ridge;
{75 Medial_edge_of_palatine_below_posterior_part_of_palatal_vault;
{76 Dorsal_surface_of_surangular;
{77 Shape_of_retroarticular_process_in_lateral_view;
{78 Snout_dorsal_surface_cross_sectional_shape;
{79 Anterior_separation_of_the_septomaxillae;
{80 Shape_of_AOF;
{81 Lateral_surface_of_maxilla_and_jugal_ventral_posteroventral_to_AOF;

{82 Lateral_surface_of_main_body_of_jugal;
{83 Anterior_extension_of_the_sub_temporal_shelf;
{84 Dorsal_extension_of_sub_temporal_shelf;
{85 Jugal_foramen_in_anteroventral_corner_of_the_subTF;
{86 Relative_robusticity_of_the_jugal;
{87
Proximal_section_of_postorbital_descending_process_where_posterior_border_of_orbit_m
eets_skull_roof_;
{88 SubTF_diagonal_aspect_ratio;
{89
Additional_ridge_on_lateral_surface_of_posterior_process_of_squamosal_below_ridge_or_r
ugosity_from_po_sq_bar;
{90 Posterior_border_of_quadrate_in_lateral_view;
{91 Internarial_septum;
{92 Triangular_projection_ventral_to_articular_condyle;
{93 Relative_length_of_mandibular_symphysis;
{94 Degree_heterodonty;
;
;
Ancstates
 -0   -1   -2   -3   -4   -5   -6   -7   -8   -9
 -10   -11   -12   -13   -14   -15   -16   -17   -18   -19
 -20   -21   -22   -23   -24   -25   -26   -27   -28   -29
 -30   -31   -32   -33   -34   -35   -36   -37   -38   -39
 -40   -41   -42   -43   -44   -45   -46   -47   -48   -49
 -50   -51   -52   -53   -54   -55   -56   -57   -58   -59
 -60   -61   -62   -63   -64   -65   -66   -67   -68   -69
 -70   -71   -72   -73   -74   -75   -76   -77   -78   -79
 -80   -81   -82   -83   -84   -85   -86   -87   -88   -89
 -90   -91   -92   -93   -94   ;

xgroup

;
agroup

;
taxcode
+0   +1   +2   +3   +4   +5   +6   +7
+8   +9   +10   +11   +12   +13   +14   +15
+16   +17   +18   +19   +20   +21   +22   +23
+24   +25   +26   +27   +28   +29   +30   +31
+32   +33   +34   +35   +36   +37   +38   +39
+40   +41   +42   +43
;

blocks 0;

tshrink

;

tread

'30 trees'

(37 (((25 (39 (1 (31 (0 41)))))(((20 ((4 (5 (21 (14 (2 15)))))(28 35)))(26 27))((22 ((7 ((6 (10 (36 38)))(34 (8 (23 (24 33)))))))(9 11)))(30 (32 (12 (13 43)))))))((16 (42 (3 (17 (18 19)))))(29 40))))*

(37 (40 (((25 (39 (1 (31 (0 41)))))(((20 ((4 (5 (21 (14 (2 15)))))(28 35)))(26 27))((22 ((7 ((6 (10 (36 38)))(34 (8 (23 (24 33)))))))(9 11)))(30 (32 (12 (13 43)))))))(29 (16 (42 (3 (17 (18 19)))))))))))*

(37 (((25 (39 (1 (31 (0 41)))))(((20 ((4 (5 (21 (14 (2 15)))))(28 35)))(26 27))((22 ((7 ((6 (10 (36 38)))(34 (8 (23 (24 33)))))))(9 11)))(30 (32 (12 (13 43)))))))(40 (29 (16 (42 (3 (17 (18 19)))))))))))*

(37 (((25 (39 (1 (31 (0 41)))))(((20 ((4 (5 (21 (14 (2 15)))))(28 35)))(26 27))((22 ((7 ((6 (10 (36 38)))(34 (8 (23 (24 33)))))))(9 11)))(30 (32 (12 (13 43)))))))(29 (16 (40 (42 (3 (17 (18 19)))))))))))*

(37 (((25 (39 (1 (31 (0 41)))))(((20 ((4 (5 (21 (14 (2 15)))))(28 35)))(26 27))((22 ((7 ((6 (10 (36 38)))(34 (8 (23 (24 33)))))))(9 11)))(30 (32 (12 (13 43)))))))(29 ((42 (3 (17 (18 19))))(16 40)))))*

(37 (((25 (39 (1 (31 (0 41)))))(((20 ((4 (5 (21 (14 (2 15)))))(28 35)))(26 27))((22 ((7 ((6 (10 (36 38)))(34 (8 (23 (24 33)))))))(9 11)))(30 (32 (12 (13 43)))))))(29 (16 ((3 (17 (18 19)))(40 42))))))*

(37 (((25 (39 (1 (31 (0 41)))))(((20 ((4 (5 (21 (14 (2 15)))))(28 35)))(26 27))((22 ((7 ((6 (10 (36 38)))(34 (8 (23 (24 33)))))))(9 11)))(30 (32 (12 (13 43)))))))(29 (16 (42 (40 (3 (17 (18 19)))))))))))*

(37 (((25 (39 (1 (31 (0 41)))))(((20 ((4 (5 (21 (14 (2 15)))))(28 35)))(26 27))((22 ((7 ((6 (10 (36 38)))(34 (8 (23 (24 33)))))))(9 11)))(30 (32 (12 (13 43)))))))(29 (16 (42 (3 (40 (17 (18 19)))))))))))*

(37 (((25 (39 (1 (31 (0 41)))))(((20 ((4 (5 (21 (14 (2 15)))))(28 35)))(26 27))((22 ((7 ((6 (10 (36 38)))(34 (8 (23 (24 33)))))))(9 11)))(30 (32 (12 (13 43)))))))((16 (42 (17 (3 (18 19)))))(29 40))))*

(37 (((25 (39 (1 (31 (0 41)))))(((20 (((21 (14 (2 15)))(4 5))(28 35)))(26 27))((22 ((7 ((6 (10 (36 38)))(34 (8 (23 (24 33)))))))(9 11)))(30 (32 (12 (13 43)))))))((16 (42 (3 (17 (18 19)))))(29 40))))*

(37 (((25 (39 (1 (31 (0 41)))))(((20 ((4 (5 (21 (14 (2 15)))))(28 35)))(26 27))((22 ((7 ((6 (10 (36 38)))(34 (8 (23 (24 33)))))))(9 11)))(30 (32 (12 (13 43)))))))(29 (40 (16 (42 (3 (17 (18 19)))))))))))*

(37 (40 (((25 (39 (1 (31 (0 41)))))(((20 ((4 (5 (21 (14 (2 15)))))(28 35)))(26 27))((22 ((7 ((6 (10 (36 38)))(34 (8 (23 (24 33)))))))(9 11)))(30 (32 (12 (13 43)))))))(29 (16 (42 (17 (3 (18 19)))))))))))*

(37 (40 (((25 (39 (1 (31 (0 41)))))(((20 (((21 (14 (2 15)))(4 5))(28 35)))(26 27))((22 ((7 ((6 (10 (36 38)))(34 (8 (23 (24 33)))))))(9 11)))(30 (32 (12 (13 43)))))))(29 (16 (42 (3 (17 (18 19)))))))))))*

(37 (((25 (39 (1 (31 (0 41)))))(((20 ((4 (5 (21 (14 (2 15)))))(28 35)))(26 27))((22 ((7 ((6 (10 (36 38)))(34 (8 (23 (24 33)))))))(9 11)))(30 (32 (12 (13 43)))))))(40 (29 (16 (42 (17 (3 (18 19)))))))))))*

(37 (((25 (39 (1 (31 (0 41)))))(((20 (((21 (14 (2 15)))(4 5))(28 35)))(26 27))((22 ((7 ((6 (10 (36 38)))(34 (8 (23 (24 33)))))))(9 11)))(30 (32 (12 (13 43)))))))(40 (29 (16 (42 (3 (17 (18 19)))))))))))*

(37 (((25 (39 (1 (31 (0 41)))))(((20 ((4 (5 (21 (14 (2 15)))))(28 35)))(26 27))((22 ((7 ((6 (10 (36 38)))(34 (8 (23 (24 33)))))))(9 11)))(30 (32 (12 (13 43)))))))(29 (16 (40 (42 (17 (3 (18 19)))))))))))))*
(37 (((25 (39 (1 (31 (0 41)))))(((20 (((21 (14 (2 15)))(4 5))(28 35)))(26 27))((22 ((7 ((6 (10 (36 38)))(34 (8 (23 (24 33)))))))(9 11)))(30 (32 (12 (13 43)))))))(29 (16 (40 (42 (3 (17 (18 19)))))))))))))*
(37 (((25 (39 (1 (31 (0 41)))))(((20 (((21 (14 (2 15)))(4 5))(28 35)))(26 27))((22 ((7 ((6 (10 (36 38)))(34 (8 (23 (24 33)))))))(9 11)))(30 (32 (12 (13 43)))))))(29 ((42 (3 (17 (18 19))))(16 40))))))*
(37 (((25 (39 (1 (31 (0 41)))))(((20 (((21 (14 (2 15)))(4 5))(28 35)))(26 27))((22 ((7 ((6 (10 (36 38)))(34 (8 (23 (24 33)))))))(9 11)))(30 (32 (12 (13 43))))))))(29 (16 ((3 (17 (18 19)))(40 42))))))))*
(37 (((25 (39 (1 (31 (0 41)))))(((20 (((21 (14 (2 15)))(4 5))(28 35)))(26 27))((22 ((7 ((6 (10 (36 38)))(34 (8 (23 (24 33)))))))(9 11)))(30 (32 (12 (13 43))))))))(29 (16 (42 (40 (3 (17 (18 19)))))))))))))*
(37 (((25 (39 (1 (31 (0 41)))))(((20 (((21 (14 (2 15)))(4 5))(28 35)))(26 27))((22 ((7 ((6 (10 (36 38)))(34 (8 (23 (24 33)))))))(9 11)))(30 (32 (12 (13 43)))))))(29 (16 (42 (3 (40 (17 (18 19)))))))))))))*
(37 (((25 (39 (1 (31 (0 41)))))(((20 (((21 (14 (2 15)))(4 5))(28 35)))(26 27))((22 ((7 ((6 (10 (36 38)))(34 (8 (23 (24 33))))))))(9 11)))(30 (32 (12 (13 43)))))))((16 (42 (17 (3 (18 19)))))(29 40))))*
(37 (((25 (39 (1 (31 (0 41)))))(((20 ((4 (5 (21 (14 (2 15)))))(28 35)))(26 27))((22 ((7 ((6 (10 (36 38)))(34 (8 (23 (24 33)))))))(9 11)))(30 (32 (12 (13 43)))))))(29 (40 (16 (42 (17 (3 (18 19)))))))))))))*
(37 (((25 (39 (1 (31 (0 41)))))(((20 ((4 (5 (21 (14 (2 15)))))(28 35)))(26 27))((22 ((7 ((6 (10 (36 38)))(34 (8 (23 (24 33)))))))(9 11)))(30 (32 (12 (13 43)))))))(29 (16 (42 (17 ((3 40)(18 19)))))))))))*
(37 (((25 (39 (1 (31 (0 41)))))(((20 (((21 (14 (2 15)))(4 5))(28 35)))(26 27))((22 ((7 ((6 (10 (36 38)))(34 (8 (23 (24 33)))))))(9 11)))(30 (32 (12 (13 43)))))))(29 (40 (16 (42 (3 (17 (18 19)))))))))))))*
(37 (40 (((25 (39 (1 (31 (0 41)))))(((20 (((21 (14 (2 15)))(4 5))(28 35)))(26 27))((22 ((7 ((6 (10 (36 38)))(34 (8 (23 (24 33)))))))(9 11)))(30 (32 (12 (13 43)))))))(29 (16 (42 (17 (3 (18 19)))))))))))))*
(37 (((25 (39 (1 (31 (0 41)))))(((20 (((21 (14 (2 15)))(4 5))(28 35)))(26 27))((22 ((7 ((6 (10 (36 38)))(34 (8 (23 (24 33)))))))(9 11)))(30 (32 (12 (13 43)))))))(40 (29 (16 (42 (17 (3 (18 19)))))))))))))*
(37 (((25 (39 (1 (31 (0 41)))))(((20 (((21 (14 (2 15)))(4 5))(28 35)))(26 27))((22 ((7 ((6 (10 (36 38)))(34 (8 (23 (24 33)))))))(9 11)))(30 (32 (12 (13 43)))))))(29 (16 (40 (42 (17 (3 (18 19)))))))))))))*
(37 (((25 (39 (1 (31 (0 41)))))(((20 (((21 (14 (2 15)))(4 5))(28 35)))(26 27))((22 ((7 ((6 (10 (36 38)))(34 (8 (23 (24 33)))))))(9 11)))(30 (32 (12 (13 43)))))))(29 (40 (16 (42 (17 (3 (18 19)))))))))))))*
(37 (((25 (39 (1 (31 (0 41)))))(((20 (((21 (14 (2 15)))(4 5))(28 35)))(26 27))((22 ((7 ((6 (10 (36 38)))(34 (8 (23 (24 33)))))))(9 11)))(30 (32 (12 (13 43)))))))(29 (16 (42 (17 ((3 40)(18 19)))))))))
;
tgroup

=0 (random_addseqs)   0 1 2 3 4 5 6 7 8 9 10 11 12 13 14 15 16 17 18 19 20 21 22 23 24 25 26 27 28 29

;

proc/;